Novel allosteric modulators of the M1 muscarinic acetylcholine receptor provide new insights into M1-dependent synaptic plasticity and receptor signaling

By

Sean P Moran

Dissertation

Submitted to the Faculty of the

Graduate School of Vanderbilt University

in partial fulfillment of the requirements

for the degree of

DOCTOR OF PHILOSOPHY

in

Neuroscience

December 14, 2019

Nashville, Tennessee

Approved:

Sachin Patel M.D., Ph.D.

Colleen Niswender, Ph.D.

Danny Winder, Ph.D.

P. Jeffrey Conn, Ph.D.

ACKNOWLEDGMENTS

Throughout my scientific career, there have been many people instrumental in my scientific journey. I would first like to thank Jeff Conn for providing a very supportive research atmosphere, for always making me laugh, for his insight and constructive criticism in our one-on-one meetings and for occasionally getting my name correct. I would also like to thank my thesis committee of Sachin Patel, Colleen Niswender and Danny Winder for their unwavering support during my time here at Vanderbilt. Additionally, I have very much enjoyed collaborating with Jerri Rook on many projects and would like to thank her for her sage behavioral pharmacology advice over the years. Also, thanks to the many members of the VCNDD including: Zixiu, Craig, Jon Dickerson, Dan Foster, Max, Nicole, Mark and Carrie who provided intellectual contributions, technical training or research support throughout my graduate career. Thank you to the many other members of the VCNDD, past and present, that have contributed to my various projects over the years. Thanks to the better half of Shames (James). I will our miss our long winded, highly pedantic and semantic discussions that occasionally touched on pharmacology topics…and thanks for making me not homeless. Thank you to my previous mentor Anthony Chan who introduced me to translational neuroscience research, allowed me to drive independent projects forward and provided the unique opportunity to both create and then play with baby monkeys.

Overall, my family has been incredibly supportive of my scientific career and I could not have gotten through graduate school without them. I will be forever thankful for my mom and dad who provided endless education opportunities that were not afforded to

them. Thank you to my sister and brother-in-law who have always provided support. Thank you, David, for providing endless laughs throughout graduate school but since you missed my thesis defense, I am not that thankful. I will miss living with you and conversing exclusively in LOTR quotes. Lastly, thank you to my incredibly smart and supportive girlfriend Carolyn, who has been my partner in crime over these many years. Our many fun vacations always provided a great getaway from science. I look forward to living in the same time zone for once. Lastly, and most importantly, thank you to the Conn Lab coffee. Without you, none of this would have been possible.

TABLE OF CONTENTS

LIST OF TABLES

Table Page

LIST OF FIGURES

CHAPTER 1

INTRODUCTION

Background

Acetylcholine plays a major role as a neurotransmitter and neuromodulator throughout the central nervous system (CNS) as well as multiple peripheral systems (*1*, *2*). In the CNS, cholinergic sources include local interneurons found in multiple brain regions, projections originating from the brainstem pedunculopontine and lateral dorsal tegmental nuclei as well as from the basal forebrain nuclei (*1*). The latter provides long-range cholinergic projections and is the major source of acetylcholine in the neocortex, hippocampus and amygdala (Figure 1A), brain regions important in learning and memory.

Acetylcholine can signal through two distinct classes of receptors that include ligand-gated cation channels, termed nicotinic acetylcholine receptors, and G-protein-coupled muscarinic acetylcholine receptors (mAChRs). While both receptor classes play important roles in central and peripheral systems, in the CNS, acetylcholine acts primarily through mAChRs as a neuromodulator to shape ensembles of neurons and alter neuronal firing in response to changing environmental conditions (*1*, *3*), The five member mAChR G-protein coupled receptor (GPCR) family consist of M_1, M_3 and M_5, which primarily couple to G_q to activate phospholipase C, and M_2 and M_4, which primarily couple to $G_{i/o}$ to inhibit adenylyl cyclase and modulate ion channels (Fig. 1B).

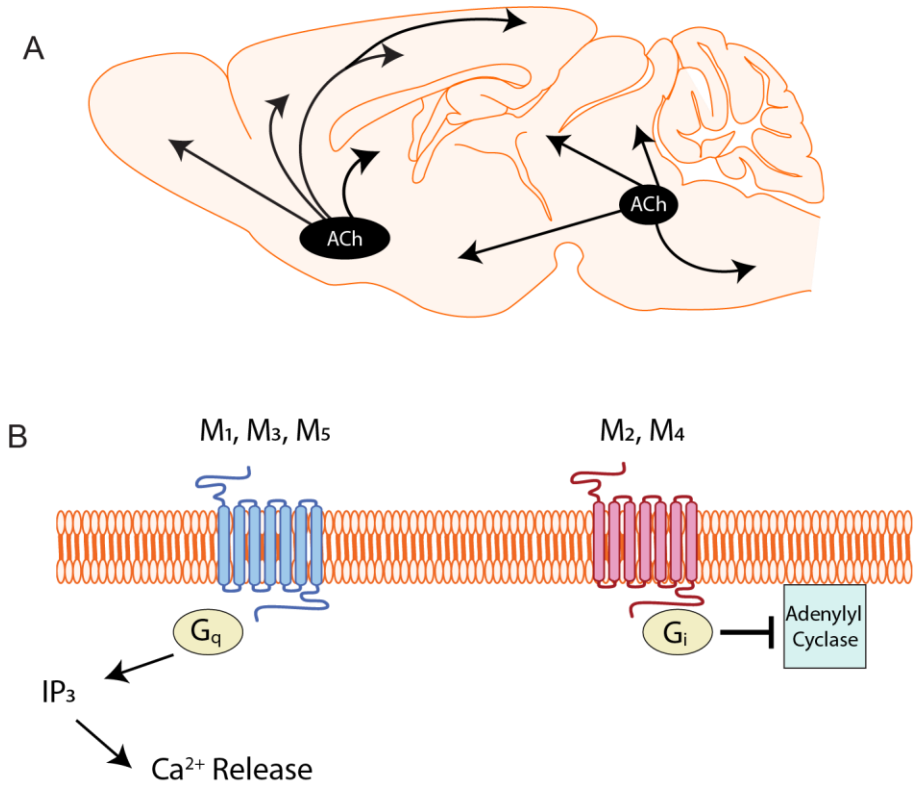

Figure 1: Schematic of cholinergic signaling in the brain.
(A) Cartoon schematic of cholinergic projection neurons in the rodent brain. (B) M_1, M_3, and M_5 primarily couple to $G_{\alpha q}$ whereas M_2 and M_4 primarily couple to $G_{\alpha i}$.

Considerable evidence suggests that mAChRs are critically involved in modulating cognition, substance use disorder (SUD) (*4*, *5*) motivation, as well as additional behaviors and their localization both pre- and postsynaptically throughout the CNS makes mAChRs uniquely situated as potential targets for the treatment of multiple CNS disorders.

Cognitive disruptions in schizophrenia and Alzheimer's disease

Schizophrenia is a devastating psychiatric disorder that afflicts approximately 1% of the worldwide population, affects women and men equally, and spans all

socioeconomic groups (*6*). The disease is characterized by three major symptom domains: positive, negative, and cognitive symptoms (*6*–*8*) . Current antipsychotics are effective at treating the positive symptoms such as auditory and visual hallucinations, delusions, and disorganized thoughts; however, they do not address the negative or the cognitive symptoms. Negative symptoms (e.g. flattened affect, social withdrawal) and cognitive symptoms (e.g. deficits in working memory, and cognitive flexibility) are believed to be the best predictors of long-term outcome and the costs of treatment along with the loss of productivity associated with schizophrenia are estimated to cost the U.S. healthcare system over $60 billion per year (*8*, *9*). Additionally, most patients discontinue currently available pharmacological treatments due to adverse effects including extrapyramidal side effects (EPS) (i.e. dystonia, akathisia, parkinsonism, bradykinesia, tremor, and tardive dyskinesia) induced by first-generation typical antipsychotics and metabolic side effects (i.e. weight gain, type II diabetes, and hyperlipidosis) induced by second generation atypical antipsychotics (*10*, *11*). Therefore, there is a critical need to identify and develop novel therapeutic targets for the treatment of the cognitive disruptions in patients with schizophrenia.

Another well characterized CNS disorder that produces cognitive disruptions is Alzheimer's disease (AD), a debilitating neurodegenerative disorder that afflicts 5.8 million Americans and this number is believed to grow up to 14 million by the year 2050 (National Institute on Aging). AD is an irreversible, progressive brain disorder that slowly destroys memory and thinking skills, and, eventually, the ability to carry out the simplest tasks. In most patients with AD, symptoms first appear in their mid-60s; however there is a small subpopulation of patients that develop early onset AD (*12*). AD is the most

common cause of dementia among older adults (*13*). Dementia is defined by the progressive loss of cognitive functioning, thinking, remembering, logic and reasoning and these changes result in a dramatically diminished quality of life for the patient as well as the caregiver(s) (*13*, *14*). Dementia ranges in severity from the mildest stage, when it is just beginning to affect a person's functioning, to the most severe stage, when the person must depend completely on others for basic activities of daily living (*13*, *14*). To date, the exact mechanism of action underlying the cause of AD is not known, however, there is well established AD-brain pathology that includes an accumulation of intracellular Aβ plaques as well as extracellular hyperphosphorylated tau tangles (*14*).

Targeting muscarinic acetylcholine receptors for the treatment of AD and schizophrenia

Cholinergic signaling is disrupted in Alzheimer's disease (AD) and several post-mortem studies have demonstrated a significant reduction in cholinergic projection neurons originating in the basal forebrain of patients with AD (*15*). Current clinical strategies to combat the loss of cholinergic neurons and restore memory and cognition in AD include raising total cholinergic tone through systemic administration of acetylcholinesterase (AChE) inhibitors that block the breakdown of acetylcholine (*16*). While AChE inhibitors such as tacrine and donepezil have demonstrated dose-dependent efficacy in improving cognition in patients with early stage AD, they suffer from dose-limiting adverse effects attributed to generalized non-selective activation of cholinergic receptors in the CNS and periphery, thereby limiting their clinical utility (*16*). Therefore,

there is intense interest in developing more selective agents that activate specific receptor subtypes within the cholinergic system.

Robust preclinical and clinical evidence suggests that mAChRs are critically involved in learning and memory (*4*) and significant investments have been made in developing ligands that engage mAChRs for the treatment of cognitive disruptions associated with AD, including the nonselective M_1/M_4 receptor preferring agonist xanomeline. In a phase III clinical study in patients with AD, xanomeline significantly reduced behavioral disturbances including vocal outbursts, suspiciousness, delusions, agitation, hallucinations, and had trending but not statistically significant improvements in cognition (*17*). While the clinical effects were promising, xanomeline has activity on all mAChR subtypes and induced severe dose-limiting gastrointestinal (GI) and other adverse effects that are mediated by activation of peripheral mAChRs (*17*, *18*). Despite these peripheral effects, the promising reduction in behavioral disturbances and the trending effect on cognition prompted a small follow up phase II clinical trial in patients with schizophrenia (*19*). Here, xanomeline produced significant improvements in the Brief Psychiatric Rating Scale (BPRS, see Glossary), Positive and Negative Syndrome Scale (PANSS), and Clinical Global Impression Scale, compared to the placebo-controlled group (*19*). Similar to the AD study, xanomeline produced GI disturbances, which halted further clinical development of xanomeline (*18*, *19*). Follow up preclinical studies suggest that activation of M_2 and M_3 in the periphery are responsible for the peripheral adverse effects of xanomeline (*18*). Recently, Karuna Pharmaceuticals renewed interest in xanomeline by advancing KarXT, a combination therapy of xanomeline with the peripherally restricted mAChR antagonist trospium chloride (*20*), into a phase II clinical

trial for schizophrenia (Clinical Trial Number: NCT03697252). While this combination therapy may reduce the adverse effects of xanomeline in the periphery and thereby increase the therapeutic window of xanomeline, a more targeted approach selectively activating specific mAChRs may provide the greatest clinical benefit.

Significant investment has been made to develop selective agonists devoid of M_2 and M_3, activation including development of the M_1 agonist HTL0018318 by Sosei Heptares, who recently partnered with Allergan to sponsor a phase I clinical trial for AD (Clinical Trial Number: NCT03456349) and phase II trial in patients with Lewy body dementia in Japan (JapicCTI-183989) (Table 1). However, an unexpected HTL0018318 chronic dosing toxicology finding in nonhuman primates placed the clinical trial in Lewy body dementia patients on hold (Table 1). Unfortunately, despite major investments in medicinal chemistry to develop highly selective M_1 or M_4 orthosteric agonists, these efforts have largely failed due to the highly conserved orthosteric acetylcholine binding site among the mAChRs.

Allosteric modulators of mAChRs

In order to develop highly selective small molecules ligands for specific mAChR subtypes, several groups have pursued development of allosteric modulators that target less well-conserved allosteric sites that are distinct from the orthosteric acetylcholine binding site (*21*, *22*). Significant progress has been made in understanding the structural basis of allosterism with the determination of the crystal structure for multiple mAChR subtypes (*23–27*), and the crystallization of several state-dependent receptor conformations (*28*). Collectively, the insights into the exact nature of orthosteric and

allosteric ligand interactions provided by these crystal structures paired with state-of-the-art *in silico* docking of digital compound libraries provide the exciting potential to screen large numbers of compounds in very little time and at low cost, thereby identifying new chemical scaffolds and novel selective ligands through rational drug design (*29*, *30*).

Positive allosteric modulators (PAMs) increase responses to orthosteric agonists, whereas negative allosteric modulators (NAMs) inhibit responses to orthosteric agonists (*22*). PAMs and NAMs exert their effects by modulating the affinity of an orthosteric ligand to the receptor or by modulating coupling to intracellular signaling (*22*). Follow up functional studies, including work utilizing receptor knockout animals have demonstrated that the procognitive and antipsychotic-like effects of xanomeline are likely mediated by M_1 and M_4 receptors, respectively (*18*, *31*, *32*). Thus, multiple drug discovery efforts have focused on developing allosteric modulators for these two mAChR subtypes.

Potential cognition enhancing effects of M_1 PAMs

The M_1 mACh receptor is the most abundant of the five mAChRs in brain regions critically involved in cognition such as the prefrontal cortex (PFC) and hippocampus (*33*, *34*). Pharmacological blockade (*35*, *36*) or genetic deletion (*37*) of M_1 produces profound disturbances in learning and memory, including significant deficits in social interaction, social discrimination, as well as working memory in the radial arm maze (*37*). Based on these studies, and extensive clinical studies implicating central mAChRs in cognitive processing (*38–40*), selective potentiation of M_1 signaling in the CNS using highly selective M_1 PAMs may hold promise to enhance cognition and reverse learning and memory disturbances.

Over the last decade, multiple M_1 PAMs have demonstrated robust efficacy in several preclinical animal models. Benzyl quinolone carboxylic acid (BQCA), the first highly selective M_1 PAM to be disclosed, reversed scopolamine-induced memory deficits in contextual fear conditioning (*41*). Interestingly, BQCA also reversed amphetamine induced hyperlocomotion (AHL), a common animal model to predict antipsychotic efficacy (*41*). Congruent with this finding, M_1 KO mice have an increased response to amphetamine, providing direct evidence for regulation of dopaminergic transmission by the M_1 receptor (*42*). Together, these findings suggest that M_1 PAMs may provide some efficacy in treating the positive symptoms of schizophrenia. However, future studies are necessary to demonstrate the potential of M_1 PAMs to reverse the positive symptoms of schizophrenia.

This initial BQCA study also revealed insights into the diverse signaling pathways that M_1 PAMs can potentiate, including ERK phosphorylation and recruitment of β-arrestin (*41*). These ground breaking results were replicated in later studies demonstrating that the M_1 PAM BQCA can reverse scopolamine-induced deficits in rodents (*43*) and does not display any signal bias in systems expressing wild-type M_1 receptors in the presence of the endogenous agonist, acetylcholine (*44*, *45*). However, BQCA was demonstrated to display a robust signal bias in M_1 Designer Receptors Exclusively Activated by Designer Drugs (DREADD) receptors that are genetically modified to no longer respond to acetylcholine and instead respond to the synthetic agonist clozapine-N-oxide (*45*). These studies suggest that the ligand-receptor dynamics for the muscarinic receptors are more complicated than initially thought and careful molecular pharmacology is necessary to fully describe each allosteric modulator's effects on a given receptor.

Further characterization of BQCA in native tissue demonstrated that M_1 PAMs can potentiate the cholinergic agonist carbachol (CCh)-induced increases in spontaneous excitatory postsynaptic currents (sEPSCs) onto layer V medial prefrontal cortex (mPFC) pyramidal neurons (*46*). BQCA was also able to potentiate layer V mPFC pyramidal neuron inward currents generated by bath application of a subeffective concentration of CCh (*46*). This study also demonstrated the first evidence that M_1 PAMs such as BQCA may be effective in reversing the learning and memory deficits in Alzheimer's disease evidenced by the ability of BQCA to restore discrimination reversal learning in a transgenic mouse model of Alzheimer's (*46*). In addition to this interesting finding, BQCA was also able to directly modulate non-amyloidogenic amyloid precursor protein processing in this same mouse model of AD. Therefore, M_1 PAMs may provide symptomatic relief as well as potentially provide disease-modifying effects in patients with Alzheimer's disease. However, further studies are necessary to determine whether M_1 PAMs can have disease modifying effects in other animal models of AD.

BQCA was also shown to improve acquisition of a visual pairwise discrimination task in mice, a highly translatable task to humans (*36*). In this study, the authors used a variant of the visual pairwise discrimination task requiring top-down processing by using two objects with unequal salience (*36*). The ability of BQCA to enhance acquisition of this top-down processing task was not surprising since M_1 KO mice have impaired acquisition of this same visual pairwise discrimination task (*36*). Another important finding from this study was that repeated BCQA administration does not alter M_1 mAChR mRNA expression in the hippocampus, PFC or striatum. Chronic dosing of small molecules can alter transcript and/or protein levels for other receptors, illustrated by some group II mGlu

agonists, and these changes in transcript and/or protein levels can result in tolerance and loss of efficacy (*47*). Thus, the lack of change in M_1 mAChR transcript levels after chronic BQCA dosing further supports M_1 PAMs as potentially efficacious therapeutics. However, we do not know if this is finding will hold true for all other M_1 PAMs, and future studies are necessary to confirm this BQCA finding.

While BQCA has been used extensively as a tool compound in preclinical animal studies, BQCA lack suitable “drug like” properties. Therefore, Merck invested considerable efforts to develop the next generation of M_1 PAMs with improved pharmacokinetic properties, selectivity and brain penetrance. These efforts resulted in the disclosure of the newer M_1 PAM 1-((4-cyano-4-(pyridine-2-yl)piperidin-1-yl)methyl-4-oxo-4H-quinolizine-3-carboxylic acid) (PQCA), which also demonstrated substantial preclinical efficacy by attenuating scopolamine-induced deficits in: novel object recognition in rats, self-ordered spatial search in cynomolgus macaques as well as object retrieval detour task in rhesus macaques (*48*). Subsequent studies revealed that PQCA also reversed scopolamine-induced deficits in the object retrieval detour cognition task in monkeys (*49*) as well as improved object recognition in the Tg2576 AD mouse model alone or in the presence of subeffective doses of donepezil (*50*). Further support for the potential efficacy of M_1 PAMs in treating neurodegenerative disorders is evidenced by the ability of 2 distinct M_1 PAMs to reverse cognitive disruptions in a prion mouse model of neurodegeneration (*51*). In addition to reversing the cognition deficits induced by pathogenic prions, the authors in this study demonstrated that chronic M_1 PAM dosing greatly extended the lifespan of the diseased mice (*51*).

In parallel to Merck's medicinal chemistry efforts, several other research groups including our group at Vanderbilt University as well as teams at Monash University, and Pfizer have identified, developed and characterized M_1 PAMs for the potential treatment of the cognitive disruptions in AD and schizophrenia. The prototypical M_1 PAM VU0453595 was recently demonstrated to rescue cognitive disruptions in mice treated subchronically with phencyclidine (PCP), a commonly used NMDA hypofunction mouse model of schizophrenia (*52*). Mechanistically, VU0453595 was shown to reverse PCP-induced deficits in a M_1-mediated form of synaptic plasticity in the PFC. Important for translating brain slice electrophysiological responses to responses in vivo, VU0453595 potentiated LTD induced by optically-evoked release of acetylcholine in PFC containing brain slices (*52*). Therefore, the effects of M_1 PAMs on synaptic plasticity in the brain are not solely dependent on introduction of exogenous cholinergic agonists. Additional studies using the more potent M_1 PAM VU6004256 demonstrated M_1 PAM efficacy in reversing cognitive disruptions in GluN1 knockdown mice, a genetic mouse model of NMDA hypofunction in which expression of the GluN1 subunit of the NMDA receptor is greatly reduced (*53*). To this same end, a study from Monash University demonstrated that BQCA could improve the efficacy of antipsychotics in mouse models of schizophrenia (*54*). While these results are very promising, BQCA effectively potentiated subeffective doses of atypical but not typical antipsychotics (*54*) therefore suggesting that M_1 PAM clinical trials in schizophrenia may be more complicated than originally thought.

In addition to both Merck and Vanderbilt University, Pfizer has spent considerable effort in developing M_1 PAMs. The highly selective and potent M_1 PAM PF-06764427 reversed AHL in mice (*55*). Shortly after disclosure of PF-06764427, Pfizer published

studies with PF-06767832, a newer M_1 PAM that reversed AHL in rats in a dose-dependent manner. In this same study, the authors demonstrated that PF-06767832 could reverse scopolamine-induced deficits in Morris water maze, a commonly used spatial learning task (*56*). While preclinical animal models of schizophrenia suffer from many caveats including the lack of construct validity, together, these studies provide support for the idea that M_1 PAMs may be efficacious in treating the cognitive disruptions in patients with schizophrenia.

Mechanistically, preliminary investigation into how M_1 PAMs may exert their procognitive effects at the molecular and cellular level have revealed that M_1 PAMs can potentiate normal synaptic plasticity (*52*, *57*) and neuronal excitability (*46*) in the PFC and can reverse synaptic plasticity disruptions in the PFC. Additionally, several studies have demonstrated a role of M_1 mAChRs in hippocampal function, since M_1 PAMs can specifically potentiate synaptic plasticity occurring at the hippocampus-PFC synapse (*58*) and activation of M_1 mAChRs in the hippocampus can induce synaptic plasticity (*59*, *60*) as well as facilitate spatial reversal learning, an important hippocampal dependent task (*61*).

The ability of M_1 PAMs to improve cognitive deficits in multiple distinct animal models as well as in multiple relevant preclinical species provides substantial support for the potential for M_1 PAMs to exhibit efficacy in reversing deficits in cognition in human patients suffering from AD and schizophrenia.

CHAPTER 2

DIVERSE M_1 PAM PHARMACOLOGY

Agonist activity in addition to PAM activity

While these findings are very promising, recent studies have revealed that some but not all M_1 PAMs display adverse effects including GI distress and behavioral convulsions in rodents and dogs (*34*, *57*, *62*). Previously, it was demonstrated that the nonselective mAChR orthosteric agonist pilocarpine induced robust seizures in healthy adult mice and mice in which M_2, M_3, M_4 or M_5 was genetically knocked out (KO) but produced no effect in M_1-KO mice, suggesting that overactivation of the M_1 receptor mediates these adverse effects (*63*, *64*). Therefore, one possibility to account for the stark contrast between M_1 PAMs that produce adverse effects and those that do not is the hypothesis that some M_1 PAMs can overactivate the M_1 receptor and therefore lead to similar adverse effects as traditional orthosteric agonists (*57*, *62*, *65*, *66*). This is reminiscent of studies from allosteric modulators for other GPCRs, such as the metabotropic glutamate receptor subtype 5 ($mGlu_5$), which demonstrated that the presence of allosteric agonist activity of $mGlu_5$ PAMs can result in severe behavioral convulsions in rodents (*67*).

We now report a series of studies in which we characterize two M1 PAMs that exhibit robust M_1 agonist activity (MK-7622 and PF-06764427) and two structurally distinct M_1 PAMs, VU0453595 (*52*) and VU0550164, that are devoid of agonist activity in cell lines. We then evaluate the physiological effects of PAMs with and without agonist

activity in the medial PFC (mPFC), a brain region important in cognition, and the potential cognitive and pro-convulsive effects in awake healthy rodents.

MK-7622 and PF-06764427 display robust agonist activity in an *in vitro* calcium mobilization assay

To assess the *in vitro* activity of the M_1 PAMs used in this study, compounds were tested using Chinese Hamster Ovary (CHO) cells stably expressing the M_1 receptor. The previously published M_1 PAM PF-06764427 (*55*, *62*) (Fig.1A, *left*) and Merck's MK-7622 (*68*) (Fig.1A, *right*) were evaluated for their ability to mobilize intracellular calcium (Ca^{2+}) in the M_1-CHO cells. The raw calcium traces (Fig. 1B) indicate that both PF-06764427 and MK-7622 induce robust increases in Ca^{2+} mobilization in the absence of an orthosteric mAChR agonist. PF-06764427 alone causes a concentration-dependent increase in the mobilization of intracellular Ca^{2+} (Ago EC_{50} 610 nM ± 14, Fig. 1C). Interestingly, we report a similar degree of intracellular Ca^{2+} mobilization with MK-7622 alone (Ago EC_{50} 2930 nM ± 95, Fig. 1D). Both PF-06764427 (PAM EC_{50} 30 nM ± 3, Fig. 1E) and MK-7622 (PAM EC_{50} 16 nM ± 4, Fig. 1F) act as potent and selective (*55*) (Fig. 2) M_1 PAMs in the presence of the orthosteric agonist ACh. Therefore, in addition to their PAM activity both PF-06764427 and MK-7622 have significant intrinsic agonist activity in this cell-based Ca^{2+} mobilization assay.

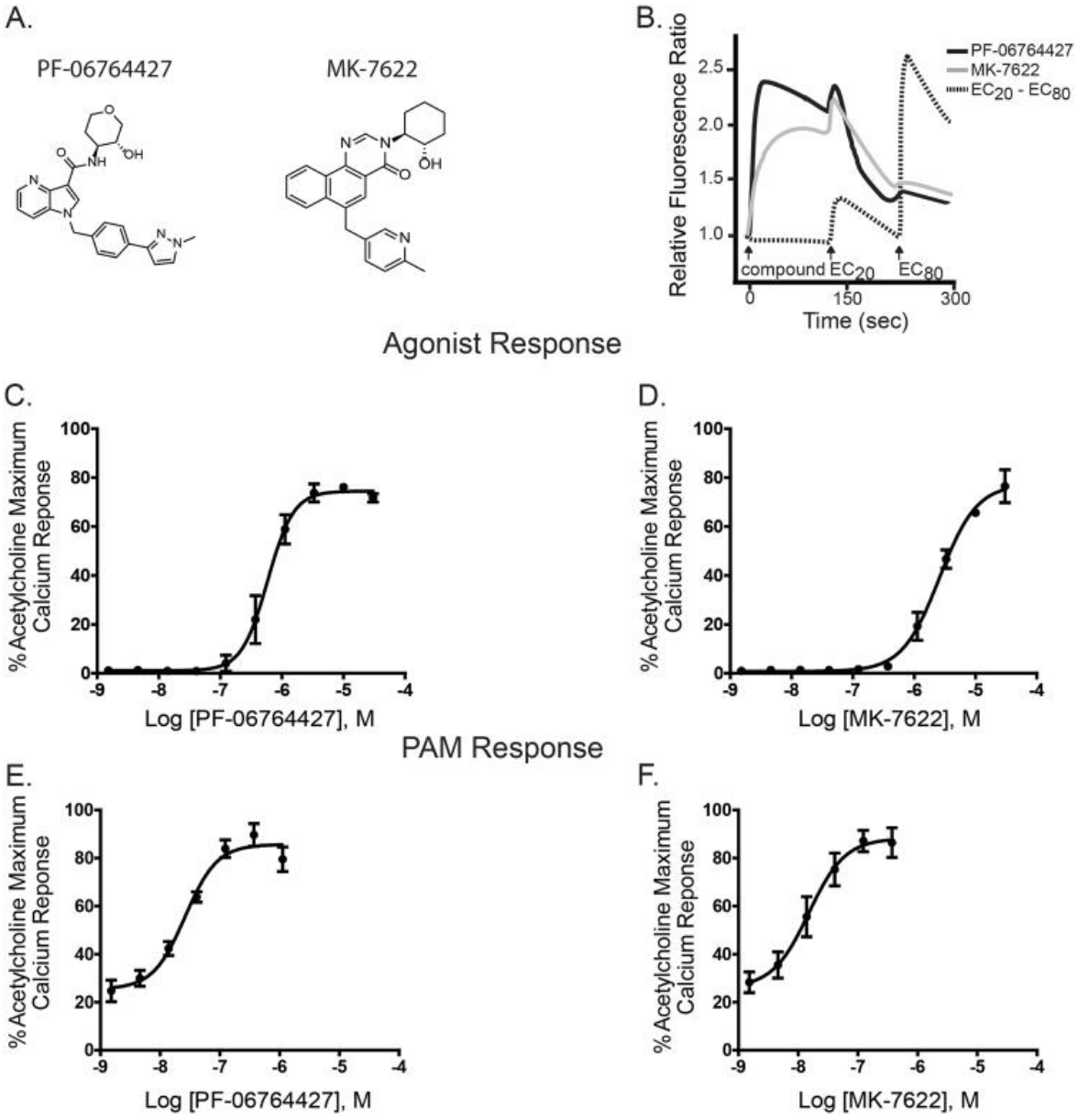

Figure 2: PF-06764427 and MK-7622 display robust intrinsic agonist activity in M_1-expressing CHO cells.

Structures of the M_1 PAMs PF-06764427 (left) and MK-7622 (right). (B) Representative raw calcium traces following the addition of 10 μM PF-06764427 (black), MK-7622 (light gray), and the subsequent additions of EC_{20} and EC_{80} concentrations of acetylcholine (ACh) (dotted line). (C) Agonist concentration-response curves of rM_1-CHO calcium mobilization assay for PF-06764427 and (D) MK-7622 in the absence of ACh. (E) PAM concentration-response curves of rM_1-CHO calcium mobilization assay for PF-06764427 and (F) MK-7622 in the presence of an EC_{20} of ACh. Data represent mean ± S.E.M. from 3 independent experiments performed in triplicate.

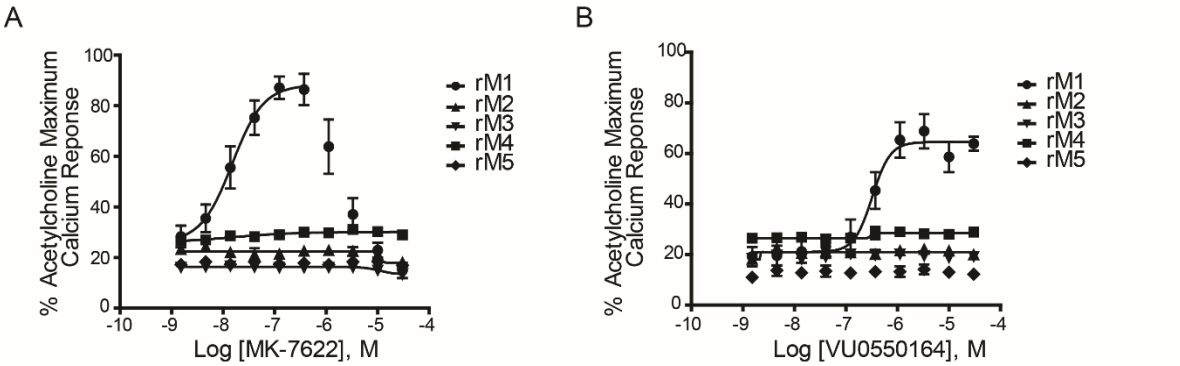

Figure 3: Selectivity of MK-7622 and VU0550164.
Calcium mobilization assays were performed using CHO cells stably expressing M_2-M_5 muscarinic receptors (M_2 and M_4 containing cells were co-transfected with G_{qi5}) to assess selectivity of MK-7622 and VU0550164. Neither MK-7622 (A) nor (B) VU0550164 exhibits any functional activity at the other rat muscarinic receptor subtypes. Data represent mean ± S.E.M. from 3 independent experiments performed in triplicate.

VU0453595 and VU0550164 act as highly selective PAMs lacking agonist activity in the M_1 *in vitro* calcium mobilization assay

Previous studies suggest that over activation of the M_1 mAChR can induce cholinergic adverse effects (*62*, *69*). Based on these studies, we initiated an effort to optimize M_1 PAMs that lack intrinsic agonist activity. We have previously reported characterization VU0453595 (*52*, *70*) (Fig. 3A, *left*) and now disclose the novel M_1 PAM VU0550164 (Fig. 3A, *right*). The raw Ca^{2+} traces (Fig. 3B) illustrate the lack of agonist activity of both VU0453595 and VU0550164 in the calcium mobilization assay even at high concentrations (>10 μM). As expected, VU0453595 had little to no effect on intracellular Ca^{2+} mobilization when applied alone (Fig. 3C). Similarly, the optimized M_1 PAM VU0550164 lacks agonist activity (Fig. 3D). However, both VU0453595 (PAM EC_{50} 2140 nM ± 436, Fig. 3E) and VU0550164 (PAM EC_{50} 330 nM ± 44, Fig. 3F) can strongly

potentiate an EC_{20} concentration of ACh in a concentration-dependent manner. These data reveal that at concentrations significantly above the PAM EC_{50}, VU0453595 and VU0550164 lack agonist activity in this assay, thereby demonstrating that these compounds are highly selective (*52*) (Fig. 2) PAMs devoid of agonist activity with respect to *in vitro* Ca^{2+} mobilization.

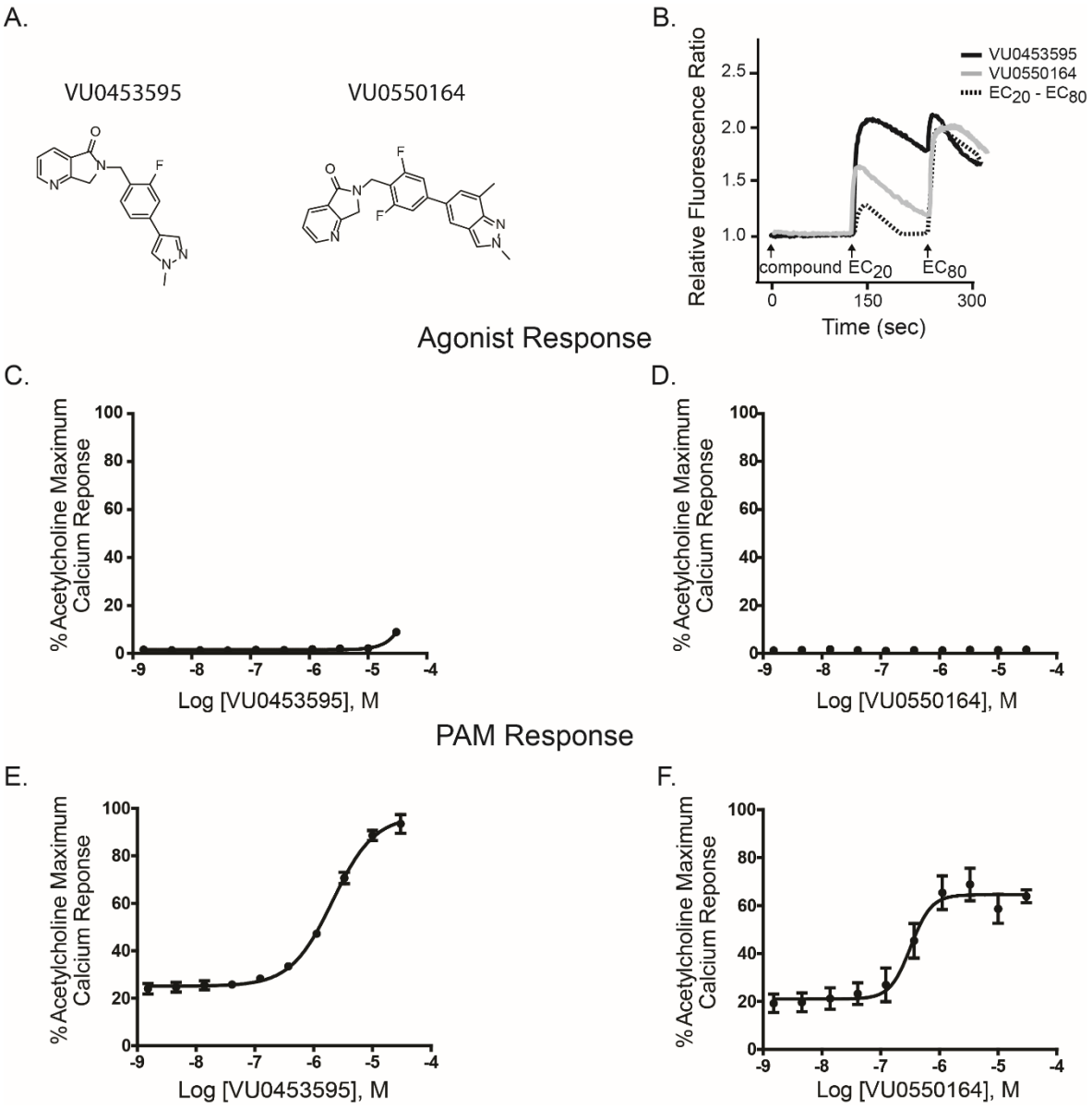

Figure 4: VU0453595 and VU0550164 lack significant agonist activity and are potent PAMs in M_1 expressing CHO cells.

(A) Structure of M_1 PAM VU0453595 (left) and VU0550164 (right). (B) Representative raw calcium traces following the addition of 10 μM VU0453595 (black) and VU0550164 (light gray) and the subsequent additions of EC_{20} and EC_{80} concentrations of acetylcholine (ACh) (dotted line). (C) Agonist concentration-response curves of rM1-CHO calcium mobilization assay for VU0453595 and (D) VU0550164 in the absence of ACh. (E) PAM concentration-response curves of rM1-CHO calcium mobilization assay for VU0453595 and (F) VU0550164 in the presence of an EC_{20} of ACh. Data represent mean ± S.E.M. from 3 independent experiments performed in triplicate.

Ago-PAMs but not PAMs lacking agonist activity increase sEPSC in layer V mPFC pyramidal neurons

To test whether PAMs displaying agonist activity in cell-based assays would have agonist activity in a native system, we evaluated the various M_1 PAMs in a series of whole cell electrophysiology experiments in native brain tissue. Previously, we reported that activation of M_1 can dramatically increase the activity of excitatory synaptic inputs onto layer V pyramidal cells in acute mPFC-containing brain slices (*46*). We now report that bath application of M_1 ago-PAM PF-06764427 (1 μM) induces a marked increase in frequency of spontaneous excitatory post synaptic currents (sEPSCs) in mPFC layer V pyramidal cells (Fig. 4A, paired t-test, $p < 0.05$). In addition, the second M_1 ago-PAM, MK-7622 (1 μM), also increased sEPSC frequency (Fig. 4B, paired t-test, $p < 0.05$). However, neither 10 μM VU0453595 (Fig. 4C) nor 10 μM VU0550164 (Fig. 4D) caused any significant change in sEPSC frequency (paired t-test, $p > 0.05$) at concentrations well above those required for maximal PAM activity. These results show that MK-7622 and PF-06764427 but not VU0453595 or VU0550164 have agonist activity in this native cortical preparation.

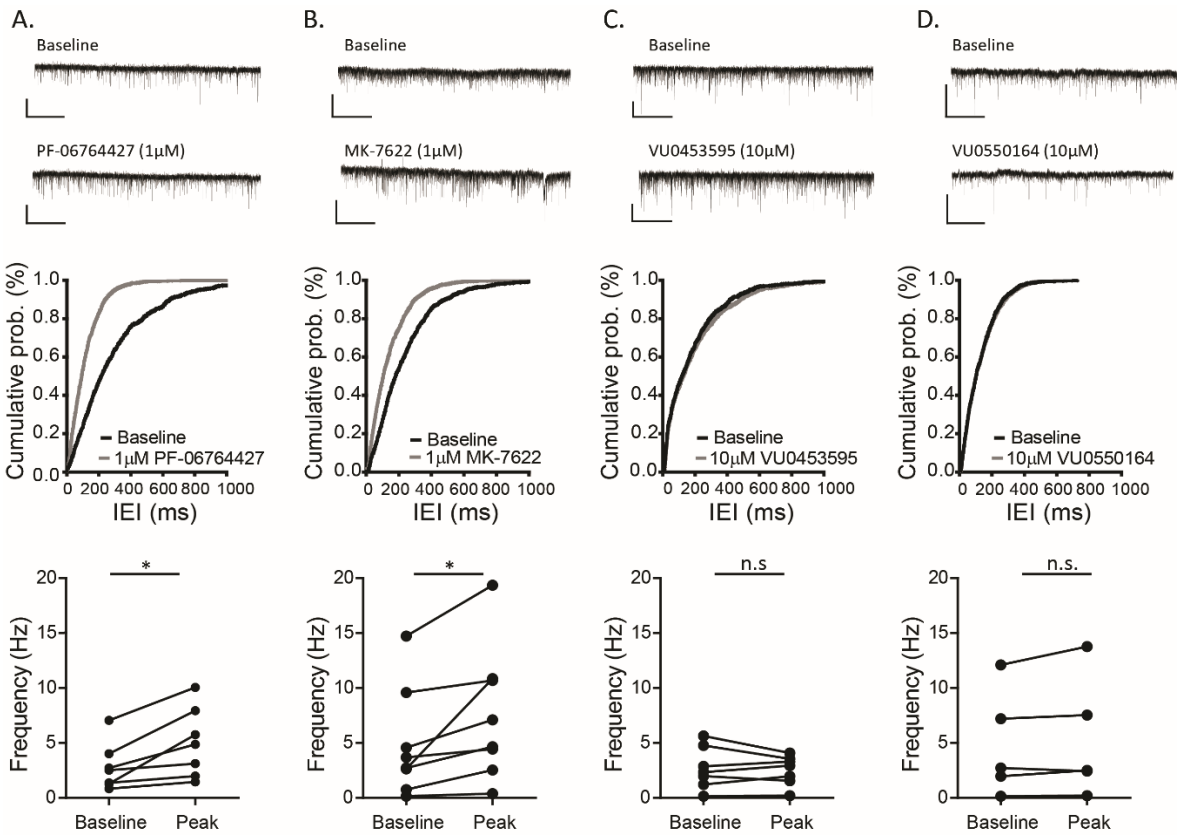

Figure 5: Ago-PAMs, but not PAMs devoid of agonist activity increase sEPSC frequency in layer V mPFC neurons.

(A) Whole-cell recordings from pyramidal neurons (regular spiking firing) clamped at −70 mV were performed in layer V of the prelimbic prefrontal mouse cortex. A sample trace of baseline (*upper-trace*) and during drug add (*bottom-trace*) and the cumulative probability of interevent intervals for a typical cell are shown in the (*middle*) during baseline and drug-add. Histogram summarizing the change in frequency of baseline to the drug peak effect (*lower*). Similar to 1 μM PF-06764427, bath application of 1 μM MK-7622 (B) produced a statistically significant increase in sEPSC frequency, in contrast to bath application of (C) 10 μM VU0453595 and (D) 10 μM VU0550164 which induced no significant change in sEPSC frequency. Scale bars denote 50pA and 10 seconds. *p<0.05, paired t-test.

Ago-PAMs but not PAMs lacking agonist activity induce robust depression of fEPSP slopes in the mPFC

We next tested the various M_1 PAMs in a more circuit-level brain slice electrophysiology assay by measuring changes in layer V field excitatory post synaptic potentials (fEPSPs) evoked by electrical stimulation of afferents in layer II/III of the mPFC. Previously, we and others found that cholinergic agonists can induce an M_1-dependent long-term depression (LTD) of fEPSP slope at this synapse (*52*, *53*, *71*). Consistent with the effects on sEPSCs, bath application of 1 µM PF-06764427 (Fig. 5A) induces a significant LTD of fEPSP slope 46-50 min (*shaded area*) after drug washout compared to baseline (paired t-test, $p<0.05$, Fig. 4B); this effect was absent in the presence of the selective M_1 antagonist VU0255035 (*72*) (Fig. 6A) as well as in M_1-KO mice (Fig. 6B). Quantification of LTD measured at 46-50 min after drug washout (*shaded area*) indicates a significant difference in the magnitude of LTD observed with application of 1 µM PF-06764427 + 10 µM VU0255035 as well as 1 µM PF-06764427 in M_1-KO mice compared to 1 µM PF-06764427 alone. (Fig. 6C) (one-way ANOVA, $p<0.05$).

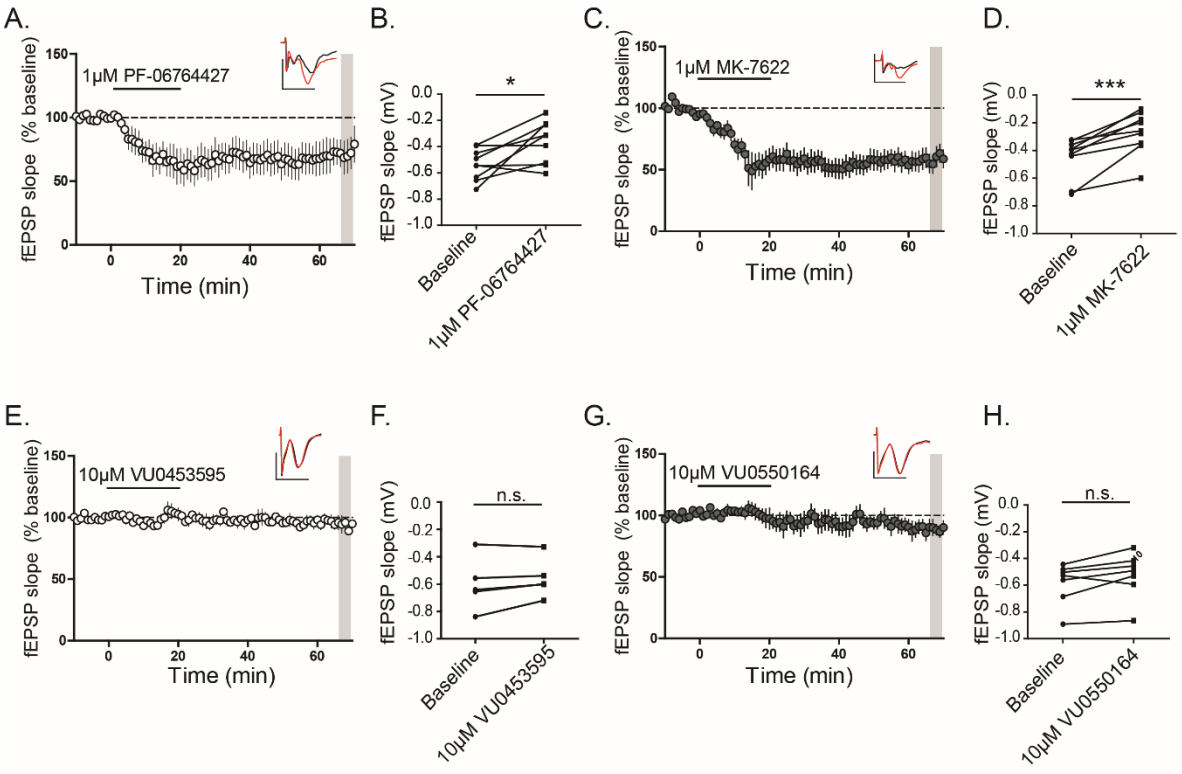

Figure 6: Ago-PAMs, but not PAMs devoid of agonist activity robustly depress fEPSP slopes recorded in layer V of the prelimbic mPFC evoked by electrical stimulation in layer II/III

(**A**) Time course graph showing that bath application of 1 μM PF-06764427 for 20 min leads to a robust long term depression (LTD) of fEPSP slope (**B**) Quantification of fEPSP slope 46-50 min following drug washout (*shaded area*) indicates a significant depression of fEPSP slope. n=9 brain slice experiments. *denotes $p<0.05$, paired t-test. (**C**) Under similar conditions bath application of 1 μM MK-7622 for 20 min led to an acute depression followed by a LTD of fEPSPs measured 46-50 min following drug washout. (**D**) Quantification of fEPSP slope 46-50 min following drug washout (*shaded area*) indicates a significant depression of fEPSP slope. n=9 brain slice experiments. ***denotes $p<0.001$, paired t-test. (**E**) Time course graph showing that bath application of 10 μM VU0453595 for 20 min led to no significant change in fEPSP slopes (**F**) measured 46-50 min following drug washout. n=4 brain slice experiments. $p>0.05$, paired t-test. (**G**) Similar to VU04553595, 10 μM VU0550164 failed to induce any significant change in fEPSP 46-50 min following drug washout (**H**). n=7 brain slice recordings, $p<0.05$. paired t-test. Time course data are expressed as mean ± S.E.M. Insert contains fEPSP sample traces during baseline (red) and 46-50 min following drug washout (black). Scale bar denotes 0.5 mV and 5 ms.

Similarly, bath application of 1 μM MK-7622 for 20 minutes (Fig. 5C) induces a robust and statistically significant LTD measured at 46-50 min following drug washout (paired t-test, $p<0.001$) (Fig. 5D). This LTD was absent in the presence of VU0255035 (Fig. 6D) as well as in brain slices obtained from M_1-KO mice (Fig. 6E). Quantification of LTD (normalized fEPSP slopes) 46-50 min after drug washout (*shaded area*) indicates a significant difference in the magnitude of LTD observed with application of 1 μM MK-7622 + 10 μM VU0255035 as well as 1 μM MK-7622 in M_1-KO mice compared to 1 μM MK-7622 alone (one-way ANOVA, $p<0.01$) (Fig. 6F).

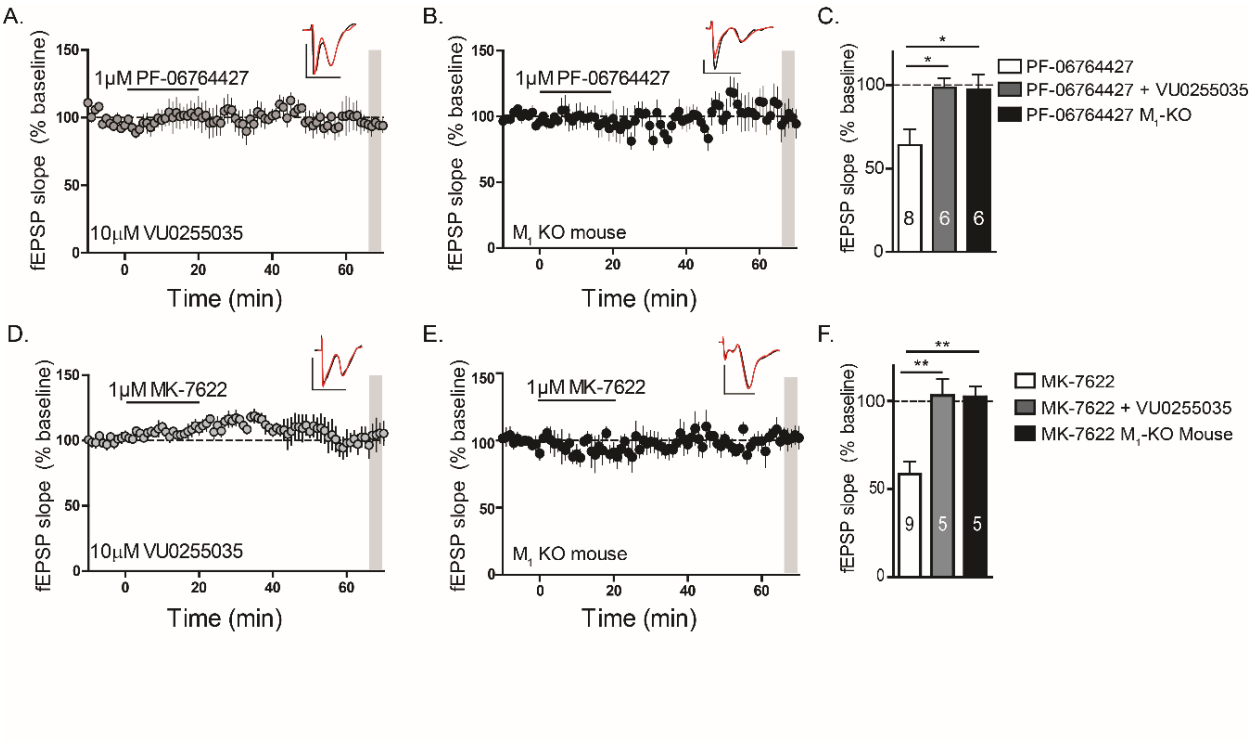

Figure 7: M_1 Ago-PAM LTD in the mPFC is M_1-dependent.
Time course graph showing that bath application of 1 μM PF-06764427 fails to induce LTD in the presence of (**A**) 10 μM VU0255035, a highly selective M_1 antagonist, and in (**B**) brain slices from M_1-KO brain mice. Insert contains fEPSP sample traces during baseline (red) and 46-50 min following drug washout (black). (**C**) Quantification of LTD (normalized fEPSP slopes) 46-50 min after drug washout (*shaded area*) of the different experimental groups. There was a significant difference in the magnitude of LTD observed with application of 1 μM PF-06764427 + 10 μM VU0255035, as well as 1 μM PF-06764427 in M_1-KO mice, compared to 1 μM PF-06764427 alone. One-way ANOVA was carried out with Dunnett's post-hoc test, 1 μM PF-06764427 (white bar) as the control group. * $p < 0.05$. Under similar conditions bath application of 1 μM MK-7622 failed to induce LTD in the presence of (**D**) 10 μM VU0255035. (**E**) Correspondingly, 1 μM MK-7622 failed to induce LTD in M_1-KO mice brain slices. Quantification of LTD (normalized fEPSP slopes) 46-50 min following drug washout (*shaded area*). (**F**) There was a significant difference in the magnitude of LTD observed with application of 1 μM MK-7622 + 10 μM VU0255035 as well as 1 μM MK-7622 in M_1-KO mice compared to 1 μM MK-7622 alone. Data are expressed as mean ± S.E.M. One-way ANOVA was carried out with Dunnett's post-hoc test with 1 μM MK-7622 (white bar) as the control group. ** $p < 0.01$. Numbers in the bar graph denote number of individual brain slice experiments.

In contrast to the effects of MK-7622 and PF-06764427, high concentrations of M_1 PAMs VU0453595 and VU0550164 induce no change in fEPSP slope. As illustrated in

Fig. 4E-F, bath application of 10 µM VU0453595, a concentration known to potentiate the LTD induced by a submaximal concentration of carbachol (CCh) (*52*), for 20 minutes did not significantly change fEPSP slope compared to baseline ($p>0.05$). Furthermore, the second M_1 PAM devoid of agonist activity *in vitro*, VU0550164 (10 µM) did not significantly change fEPSP slope compared to baseline when bath applied alone ($p>0.05$) (Fig. 5G-H), but potentiated the response to 10 µM CCh (Fig. 7A) and induced a robust LTD only in the presence of an orthosteric agonist (Fig. 7B). Quantification of LTD indicates a significant difference in the magnitude of LTD observed with co-application of 10 µM VU0550164 + 10 µM CCh compared to 10 µM alone ($p<0.05$) (Fig. 7C). Taken together, these data demonstrate that MK-7622 and PF-06764427 display strong intrinsic M_1 agonist activity in this cortical brain slice electrophysiological assay, in contrast to VU0453595 and VU0550164 which lack agonist activity and maintain activity-dependence of M_1 activation in these native brain tissue assays.

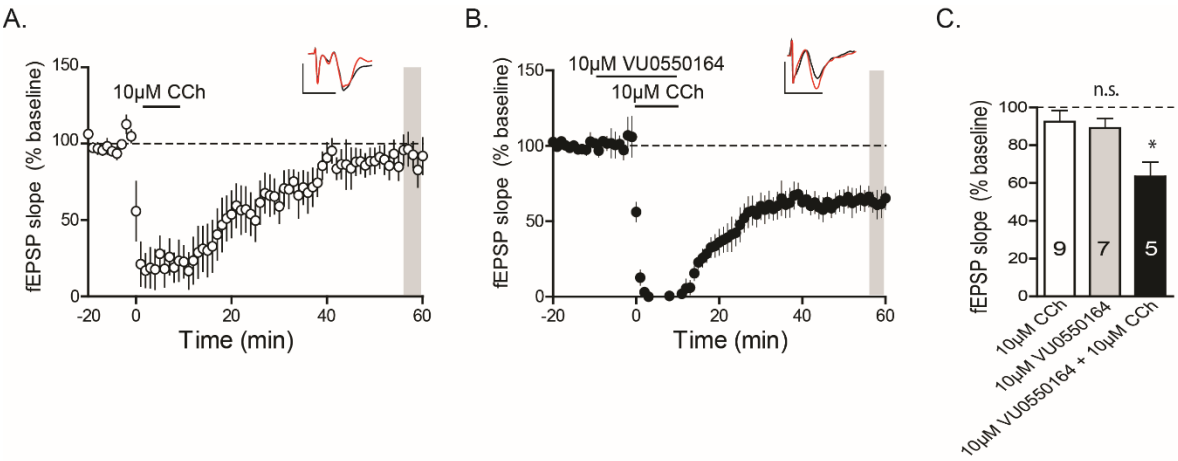

Figure 8: VU0550164 potentiates CCh-LTD in the mPFC.
(**A**) Time course graph showing that bath application 10 μM CCh induces a submaximal LTD 46-50min after drug washout (shaded area). (**B**) 10 min pretreatment of the M_1 PAM VU0550164 and 10 min co-application of VU0550164 is able to potentiate 10 μM CCh producing a maximal LTD 46-50min after drug washout. Insert contains fEPSP sample traces during baseline (red) and 46-50 min following drug washout (black). (**C**) Bar graph denoting quantification of LTD (normalized fEPSP slopes) of the different experimental groups. There was a significant difference in the magnitude of LTD observed with application of 10 μM CCh compared to 10 μM VU0550164 + 10 μM, but no significant difference between 10 μM CCh and 10 μM VU0550164 alone. One-way ANOVA was carried out with with Dunnett's post-hoc test. 10 μM CCh (white bar) as the control group. * $p < 0.05$. Numbers in the bar graph denote number of individual brain slice experiments. Scale bar denotes 0.5 mV and 5 ms.

MK-7622, but not VU0453595, induces behavioral convulsions in rodents

In light of our finding that both PF-06764427 and MK-7622 have robust allosteric agonist activity in both cell line and native tissue assays, we hypothesized that MK-7622 would induce behavioral convulsions in a manner similar to those observed with PF-06764427 (*62*). Therefore, we performed a dose-escalation study in mice to assess seizure liability of the M_1 ago-PAM MK-7622. Consistent with our previous study with PF-06764427, 30 mg/kg and 100 mg/kg MK-7622 induces robust convulsions that reached stage 5 on the modified Racine scale (*62*, *67*, *73*) in WT but not in M_1 KO mice (Fig. 8A).

While the M_1 PAM VU0550164 does not have suitable pharmacokinetic properties for systemic administration, VU0453595 has excellent properties for use in *in vivo* studies (*52*). Interestingly, VU0453595 induces no gross changes in behavior even at doses up to 100 mg/kg (Fig. 8A), well above doses that enhance cognition in rodents (*52*). Collectively, these findings suggest that M_1 ago-PAMs, such as MK-7622 and PF-06764427, induce behavioral convulsions that are not observed with PAMs lacking agonist activity such as VU0453595.

VU0453595 but not MK-7622 can enhance rodent object recognition

While M_1 ago-PAMs such as MK-7622 and PF-06764427 do not induce overt seizures at lower doses, it is possible that over activation of M_1 with ago-PAMs such as MK-7622 and PF-06764427 could disrupt cortical function and reduce efficacy of these compounds in enhancing cognitive function. Therefore, we performed a series of studies to evaluate the effects of the M_1 ago-PAM MK-7622 and the PAM VU0453595 in an established model of recognition memory in healthy adult rats (Fig. 8B). Rats were chosen for these studies because they do not display overt behavioral convulsions in response to administration of M_1 ago-PAMs and, for these studies, we used doses below those shown to induce behavioral convulsions in mice.

Interestingly, MK-7622 (1, and 3, and 10 mg/kg), did not significantly improve performance in the novel object recognition task ($p=0.9110$, one-way ANOVA) (Fig. 8C). In contrast, VU0453595, which lacks agonist activity induces a robust improvement in recognition memory in healthy adult rats assessed using the novel object recognition task. At 1, 3, and 10 mg/kg, VU0453595 enhances object recognition as indicated by a

significant increase in the recognition index (Dunnett's multiple comparison test: p=0.0008) (Fig. 8D).

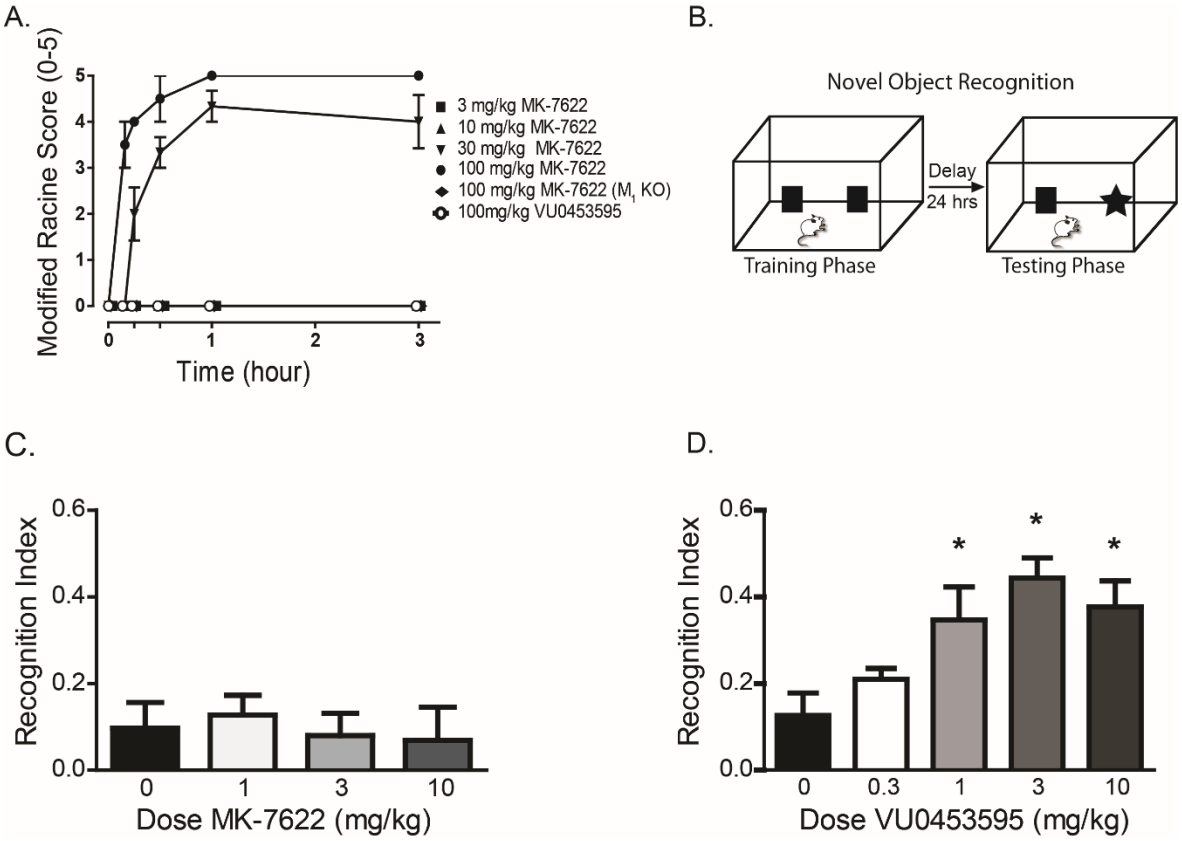

Figure 9: MK-7622 induces robust behavioral convulsions and lacks efficacy in enhancing rodent cognition.
(**A**) C57Bl6/j mice were administered 3, 10, 30, 100 mg/kg MK-7622, and behavioral convulsions were measured for 3 h using the modified Racine scale (0−5). M_1-KO mice exhibit no behavioral convulsions, suggesting that MK-7622 induces behavioral convulsions in a M_1-dependent fashion. Compounds were formulated in 10% Tween 80 and delivered intraperitoneally. Data represent mean ± SEM (n = 3 mice per dose). This is in contrast to VU0453595, which displays no overt adverse effects at concentrations up to 100 mg/kg (n = 3 mice). (**B**) Schematic of the rodent Novel Object Recognition paradigm**.** (**C**) Pretreatment with 1, 3, and 10 mg/kg of 90min before the familiar phase failed to significantly enhance object recognition assessed 24 hr later. (p=0.9110, n=11-12 rats per group). (**D**) Under similar conditions for MK-7622, VU0453595 dose-dependently enhances object recognition in rats. Pretreatment with 1, 3, and 10 mg/kg 90 min before the familiar phase enhanced object recognition memory assessed 24 hr later (p=0.008, n=11-12 rats per group). Data are expressed as mean ± SEM. *p< 0.05.

These studies suggest that the ability of MK-7622 to activate M_1 mAChRs regardless of presynaptic acetylcholine release may lead to aberrant receptor activity and may even disruption cognition and could therefore explain why MK-7622 did not meet clinical endpoints in an proof-of-concept clinical trial in AD patients (*74*). Together, these studies provided fundamental new insights into the impact of subtle differences in modes of activity of different M_1 PAMs and the need to strictly avoid allosteric agonist activity in these compounds.

Agonist activity is dependent in part on receptor reserve

Characterization of M_1 PAM PF-06827443

In opposition to this hypothesis, the newer PF-06827443 was previously demonstrated to display minimal agonist activity in cell lines expressing human M_1 but induced severe adverse effects in some preclinical animal models (*34*). One way to account for this finding is that agonist activity can vary dramatically depending on total receptor expression, known conceptually as receptor reserve. This is the concept that a full pharmacological response can be induced at ligand concentrations that do not saturate the receptor (*75*). Therefore, an allosteric modulator in systems with low receptor expression (low receptor reserve) may display partial agonism or no agonist activity at all. However, when the same ligand is tested in a cell line or system with high receptor expression (high receptor reserve), it may unmask agonist activity not seen in low expression systems. Therefore, we hypothesized that using cell lines with varied levels of M_1 receptor reserve, we could reveal agonist activity of PF-06827443.

In order to test this hypothesis, we first evaluated the ability of PF-06827443 to directly activate M_1 as assessed by mobilization of intracellular calcium (Ca^{2+}) in Chinese Hamster Ovary (CHO) cells stably expressing the rat M_1 receptor. PF-06827443 induces a robust increase in intracellular Ca^{2+} in the absence of an orthosteric mACh receptor agonist (rat ago EC_{50} 1900 nM; 81 ± 5% ACh Max, Figure 9) and is a potent PAM in the presence of an EC_{20} concentration of acetylcholine (rat PAM EC_{50} 36.1 ± 4.9 nM; 97 ± 1% ACh Max, Figure 9B). Additionally, PF-06827443 displays similar agonist and PAM activities at the dog and human M_1 receptors (Figure 10). Furthermore, unlike other M_1 PAMs devoid of agonist activity, PF-06827443 inhibits [^{3}H]-NMS binding, which likely reflects negative cooperativity with antagonist binding at the orthosteric binding site (Figure 11).

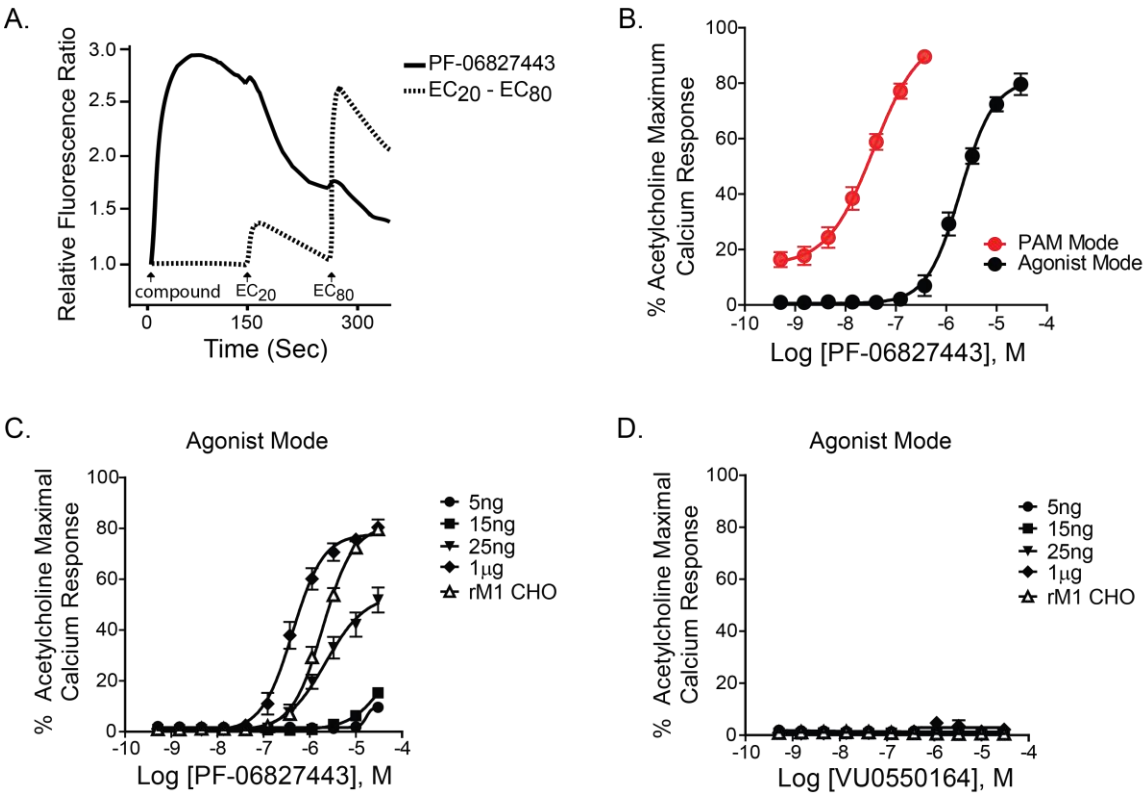

Figure 10: PF-06827443 displays intrinsic agonist activity in rM$_1$-CHO cells with high receptor expression.

(**A**) Representative raw calcium traces following the addition of 30 µM PF-06827443 (black) and the subsequent additions of EC_{20} and EC_{80} concentrations of acetylcholine (ACh) (dotted line). (**B**) Concentration-response curves (CRC) of rM$_1$-CHO calcium mobilization assay for PF-06827443 in the absence of ACh (Agonist Mode; Black) and the presence of an EC_{20} of ACh (PAM Mode; Red). Concentration-response curves for (**C**) PF-06827443 and (**D**) VU0550164, in the absence of ACh, in cell lines treated with 5 ng, 15 ng, 25 ng, and 1 µg of tetracycline as well as rM$_1$ CHO cells. Data represent mean ± S.E.M. from 3 independent experiments performed in triplicate.

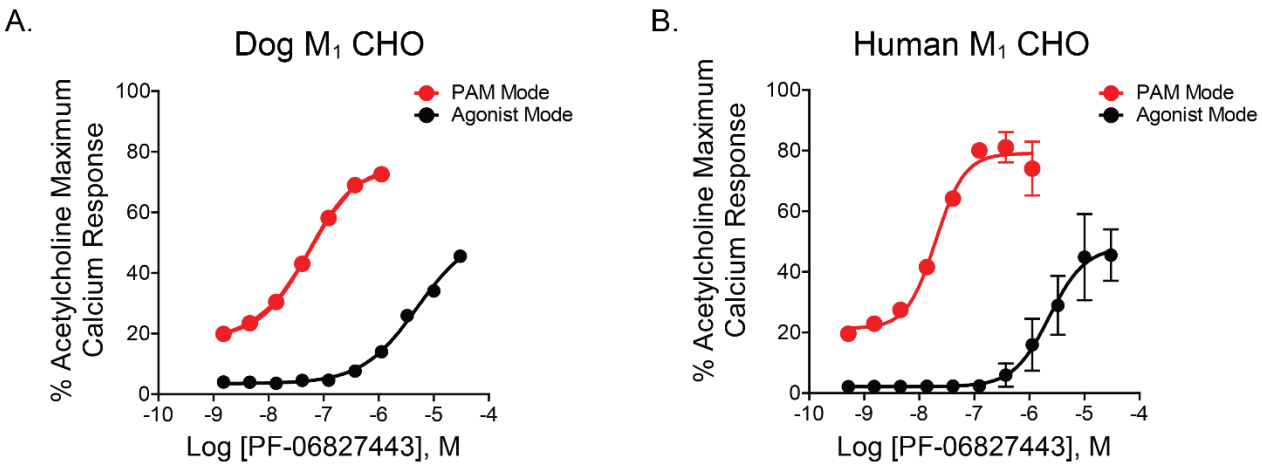

Figure 11: PF-06827443 displays intrinsic agonist activity in M_1-expressing CHO cells, independent of species.
(**A**) PF-06827443 concentration-response curves (CRC) of calcium mobilization assay in CHO cells stably expressing the dog M_1 receptor in the absence of ACh (Agonist Mode; Black) and the presence of an EC_{20} of ACh (PAM Mode; Red). (**B**) Under similar conditions, concentration response curves were generated for PF-06827443 in CHO cells stably expressing the human M_1 receptor. Data represent mean ± S.E.M. from 3 independent experiments performed in triplicate.

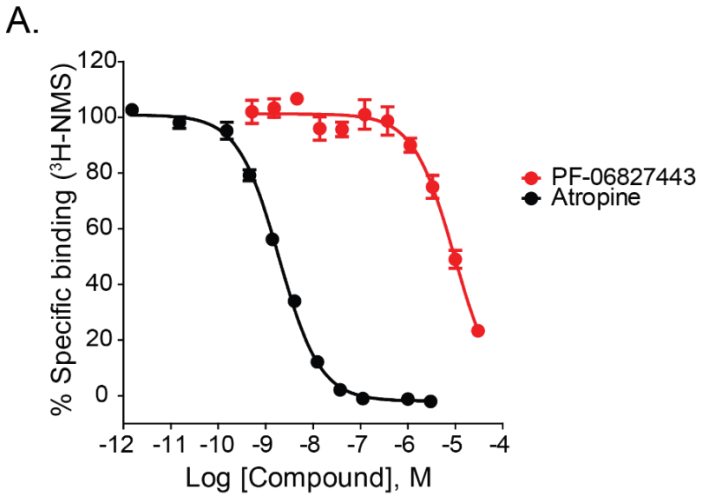

Figure 12: PF-06827443 displaces [^{3}H]-NMS at rat M_1 receptors.
(A) Inhibition of orthosteric radioligand binding with [^{3}H]-NMS by PF-06827443 and atropine control. Data are plotted as a percentage of specific [^{3}H]-NMS binding. Data represent the mean ± SEM from three separate experiments performed in triplicate.

While PF-06827443 was previously demonstrated to have minimal agonist activity at human M_1 (*34*), this discrepancy could due to the use of a cell line with lower M_1 expression as agonist activity of GPCR PAMs is dependent on receptor expression levels (*67*, *76–79*). To determine whether the robust agonist activity is dependent on levels of receptor expression, we used a TREx-CHO cell line in which the rM_1 receptor is under control of the tetracycline (TET) repressor protein, enabling us to systematically increase M_1 expression by adding increasing amounts of TET. This permits the measurement of M_1 activation in a single cellular background with different levels of receptor reserve. As shown in Table 1, increases in M_1 receptor expression was observed in a TET-concentration dependent manner and cells treated with 25ng/mL TET show comparable M_1 expression levels as CHO cells stably expressing rM1 and hM1. Similarly, increasing concentrations of TET led to a progressive increase in M_1 receptor expression, and a leftward shift in the ACh potency (Table 2). PF-06827443 shows comparable agonist activity in the cells treated with 25 ng TET (ago EC_{50} = 2300 nM; 54 ± 5% ACh Max, Figure 9C) to one in rat M_1-CHO. However, in cells with 1 µg TET, PF-06827443 exhibits robust agonist activity at high receptor expression levels (ago EC_{50} = 400 nM ; 78 ± 2% ACh Max), which is not as evident at lower expression levels, e.g. 5 ng and 15 ng TET (Figure 9C). In contrast, a previously characterized M_1 PAM optimized to lack agonist activity, VU0550164, does not exhibit agonism at any receptor expression level (Figure 9D).

Rat M_1-TREx CHO	Bmax (fmol/mg) ± SEM
5 ng TET	48 ± 4
15 ng TET	139 ± 8
25 ng TET	1066 ± 27
1000 ng TET	5859 ± 188
rM1-CHO	1305 ± 208
hM1-CHO	1479 ± 129

Table 1: Receptor densities determined from saturation binding assay
Data represents values determined from displacement of varying concentration of [^{3}H]-NMS ranging from 3nM to 0.003 nM) using the cell membranes isolated from rat M_1-TREx CHO that induced with different TET amount compared to the CHO cells stably expressing rM_1 and hM_1 receptors. Values represent the mean ± SEM of two experiments performed in triplicate.

Condition	ACh concentration (nM) (± SEM)	EC_{20} % response
5 ng TET	45.3 ± 1.3	16 ± 2
15 ng TET	19.3 ± 1.3	16 ± 1
25 ng TET	1.4 ± 0.2	15 ± 1
1 ug TET	0.2 ± 0.0	13 ± 1
rM1-CHO	1.2 ± 0.0	14 ± 1

Table 2: Comparison of acetylcholine concentration to elicit EC_{20} response in each TET condition in rat M_1 TREx-CHO and rat M_1-CHO.
There is a leftward shift of ACh potency with increasing amount of TET. Incubation with 25 ng TET shows comparable ACh potency to one in rat M_1-CHO.[a] Data values determined from ACh concentration necessary to elicit a ~EC_{20} % response in the various cell lines. Values represent the mean ± SEM of three independent experiments performed in triplicate.

PF-06827443 displays robust agonist activity in the mPFC

Native systems often have a high receptor reserve for M_1 (*76*, *78*); thus, it is important to evaluate the potential agonist activity of PF-06827443 in a native system relevant to rodent cognition. Previously, we and others found that cholinergic agonists, as well as M_1 ago-PAMs, can induce an M_1-dependent long-term depression (LTD) of layer V field excitatory post synaptic potentials (fEPSPs) electrically evoked by stimulation of layer II/III in the mouse PFC (Figure 12A) (*52*, *53*, *57*, *71*). Therefore, we tested the hypothesis that PF-06827443 would induce an LTD of fEPSPs at this cortical synapse similar to previously described ago-PAMs (*57*). Consistent with previous studies, 1 µM

(77.8 ± 4.27%, Figure 12B) and 10 µM PF-06827443 (51.8 ± 3.78%, Figure 12C) induce a sustained LTD of fEPSPs in the PFC. This effect of PF-06827443 was completely blocked by the highly selective M_1 antagonist VU0255035 (*72*), confirming that this PF-06827443 induced-LTD is M_1-dependent (101.6 ± 9.30%, Figure 12D). Quantification of LTD measured at 46-50 min after drug washout (shaded area) indicates a significant difference in the magnitude of LTD observed with application of 1 µM PF-06827443 + 10 µM VU0255035 compared to 1 µM PF-06827443 alone (Figure 12E, one-way ANOVA, $p<0.05$). Therefore, similar to other M_1 ago-PAMs, PF-06827443 displays robust agonist activity in the mouse PFC, a brain region heavily implicated in cognition.

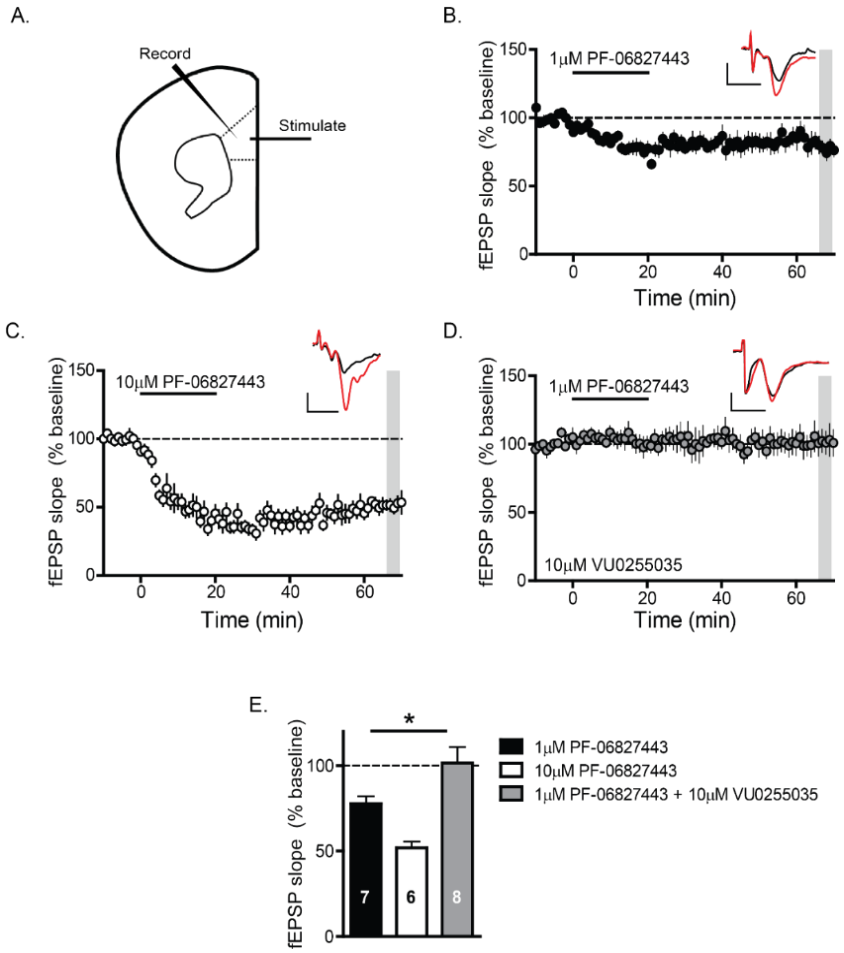

Figure 13: PF-06827443 robustly depresses fEPSP slopes recorded in layer V of the prelimbic mPFC evoked by electrical stimulation in layer II/III.
(**A**) Schematic the fEPSPs recorded from layer V of the mouse PFC in response to electrical stimulation in the superficial layers II–III. Time-course graph showing that bath application of (**B**) 1 μM PF-06827443 and (**C**) 10 μM PF-06827443 for 20 min leads to a robust long-term depression (LTD) of fEPSP slope. (**D**) Time course graph showing that bath application of 1 μM PF-06827443 fails to induce LTD in the presence of 10 μM VU0255035, a highly selective M_1 antagonist. Insert contains fEPSP sample traces during baseline (red) and 46-50 min following drug washout (black). Scale bars denote 0.2 mV and 5 seconds. n=6-8 brain slice experiments per group. (**E**) Quantification of LTD (normalized fEPSP slopes) 46-50 min after drug washout (shaded area) of the different experimental groups. There was a significant difference in the magnitude of LTD observed with application of 1 μM PF-06827443 + 10 μM VU0255035 compared to 1 μM PF-06827443 alone. One-way ANOVA was carried out with Dunnett's post-hoc test, 1 μM PF-06827443 (black bar) as the control group. * $p < 0.05$.

PF-06827443 increases sEPSC frequency in layer V prelimbic mPFC neurons

In addition, we performed studies to test the hypothesis that bath application of PF-06827443 would increase the frequency of spontaneous excitatory postsynaptic currents (sEPSCs) measured in layer V pyramidal cells of the PFC (Figure 13A) similar to previously characterized M_1 ago-PAMs (*57*). In agreement with previous studies, 10 μM PF-06827443 decreases the inter-event-interval (IEI) (Figure 13B) and consequently, significantly increases sEPSC frequency in layer V pyramidal cells (Figure 13C, paired t-test, $p<0.05$). Together, these results show that PF-06827443 displays robust agonist activity in two native tissue electrophysiological assays.

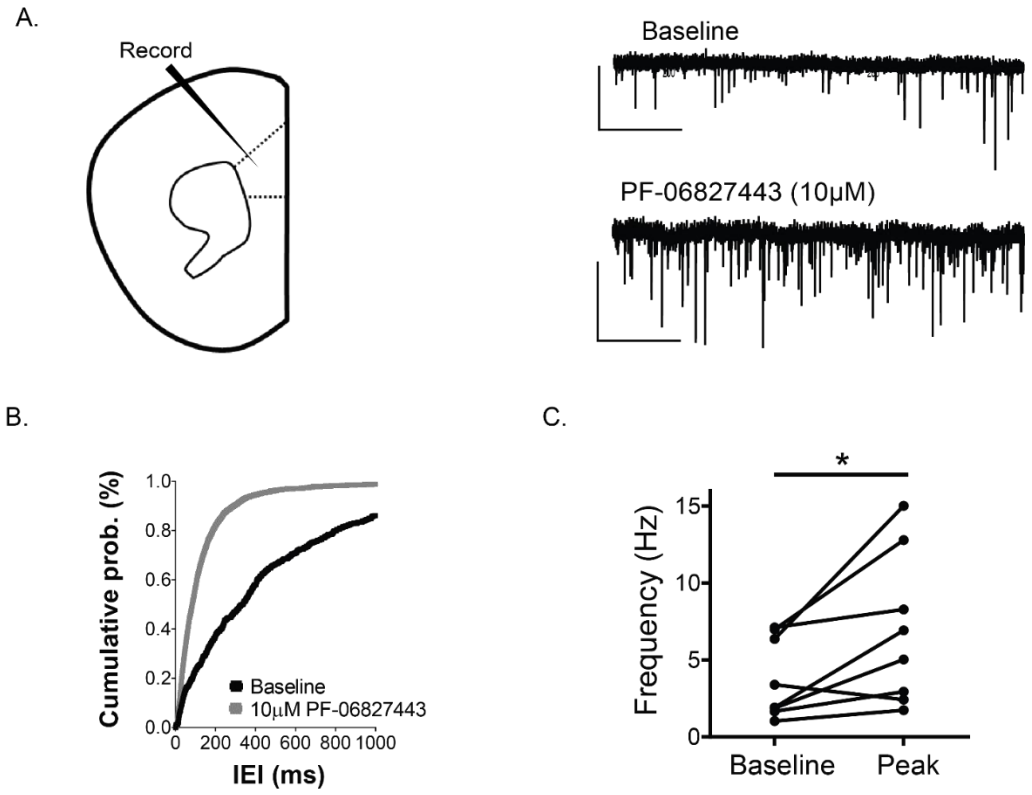

Figure 14: PF-06827443 increases sEPSC frequency in layer V prelimbic mPFC neurons.
(**A**) Whole-cell recordings from pyramidal neurons (regular spiking firing) clamped at −70 mV were performed in layer V of the prelimbic prefrontal mouse cortex. A sample trace of baseline (upper-trace) and during drug add (bottom-trace) for a typical cell are shown. Scale bars denote 50 pA and 2 seconds. (**B**) Histogram summarizing the change in the inter-event-interval of baseline (black) to the drug peak effect (grey). (**C**) 10 μM PF-06827443 produced a statistically significant increase in sEPSC frequency. n=8 slices. Student's t-Test; * $p < 0.05$.

PF-06827443 induces behavioral convulsions in mice

As seen with other ago-PAMs (*57*, *62*), we hypothesized that this overactivation of M_1 by PF-06827443 in native brain tissue preparations is responsible for M_1-induced behavioral convulsions. We next tested the hypothesis that the agonist activity of PF-06827443 seen in *in vitro* and native tissue assays would correlate to behavioral

convulsions when administered in mice. Therefore, we performed a single high dose (100 mg/kg) PF-06827443 study in M_1 knockout (KO) mice and littermate controls to assess seizure liability. Consistent with our previous ago-PAM studies, 100 mg/kg PF-06827443 induced behavioral convulsions that reached stage 3 on the modified Racine scale (*62*, *73*) in wildtype littermate mice that were absent in M_1 KO mice (Figure 14). Collectively, these findings demonstrate that high doses of PF-06827443 induce behavioral convulsions in mice similar to the adverse effects previously published in dogs (*34*).

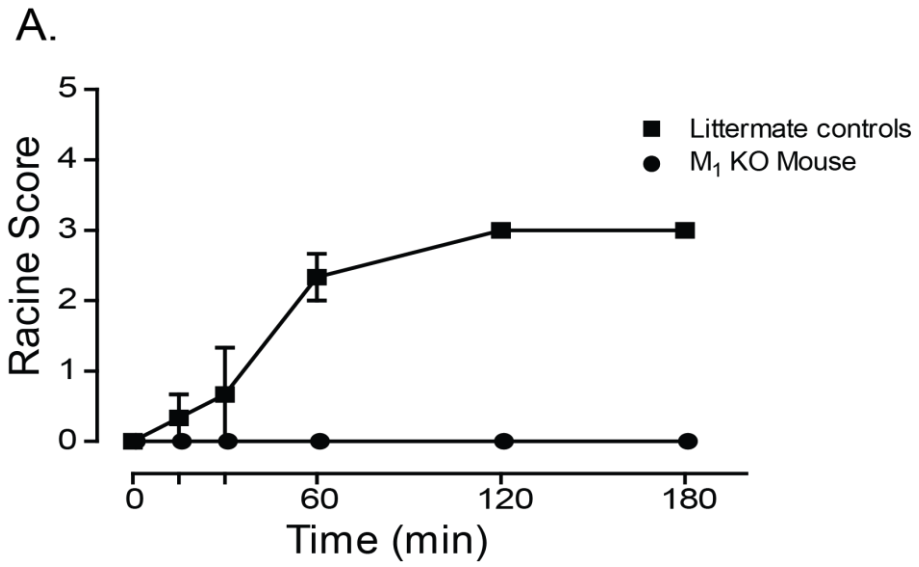

Figure 15: PF-06827443 induces behavioral convulsions in mice.
(**A**) C57Bl6/J mice were administered a single 100 mg/kg dose of PF-06827443 and behavioral convulsions were measured for 3 h using the modified Racine scale (0−5). M_1-KO mice treated with PF-06827443 exhibit no behavioral convulsions, suggesting that PF-06827443 induces behavioral convulsions in an M_1-dependent fashion. Compounds were formulated in 10% Tween 80 and delivered intraperitoneally. Data represent mean ± SEM (n = 3 mice per dose).

Discussion

Overactivation of the M_1 mAChR may be detrimental to M_1 PAM efficacy

Over the last decade, multiple M_1 PAMs have demonstrated robust efficacy in reversing cognitive disruptions in preclinical animal models relevant for AD (*41*, *51*, *80*) and schizophrenia (*48*, *49*, *52*, *53*, *81*, *82*). While these findings are very promising, recent studies have revealed that some but not all M_1 PAMs display adverse effects including GI distress and behavioral convulsions in rodents and dogs (*34*, *57*, *62*). Previously, it was demonstrated that the nonselective muscarinic orthosteric agonist pilocarpine induced robust seizures in healthy adult mice and mice in which M_2, M_3, M_4 or M_5 was genetically knocked out (KO) but produced no effect in M_1-KO mice, suggesting that overactivation of the M_1 receptor mediates these adverse effects (*63*, *64*). Therefore, one possibility to account for the stark contrast between M_1 PAMs that produce adverse effects and those that do not is the hypothesis that some M_1 PAMs can overactivate the M_1 receptor and therefore lead to similar adverse effects as traditional orthosteric agonists (*57*, *62*, *65*, *66*). This is reminiscent of studies from allosteric modulators for other GPCRs, such as the metabotropic glutamate receptor subtype 5 ($mGlu_5$), which demonstrated that the presence of allosteric agonist activity of $mGlu_5$ PAMs can results severe behavioral convulsions in rodents (*67*, *73*).

In agreement with this hypothesis, M_1 PAMs such PF-06764427 and MK-7622 demonstrate robust agonist activity in addition to PAM activity (ago-PAM) and when dosed at high concentrations display M_1-dependent behavioral convulsions in rodents (*57*, *62*). This contrasts with two structurally distinct M_1 PAMs, VU0453595 and

VU0550164, optimized to eliminate agonist activity (*57*). Similar to previously described M_1 PAMs, VU0453595 and VU0550164 robustly potentiate responses to ACh (*57*). However, in contrast with PF-06764427 and MK-7622, VU0453595 and VU0550164 lack agonist activity in all assays tested (*57*). Furthermore, both PF-06764427 and MK-7622 induce robust behavioral convulsions in adult mice that were absent in M_1-KO mice, suggesting that overactivation of M_1 is responsible for the ago-PAM-induced behavioral convulsions (*57*). These severe adverse effects were not present at any concentration of VU0453595, an M_1 PAM optimized to avoid allosteric agonist activity (*57*). Finally, VU0453595, but not MK-7622, exhibited robust efficacy in improving object recognition memory in rats (*57*). Together, these studies greatly expand our knowledge into the impact of subtle differences in modes of activity of different M_1 PAMs and the need to strictly avoid allosteric agonist activity in these compounds.

In opposition to the hypothesis that agonist activity is a strong contributor of adverse effect liability was the disclosure of PF-06827443, a highly selective and potent M_1 PAM with weak agonist activity at the human M_1 receptor but which induces severe seizures when administered to dogs (*34*). Based on the relatively weak agonist activity of PF-06827443, the authors suggested that severe adverse effect liability is not dependent on agonist activity of M_1 PAMs. However, this study relied on a single cell line expressing the human M_1 mAChR, and PF-06827443 was not extensively characterized to establish the level of agonist activity of this M_1 PAM in other preclinical systems. Allosteric agonist activity is highly dependent on receptor expression levels (*67*, *79*) and there are documented species differences in the pharmacological profiles for other muscarinic allosteric modulators (*83*, *84*). Since animal models, such as rodent, dog and monkey,

often drive preclinical drug discovery, it is therefore critical to fully assess agonist activity across different levels of receptor expression, in different species, and in native systems to fully evaluate intrinsic agonist activity of M_1 PAMs.

In contrast to their molecular pharmacology findings, we found that PF-06827443 displays robust agonist activity across cell lines expressing rat, dog and human M_1 (*66*). Furthermore, we used an inducible cell line to control M_1 receptor expression and found that PF-06827443 displays agonist activity in systems with moderate to high receptor reserve (*66*). In contrast, VU0550164, an M_1 PAM optimized to avoid ago-PAM activity (*57*) exhibits no agonist activity at any expression level tested. Finally, unlike recently reported M_1 PAMs optimized to eliminate agonist activity (*57*), PF-06827443 displays robust agonist activity in mouse brain slices and induces behavioral convulsions in mice that is similar to other previously described ago-PAMs (e.g. MK-7622 and PF-06764427). Taken together, these findings reveal that PF-06827443 is a robust M_1 ago-PAM and add further support to the hypothesis that intrinsic agonist activity may be a detrimental quality for M_1 PAM clinical candidates.

CHAPTER 3

MULTIPLE MODES OF PAM ACTIVITY

M_1 PAMs that display bias can have differential effects in the CNS

In addition to differences in allosteric agonist activity, M_1 PAMs can also differ in their ability to confer bias to M_1 signaling. Signal bias is the phenomenon by which different GPCR ligands induce distinct active receptor-complex states that are biased toward or away from specific signaling pathways (Fig. 15) (*85*). To date, GPCR signal bias has been well characterized for μ opioid agonists that can signal through G-proteins as well as β-arrestin or both (*86*, *87*). Recent work suggests that μ opioid agonists that avoid β-arrestin activity and preferentially signal through G-proteins can induce analgesia while minimizing respiratory suppression. Recent work suggests that μ opioid receptor agonists that avoid β-arrestin activity and preferentially signal through G-proteins can induce analgesia while minimizing respiratory suppression. Therefore, these biased ligands could provide a larger therapeutic window than fentanyl, which preferentially signals through β-arrestin and produces robust respiratory depression (*88*, *89*). Thus, characterization of potential signal bias in muscarinic ligands may provide opportunities to understand specific signaling pathways involved in efficacy and potentially increase in vivo efficacy while minimizing adverse effect liability.

Characterization of a broad range of structurally diverse M_1 PAMs revealed that some M_1 PAMs confer signal bias and potentiate receptor signaling through the canonical phospholipase C (PLC) pathway, but do not potentiate M_1 receptor–mediated activation of phospholipase D (PLD) (*90*). PLD is a widely expressed enzyme that hydrolyzes the

major plasma membrane phospholipid phosphatidylcholine into the signaling molecules phosphatidic acid (PA) and choline (*91*). PLD can be activated by various receptors, including the M_1 receptor (*92*, *93*). Although there are six distinct mammalian isoforms of PLD, only PLD_1 and PLD_2 have well-established enzymatic activity within the central nervous system (CNS) (*91*, *94*).

However, little is known about the roles of PLD in regulating brain function, and the potential roles of PLD in M_1 receptor–dependent signaling has not been explored. Thus, it is unclear whether M_1 receptor PAMs that do not activate coupling of the receptor to PLD in cell lines will display functional differences in regulating M_1 signaling in the CNS relative to nonbiased M_1 receptor PAMs. For other GPCRs, signal bias provides the exciting potential advantage of selectively activating or potentiating therapeutically relevant pathways while minimizing activation of pathways responsible for adverse effects (*39*, *88*, *95*). Therefore, a better understanding of these signaling mechanisms is essential for the development of M_1 receptor PAMs as potential therapeutics for the treatment of prevalent cognitive disorders.

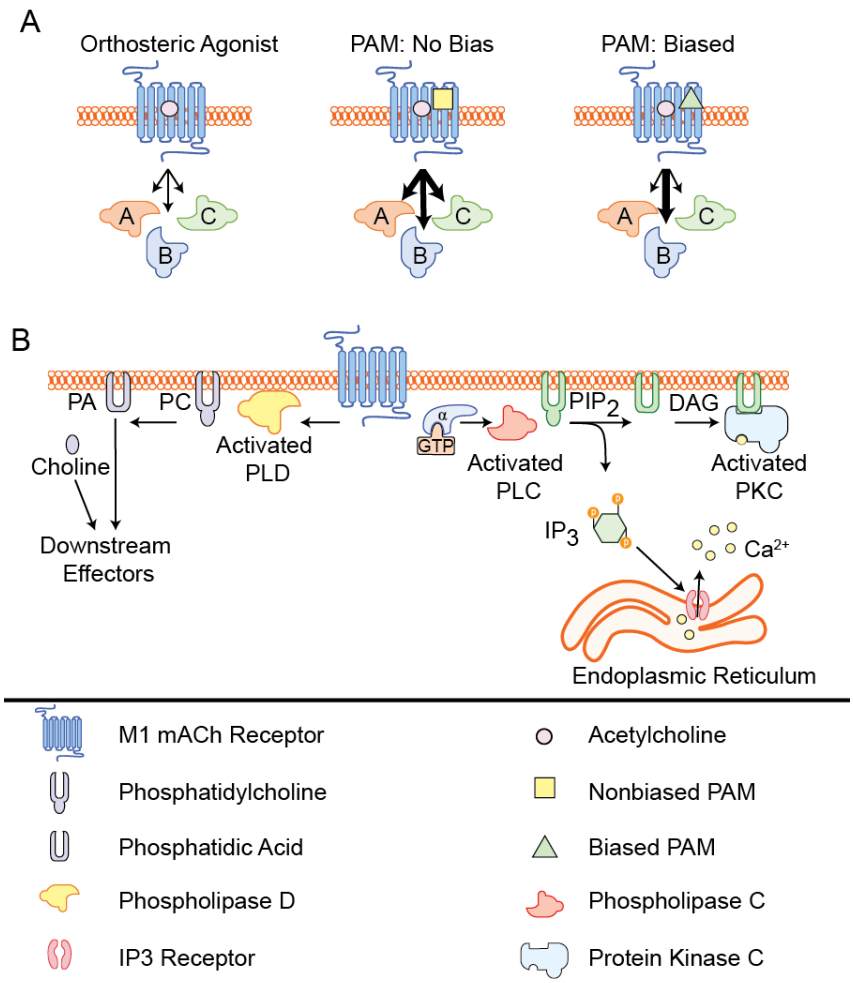

Figure 16: Biased M_1 PAM schematic.
(**A**) Cartoon depicting the effect of biased or nonbiased M_1 PAMs on mAChR signaling. (**B**) Simplified signaling cascade downstream of the M_1 mAChR involving both PLC and PLD.

Here, we report that PLD activity is necessary for a form of M_1 receptor–dependent long-term depression (LTD) in the prefrontal cortex (PFC), which was previously implicated in the potential therapeutic response to M_1 receptor PAMs (*52*, *53*, *96*). Furthermore, biased M_1 PAMs that do not potentiate M_1 receptor coupling to PLD failed to potentiate this form of LTD, but actively inhibited M_1 receptor–dependent LTD at this

synapse. In contrast, biased and nonbiased M_1 receptor PAMs functioned similarly in their ability to potentiate M_1 receptor–dependent responses in the CNS that we found to be PLD-independent. Together, these studies reveal that PLD is a critical downstream signaling node for this M_1 receptor–dependent LTD in the PFC and demonstrate that biased M_1 receptor PAMs can have fundamentally different effects, relative to those of nonbiased M_1 receptor PAMs, in regulating specific aspects of CNS function.

M_1 receptor activation leads to PLD activity in hM_1-CHO cells

M_1 receptor activation leads to an increase in PLD activity (*92*, *93*), but it is not known whether this reflects activation of PLD_1, PLD_2, or both isoforms. Therefore, we characterized the relative contribution of these two distinct PLD isoforms downstream of selective activation of M_1 in Chinese Hamster Ovary (CHO) cells stably expressing the M_1 receptor. Whereas direct measurement of the PLD product PA is challenging due to its rapid conversion into other lipids, such as diacylglycerol and lysophosphatidic acid, in the presence of a primary alcohol, such as 1-butanol, PLD generates the stable product phosphatidylbutanol (pButanol), which cannot be metabolized, and enables quantification of intracellular PLD activity (*91*, *97*, *98*). Consistent with previous findings (*90*), the cholinergic orthosteric agonist carbachol (CCh) induced an increase in pButanol accumulation, which was blocked by the selective M_1 receptor antagonist VU0255035 (Fig. 16A) (*72*). Furthermore, the $PLD_{1,2}$ inhibitor ML299 (*99*) blocked M_1-mediated pButanol production, thereby supporting the hypothesis that PLD was responsible for the generation of pButanol. Using more modern PLD_1 (VU0359595) (*100*) and PLD_2 (VU0364739) (*101*) isoform-selective inhibitors, we found that pharmacological inhibition

of PLD_1, but not PLD_2, blocked the M_1-dependent activation of PLD in this *in vitro* assay (Fig. 16A). These data suggest that in this cell-based assay, M_1-dependent activation of PLD primarily occurs through PLD_1, not PLD_2.

Although we have previously characterized M_1 PAMs that couple to PLC but not PLD (*90*), these early biased M_1 PAMs suffered from low potency and aqueous solubility. Therefore, we optomized additional M_1 PAMs that potentiate M_1 coupling to PLC, but do not potentiate coupling to PLD. Previously, we reported that the M_1 PAMs VU0453595 ((EC_{50}) = 2140 ± 440 nM), VU0405652 (EC_{50} = 2580 ± 440 nM), and VU0405645 (EC_{50} = 340 ± 30 nM) are potent M_1 PAMs with respect to their ability to potentiate Ca^{2+} mobilization in CHO cells stably expressing the M_1 receptor (Fig. 16, B and C) (*52*, *102*). We now report that unlike the prototypical M_1 PAM VU0453595, both VU0405652 and VU0405645 failed to potentiate the CCh-dependent activation of PLD in this *in vitro* assay (Fig. 16D). These findings demonstrate that VU0405652 and VU0405645, but not VU0453595, are biased M_1 receptor PAMs that do not potentiate M_1 coupling to PLD.

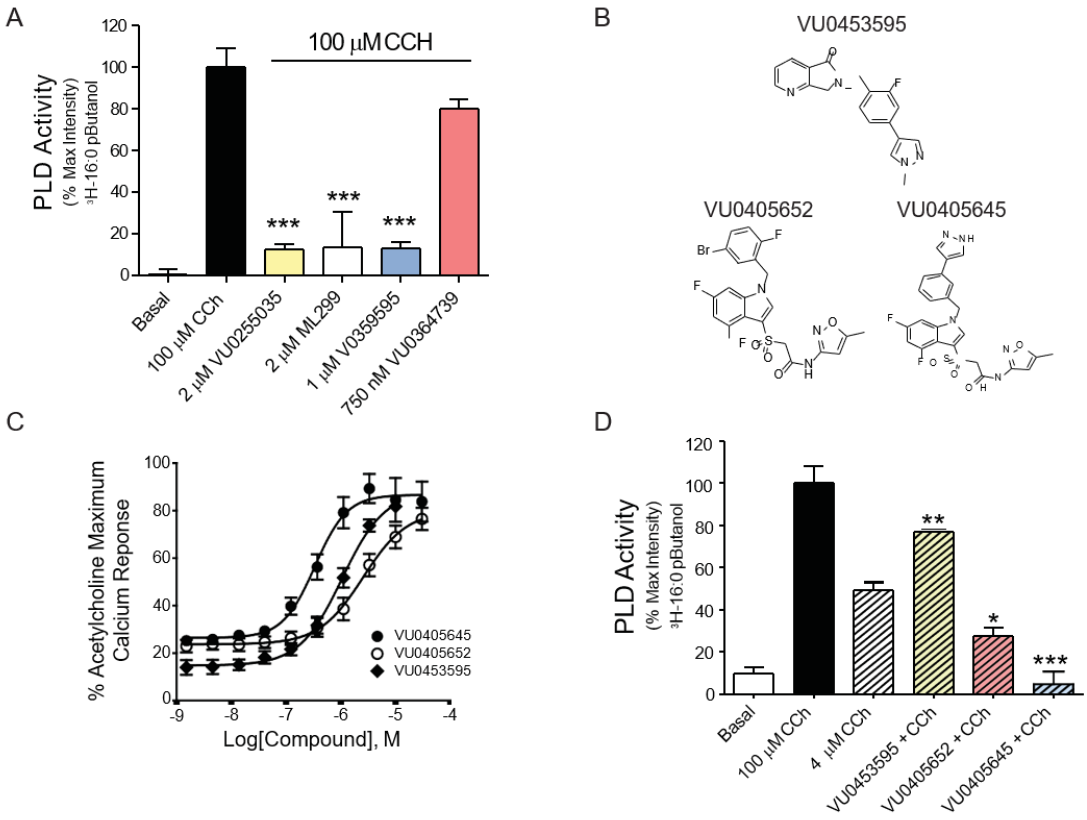

Figure 17: M_1 receptor activation leads to PLD activity in hM_1-CHO cells, and M_1 PAMs show differential signal bias in potentiating M_1-mediated PLD signaling.
(**A**) rM_1 CHO cells were treated with DMSO (basal) or 100 μM CCh alone or in combination with 2 μM VU0255035 (M_1 antagonist), 2 μM ML299 ($PLD_{1,2}$ inhibitor), 1 μM VU0359595 (PLD_1 inhibitor), or 750 nM VU0364739 (PLD_2 inhibitor). PLD activity was measured by quantification of the PLD product pButanol. The extent of PLD activity in response to 100 μM CCh alone was set at 100%. The effects of the M_1 receptor antagonist or various pharmacological inhibitors of PLD were compared to the maximal effect elicited by 100 μM CCh (one-way ANOVA $F_{4,10} = 29.34$; $P = 0.0001$, with a post-hoc Dunnett's test using 100 μM CCh alone as the control group, ***$P < 0.001$). (**B**) Structures of the M_1 receptor PAMs VU0453595, VU0405652, and VU0405645. (**C**) rM_1-CHO cells were treated with an EC_{20} concentration of acetylcholine in the presence of the indicated concentrations of VU0453595, VU0405652, and VU0405645 and then were assayed for Ca^{2+} signaling by using the Functional Drug Screening System (FDSS7000). (**D**) Using rM_1 CHO cells under the same conditions described above, the extent of PLD activation relative to a maximal response of 100 μM CCh alone was evaluated for 4 μM CCh in the presence of DMSO, 10 μM VU0453595, 10 μM VU0405652, or 10 μM VU0405645 (one-way ANOVA $F_{3,8} = 55.1$; $P = 0.0001$, with a post-hoc Dunnett's test using 4 μM CCh *$P < 0.05$, **$P < 0.01$, ***$P < 0.001$). Data in (A), (C), and (D) are means ± SEM from three independent experiments each performed in triplicate.

PLD_1, but not PLD_2, is required for M_1 receptor–mediated LTD in the mPFC

While these cell-based studies demonstrated that M_1 receptor activation can increase PLD activity, little is known about whether PLD is necessary for M_1-dependent responses in native neuronal tissue. Therefore, we characterized the role of PLD in mediating established responses to M_1 receptor activation in CNS preparations. One response to M_1 receptor activation that may be relevant to some aspects of cognitive function is induction of long-term depression (LTD) of excitatory synaptic transmission in the medial prefrontal cortex (mPFC) (*52*, *53*, *57*, *65*, *71*, *96*). We assessed the role of PLD in inducing LTD in the mPFC by measuring changes in layer V field excitatory postsynaptic potentials (fEPSP) evoked by electrical stimulation of afferents in layer II/III of the mPFC (Fig. 17A). Consistent with previous findings (*52*, *53*, *65*, *71*), a maximal concentration of CCh induced robust LTD of fEPSP slope at this synapse (Fig. 17B). In order to test whether PLD is required for CCh-induced LTD, we bath applied the $PLD_{1,2}$ inhibitor ML299 for 10 min before and throughout CCh application which resulted in a complete loss of CCh-induced LTD (Fig. 17C). Using selective inhibitors for each PLD isoform, we found that pharmacological inhibition of PLD_1 with VU0359595 fully blocked CCh-induced LTD (Fig 17D). Congruent with the cell-based assay findings, inhibition of PLD_2 with VU0364739 had no effect on CCh-induced LTD at this synapse (Fig. 17E). Quantification of fEPSP slope 46–50 min following drug washout indicated that ML299 and VU0359595 significantly attenuated CCh-induced LTD whereas inhibition of PLD_2 with VU0364739 had no significant effect (Fig. 17F).

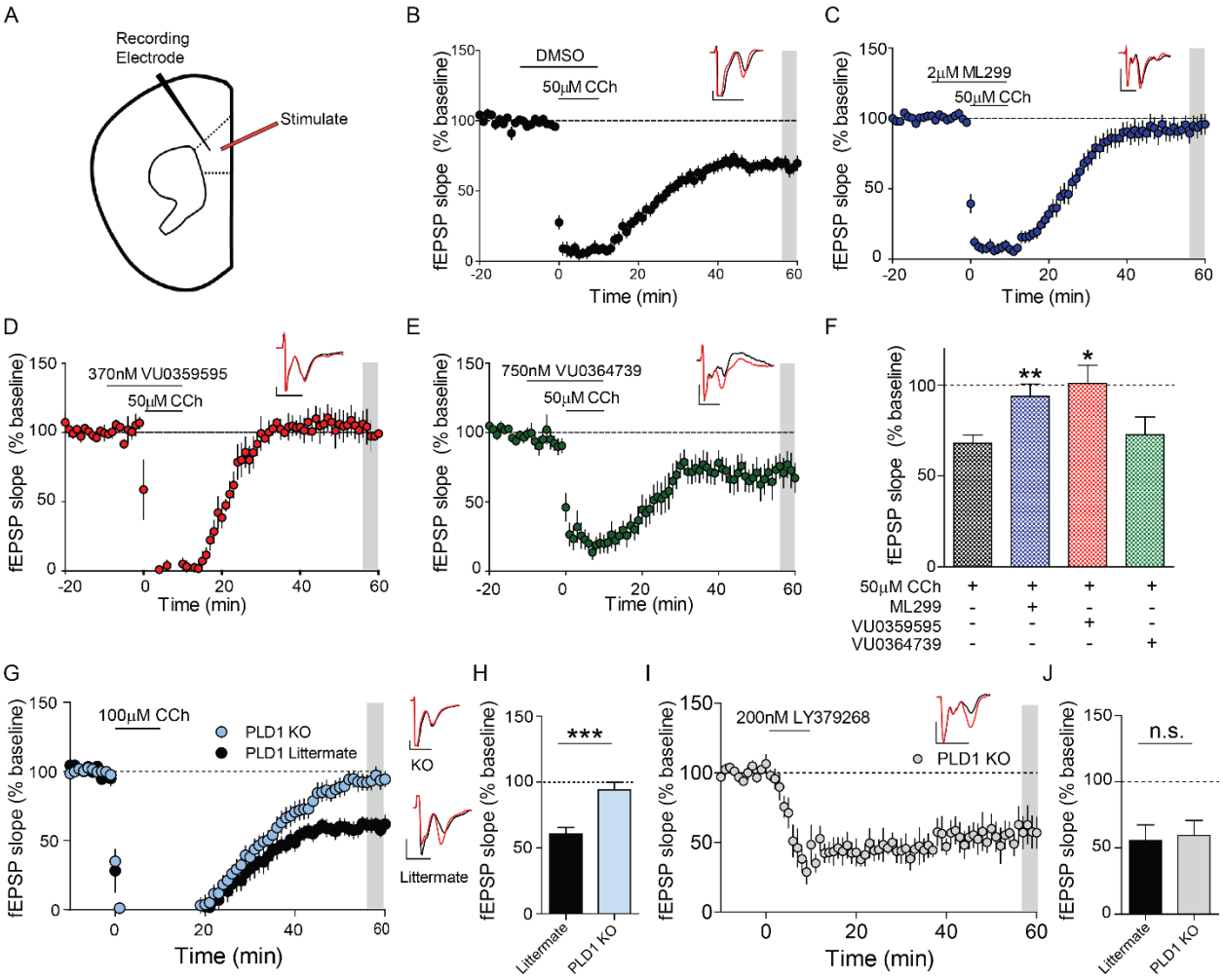

Figure 18: PLD_1 but not PLD_2, is necessary for CCh-dependent LTD in the mPFC. (**A**) Schematic of the field excitatory post-synaptic potentials (fEPSP) recorded from layer V of the mouse mPFC in response to electrical stimulation in the superficial layers II–III. (**B**) Time course graph for fEPSP slope normalized to the average baseline. 50 μM carbachol (CCh) induces a long-term depression of fEPSP slope (68.0 ± 4.44%, n/N= 26/20 slices/mice). (**C**) Time course graph for fEPSP slope with 10 min pretreatment of the $PLD_{1,2}$ inhibitor ML299 (2 μM), followed by a 10 min co-application of ML299 and 50 μM CCh (93.8 ± 6.74%, n/N= 21/10). (**D**) Time course graph for fEPSP slope normalized to baseline with 10 min pretreatment of the PLD_1-specific inhibitor VU0359595 (370 nM) and 10 min co-application of 50 μM CCh (101 ± 10.1%, n/N= 7/6). (**E)** Time course graph for fEPSP slope normalized to baseline with 10 min pretreatment of the PLD_2 selective inhibitor VU0364739 (750 nM) and 10 min co-application of 50 μM CCh (69.3 ± 13.0, n/N= 8/4). Inset shows representative fEPSP traces for each condition for baseline (red trace) and 50 min after CCh washout (black trace). (**F**) Quantification of the average fEPSP slope 46–50 min following drug washout (shaded area) (one-way ANOVA $F_{3,58} = 5.21$; P = 0.0029, with a post-hoc Dunnett's test using 50 μM CCh alone as the control group, *P < 0.05, **P < 0.01). (**G**) Left: Time course graph of fEPSP slope normalized to baseline

with bath application of CCh (100 μM) in littermate controls (59.6 ± 6.06 n/N= 9/6) and PLD_1 KO mice (92.2 ± 3.21, n/N= 9/6). Right: representative fEPSP traces for baseline (red trace) and 50 min after CCh washout (black trace) for PLD_1 KO animals (Top) and littermate controls (Bottom). (**H**) Quantification of the average fEPSP slope 46–50 min following drug washout (shaded area) (Student's t-test; P = 0.0002, ***P < 0.001). (**I**) Time course graph for fEPSP slope normalized to baseline with 10 min bath application of group II metabotropic glutamate receptor agonist LY379268 (200 nM) in PLD_1 KO mice (59.4 ± 11.4%, n/N = 5/3). (**J**) Quantification of the average fEPSP slope 46–50 min following LY379268 (200 nM) washout (shaded area) for PLD_1 KO mice and littermate controls (55.7 ± 11.6%, n/N = 7/3; Student's t-test; P = 0.828). Inset shows representative fEPSP traces for each condition for baseline (red trace) and 50 min after LY379268 washout (black trace). Scale bars denote 0.25 mV and 5 ms. Data are expressed as mean ± SEM.

To confirm these pharmacological results, we obtained PLD_1 knockout (KO) mice and subsequently confirmed that PLD_1 expression is reduced in cortical tissue compared to littermate controls (Fig. 18). In agreement with the pharmacological findings, CCh induced a robust LTD in slices obtained from littermate controls but not from PLD_1 KO mice (Fig. 17G, H). Importantly, the ability of a selective agonist of group II metabotropic glutamate receptors (LY379268) to induce LTD was intact in the PLD_1 KO mice and not significantly different than littermate controls (Fig. 17 I, J). This form of LTD has been previously characterized in detail and is mechanistically distinct from M_1-dependent LTD in the mPFC (*103–105*). Furthermore, input-output curves generated by comparing fiber volley slope to fEPSP slope (Fig. 19A) did not appear to differ between genotypes (Fig. 19B). These data together suggest that the loss of M_1-mediated LTD is not due to a general deficit in LTD in this brain region. Taken together, these data demonstrate a critical role of PLD, specifically PLD_1, in this form of cortical M_1-LTD.

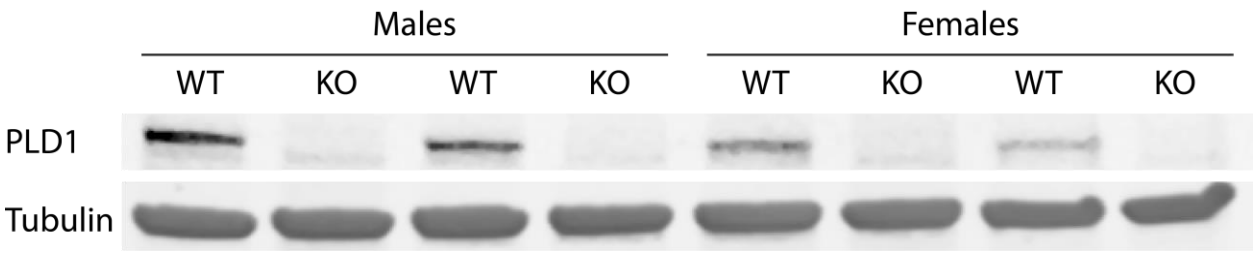

Figure 19: Western blot validation of PLD_1 KO mice.
Total protein from cortex was probed with a PLD_1 specific antibody (Cell Signaling Technology #3832). The immunoreactive band corresponding to PLD_1 (~120 kDa) was absent in samples from KO mice.

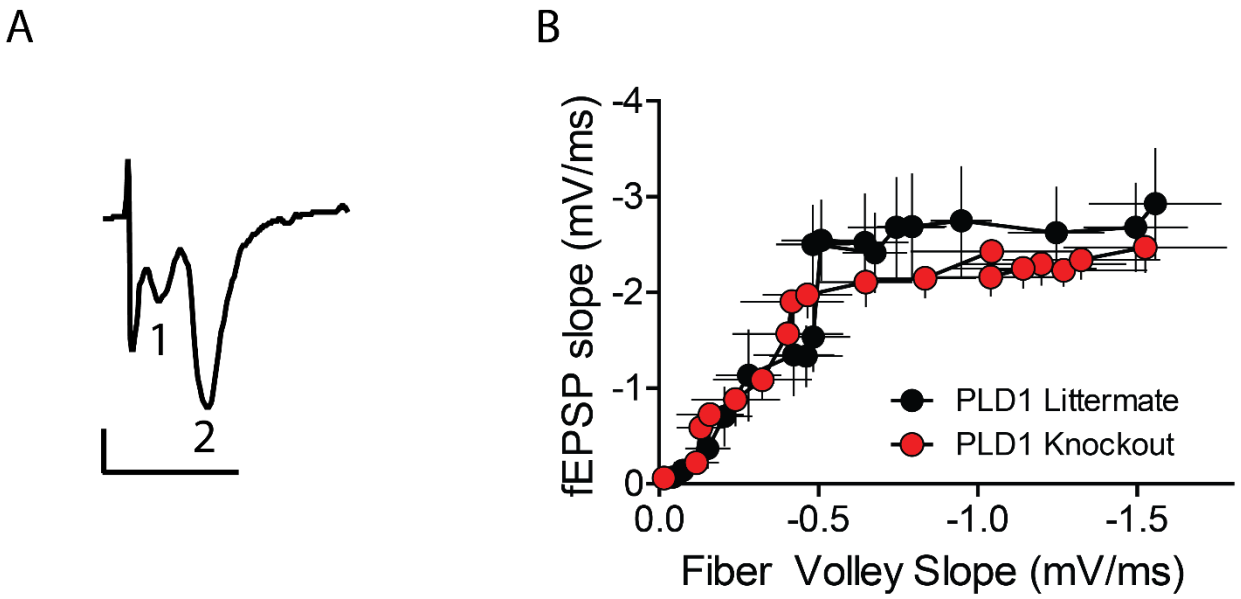

Figure 20: Input/output relationship of fEPSPs compared to fiber volley from PLD_1 KO mice and littermate controls.
(**A**) Representative sample trace generated from electrical stimulation of layer II/II and recording in layer V of the mPFC. 1: corresponds to the fiber volley and 2: corresponds to the fEPSP. Scale bars denote 0.5mV and 5 ms. (**B**) The fiber volley slope was plotted against fEPSP slope from PLD_1 littermates (n=12/N=3 slices/mice, black) and PLD_1 KO mice (n=10/N=2, red). Data are expressed as mean ± SEM.

Biased M_1 receptor PAMs fail to potentiate M_1 receptor–dependent LTD in the mPFC

We next tested the hypothesis that biased and non-biased M_1 receptor PAMs would display functional differences in their ability to potentiate this PLD-dependent CCh-induced LTD of layer V fEPSPs electrically evoked in layer II/III in the mPFC. As previously shown, a submaximal concentration of CCh (10 μM) does not induce LTD at this synapse (Fig. 20A) (*52*, *57*, *65*). Similar to previous findings, bath application of the non-biased M_1 receptor PAM VU0453595 for 10 min before and during CCh application lead to a robust LTD (Fig. 20B). Consistent with a role of PLD in inducing M_1-LTD, neither of the biased M_1 receptor PAMs, VU0405652 (Fig. 20C) nor VU0405645 (Fig. 20D), potentiated the LTD response to a submaximal concentration of CCh. Quantification of fEPSP slope following drug washout indicated a significant depression of fEPSP slope compared to baseline with the M_1 receptor PAM VU0453595 but not VU0405652 nor VU0405645 (Fig. 20E).

Theoretically, M_1 receptor PAMs that confer this form of biased M_1 receptor signaling stabilize a conformation of M_1 receptor that favors activation of signaling by PLC and not PLD (*22*, *85*, *106*, *107*). If correct, these PAMs confer true bias to M_1 signaling, and should inhibit PLD-mediated responses. Thus, we tested the hypothesis that PAMs that bias M_1 receptor signaling away from PLD would block the LTD normally induced by a maximal concentration of CCh (Fig. 20F). In agreement with our hypothesis, both VU0405645 (Fig. 20F) and VU0405652 (Fig. 20G, H) blocked CCh-induced LTD (Fig. 20H). Collectively, these findings demonstrate a role of PLD in this cortical M_1-LTD and

show that biased M_1 receptor PAMs not only fail to potentiate a submaximal concentration of CCh-LTD, but can also actively block a maximal concentration of CCh-LTD.

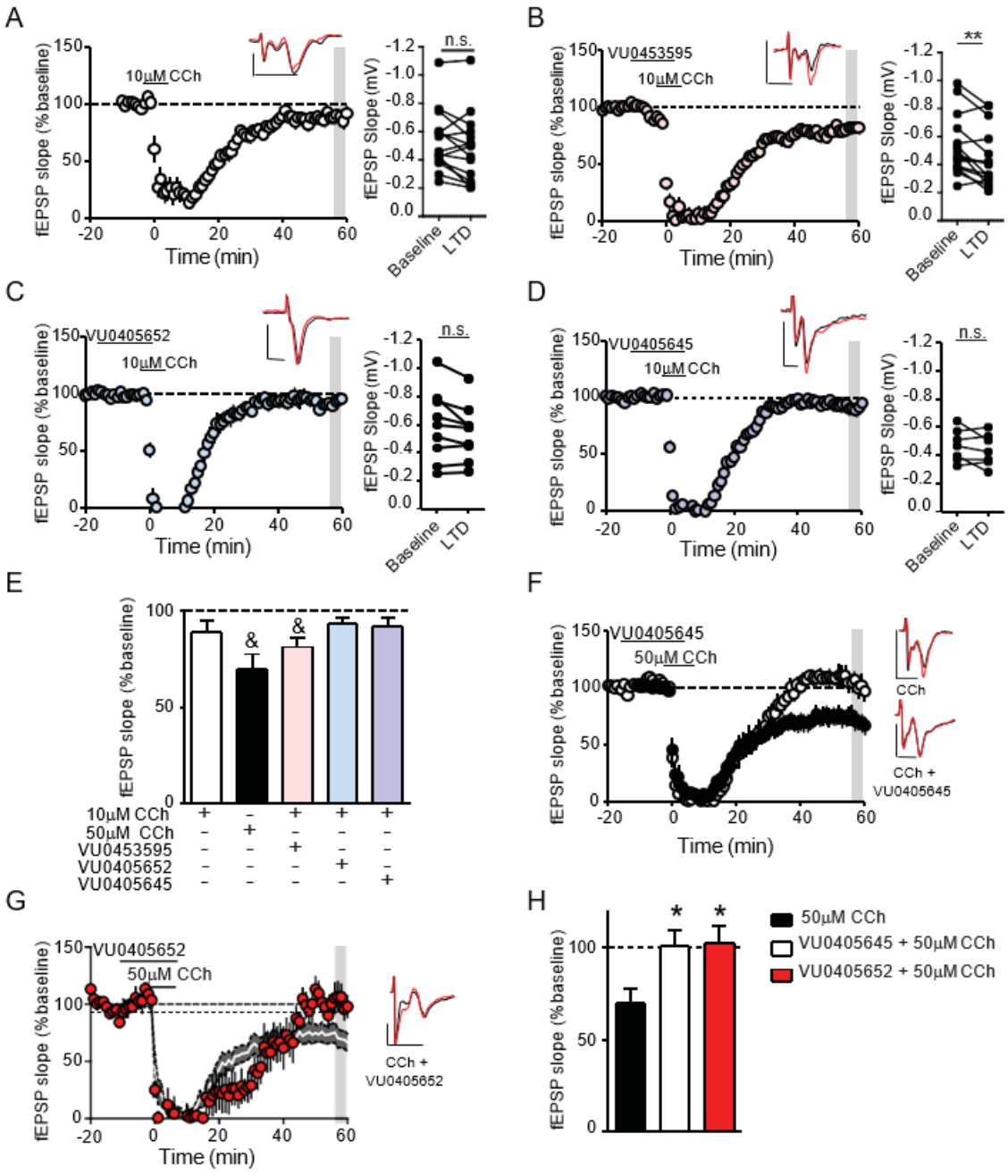

Figure 21: Biased M_1 PAMs fail to potentiate a submaximal mLTD in the mPFC and actively block CCh-dependent LTD.
(**A**) Left: Time course graph for fEPSP slope normalized to the average baseline. Right: Comparison of fEPSP slope during baseline and 46-50 min after carbachol (10 μM, CCh) washout (shaded area). 10 min bath application of CCh (10 μM) induces a minimal long-term depression (LTD) of fEPSP slope (88.9 ± 6.05, n/N= 15/13 slices/mice; paired t-test; p > 0.05). (**B**) 10 min pretreatment of the nonbiased M_1 PAM VU0453595 (10 μM), followed by a 10 min co-application of VU0453595 + CCh (10 μM) (81.5 ± 4.70%, n/N= 14/11; paired t-test P = 0.01). (**C**) 10 min pretreatment of the biased M_1 PAM VU0405652 (10 μM), followed by a 10 min co-application of VU0405652 + 10 μM CCh (93.5 ± 3.28%, n/N= 9/8; paired t-test; P > 0.05). (**D**) 10 min pretreatment of the biased M_1 PAM VU0405645 (10 μM), followed by a 10 min co-application of VU0405645 + CCh (10 μM) (91.9 ± 4.67%, n/N= 7/7; paired t-test; P > 0.05). Insets contain representative fEPSP traces for each condition for baseline (red trace) and 50 min after CCh washout (black trace), scale bars denote 0.5 mV and 5 ms and data are expressed as mean ± SEM. **P ≤ 0.01. (**E**) Summary of the last 5 min of the recordings from the time course experiments (& = P < 0.05, paired t-test). (**F**) Left: Time course graph for fEPSP slope normalized to the average baseline. CCh (50 μM, black) (70.0 ± 7.78%, n/N= 9/7) alone compared to 10 min pretreatment with VU0405645 (10 μM) and 10 min co-application of CCh (50 μM, white) (101 ± 8.59%, n/N= 11/8). Right: representative fEPSP traces for each condition for baseline (red trace) and 50 min after CCh washout (black trace), scale bars denote 0.5 mV and 5 ms. (**G**) Time course graph of normalized fEPSP slope of 10 min pretreatment VU0405652 (75 μM) and 10 min co-application of CCh (50 μM, red) (102 ± 9.46%, n/N= 7/3) compared to CCh alone (shaded time course correspond to CCh (50 μM) from the previous panel; the solid, white line represents the mean fEPSP slope and the gray-shaded region around the line shows ± SEM). (**H**) Quantification of the average fEPSP slope 46–50 min following CCh washout (shaded area) (one-way ANOVA $F_{3,25}$ = 4.554; p = 0.0216, with a post-hoc Dunnett's test using CCh alone as the control group, * P < 0.05).

PLD is not necessary for the M_1 receptor–dependent increase of layer V sEPSC in the mPFC

In light of these findings, we next set out to determine whether PLD is important in other M_1-dependent functions in the CNS. Previously, we reported that M_1 receptor activation increases the frequency of spontaneous excitatory postsynaptic currents (sEPSC) in mPFC layer V pyramidal neurons (*46*, *52*, *57*). In agreement with these previous findings, bath application of a maximal concentration of CCh induced a robust

increase in sEPSC frequency in layer V pyramidal neurons (Fig. 21A). In contrast to M_1-dependent LTD, the effect of CCh on sEPSCs was unchanged by pretreatment and co-application of the dual PLD inhibitor ML299 (Fig. 21B). Quantification of the peak CCh effect on sEPSC frequency indicated no statistically significant difference between CCh alone and CCh in the presence of ML299 (Fig. 21C). These data suggest that PLD is not necessary for this M_1-dependent increase of sEPSC frequency in mPFC layer V pyramidal neurons.

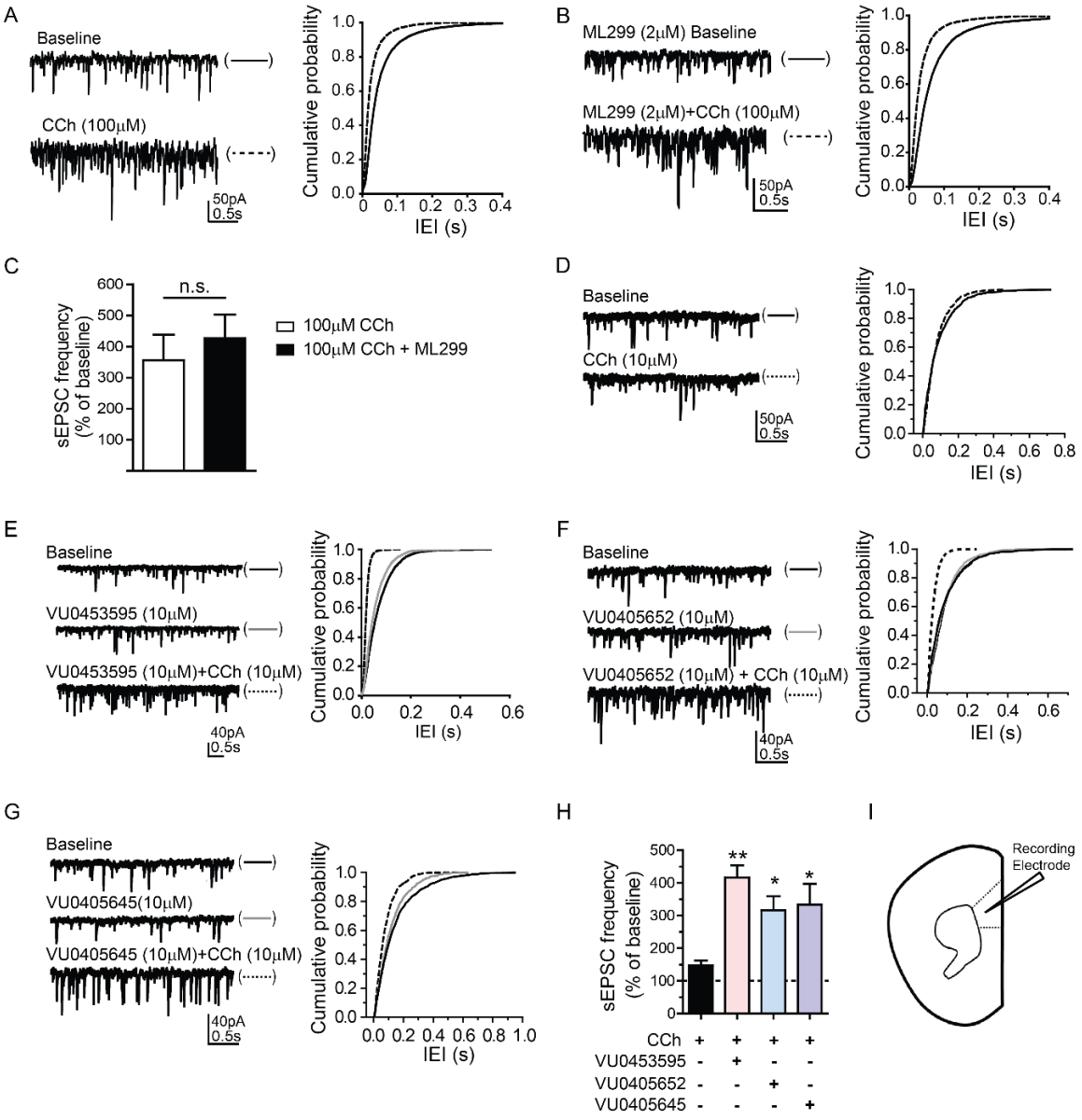

Figure 22: PLD is not required for the M_1-dependent increase in sEPSC frequency in mPFC layer V pyramidal neurons, and both biased and nonbiased M_1 PAMs potentiate this response.
(**A**) Sample traces (left) and the cumulative probability of interevent interval (IEI) (right) of sEPSCs in baseline) during application of CCh (100 µM) as indicted for a typical cell. (**B**) Sample traces (left) and the IEI cumulative probability (right) of sEPSCs in baseline with $PLD_{1,2}$ inhibitor ML299 (2 µM) and during application of a combination of ML299 and CCh (100 µM) for a typical cell. (**C**) Quantification of the average increase in sEPSC frequency between CCh alone (357.0 ± 81.6%, n/N = 7/3 cells/animals) and CCh in the presence of ML299 (427.0 ± 76.5%, n/N = 8/3) (Student's t-test; $P > 0.05$). (**D**) Sample traces (left) and IEI cumulative probability (right) of sEPSCs in baseline and during application of CCh (10 µM) from a typical cell. (**E** to **G**) Sample traces (left) and IEI cumulative probability (right) of sEPSCs in baseline, during application of a PAM) and the PAM with CCh as indicated for typical cells are shown. (**H**) Quantification of the peak effect on sEPSC frequency for CCh (10 µM) alone (147 ± 15.4%, n/N = 7/3), CCh with VU0453595 (10 µM) (416 ± 38.2%, n/N = 8/4), CCh with VU0405652 (10 µM) (316 ± 43.3%, n/N = 10/5), and CCh with VU0405645 (10 µM) (332.4 ± 63.7%, n/N = 11/4). one-way ANOVA $F_{3,35} = 5.77$; $P = 0.0026$, with a post-hoc Dunnett's test using CCh alone as the control group, *$P < 0.05$, **$P < 0.01$. Data are expressed as mean ± SEM. (I) Schematic of whole-cell recordings from mPFC layer V pyramidal neurons (regular spiking cells) clamped at −70 mV.

Next, we sought to compare the two biased M_1 receptor PAMs, VU0405652 and VU0405645, to our prototypical M_1 receptor PAM, VU0453595, in their ability to potentiate a submaximal concentration of CCh-induced increases in mPFC layer V pyramidal neuron sEPSC frequency. As expected, bath application of a submaximal concentration of CCh did not induce a significant change in sEPSC frequency (Fig. 21D). Similar to the M_1 receptor PAM BQCA (*46*), the non-biased M_1 receptor PAM VU0453595 induced a robust potentiation of the effect of a submaximal concentration of CCh on sEPSC frequency (Fig. 21E) and this effect was attenuated by pharmacological inhibition of PLC with the PLC inhibitor U73122 (Fig. 22A-D). Consistent with the studies with PLD inhibitors, both VU0405652 (Fig. 21F) and VU0405645 (Fig. 21G) potentiated agonist-induced increases in sEPSC frequency. Quantification of the peak effect on sEPSC

frequency indicated a statistically significant difference between CCh alone and all three M_1 receptor PAMs (Fig. 21H). Therefore, both biased and non-biased M_1 receptor PAMs function similarly in their ability to potentiate a submaximal concentration of agonist-induced increases in mPFC layer V pyramidal neuron sEPSC frequency (Fig. 21I).

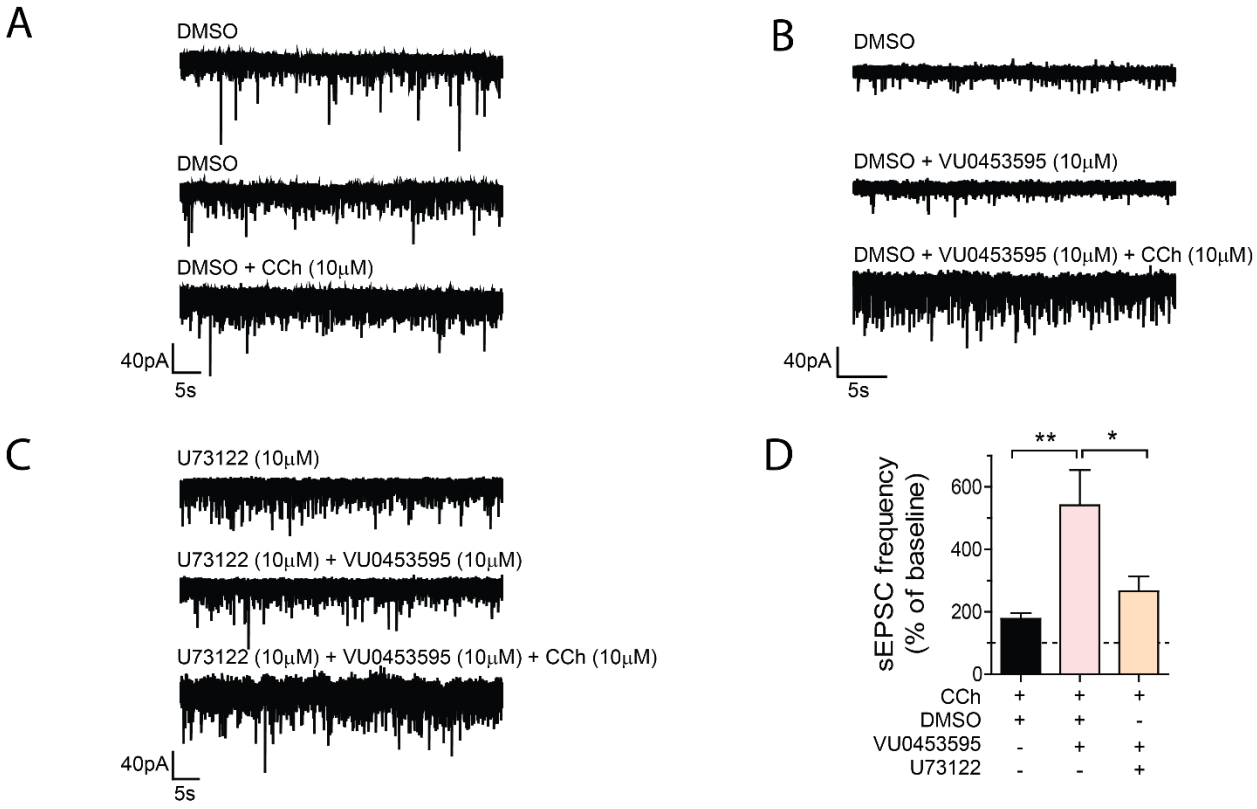

Figure 23: M_1 receptor PAM potentiation of CCh-induced increases in mPFC layer V pyramidal neuron sEPSC frequency is phospholipase C dependent.
(**A**) Sample traces during bath application of CCh (10 µM) in the presence of DMSO ACSF for a typical cell. (**B**) Sample trace during bath application of DMSO ACSF, VU0453595 (10 µM) + DMSO ACSF then VU0453595 (10 µM) + CCh (10 µM) + DMSO ACSF for a typical cell. (**C**) Sample trace during bath application of U73122 (10 µM), U73122 (10 µM) + VU0453595 (10 µM) then U73122 (10 µM) + VU0453595 (10 µM) + CCh (10 µM). (**D**) Quantification of the peak effect on sEPSC frequency for CCh (10 µM) in the presence of DMSO (177.5 ± 19.0%, n/N = 6/3), CCh + VU0453595 (10 µM) + DMSO (542.0 ± 112.3%, n/N = 7/3), CCh + VU0453595 (10 µM) + U73122 (10 µM) (265.9 ± 47.2%, n/N = 7/3. one-way ANOVA $F_{3,19} = 6.467$; P = 0.0082, with a post-hoc Dunnett's test using VU0453595 (10 µM) + CCh (10 µM) in the presence of DMSO ACSF as the control group, *P < 0.05, **P < 0.01. Data are expressed as mean ± SEM.

PLD is not necessary for the effects of the M_1 receptor on the excitability of striatal SPNs

The M_1 receptor is also highly expressed in the striatum (*34*), and we have shown that M_1 receptor activation in spiny projection neurons (SPN) in the dorsal lateral striatum leads to a robust increase in SPN excitability that can be blocked by a selective M_1 receptor antagonist (*70*, *108*). Therefore, we set out to determine whether PLD is required for this M_1-dependent response. As expected, bath application of CCh induced a robust increase in dorsal lateral striatum SPN excitability (Fig. 23A). In the presence of the dual PLD inhibitor ML299, CCh still induced a marked increase in SPN excitability compared to baseline (Fig. 23B). Quantification of the CCh-induced increase in SPN excitability showed no significant difference between the change in number of spikes per pulse between control (DMSO) and ML299 groups (Fig. 23C). Therefore, similar to the sEPSC findings, PLD is not necessary for M_1-dependent increases in dorsal lateral SPN excitability.

The finding that PLD is not involved in M_1 receptor regulation of SPN excitability suggests that biased M_1 receptor PAMs that selectively potentiate coupling to PLC and do not potentiate PLD activity would function similarly to non-biased M_1 receptor PAMs in their ability to potentiate responses to a low concentration of CCh on SPN excitability. In agreement with our previous findings (*108*), a submaximal concentration of CCh induced a minimal increase in SPN excitability (Fig. 23D) that was robustly potentiated by the prototypical M_1 receptor PAM VU0453595 (Fig. 23E). As expected, both VU0405652 (Fig. 23F) and VU0405645 (Fig. 23G) potentiated a submaximal concentration of CCh-induced increase of SPN excitability. The maximal increase in the number of spike discharges

during agonist application was significantly higher in the presence of each of the three M_1 receptor PAMs compared to the DMSO control condition (Fig. 23H-I). Interestingly, in these studies the concentration of VU0453595 used induced a more robust effect than did these concentrations of VU040652 or VU0405645. However, based on the current results, it is unclear whether the concentrations used provide a maximal effect on SPN excitability. Thus, it is not clear whether this apparent difference represents differences in relative efficacies of the different PAMs or differences in slice penetration and final concentrations at the M_1 receptor. However, these results demonstrated that biased and non-biased M_1 receptor PAMs function similarly in their ability to potentiate M_1-dependent regulation of SPN excitability and other CNS responses that are PLD-independent.

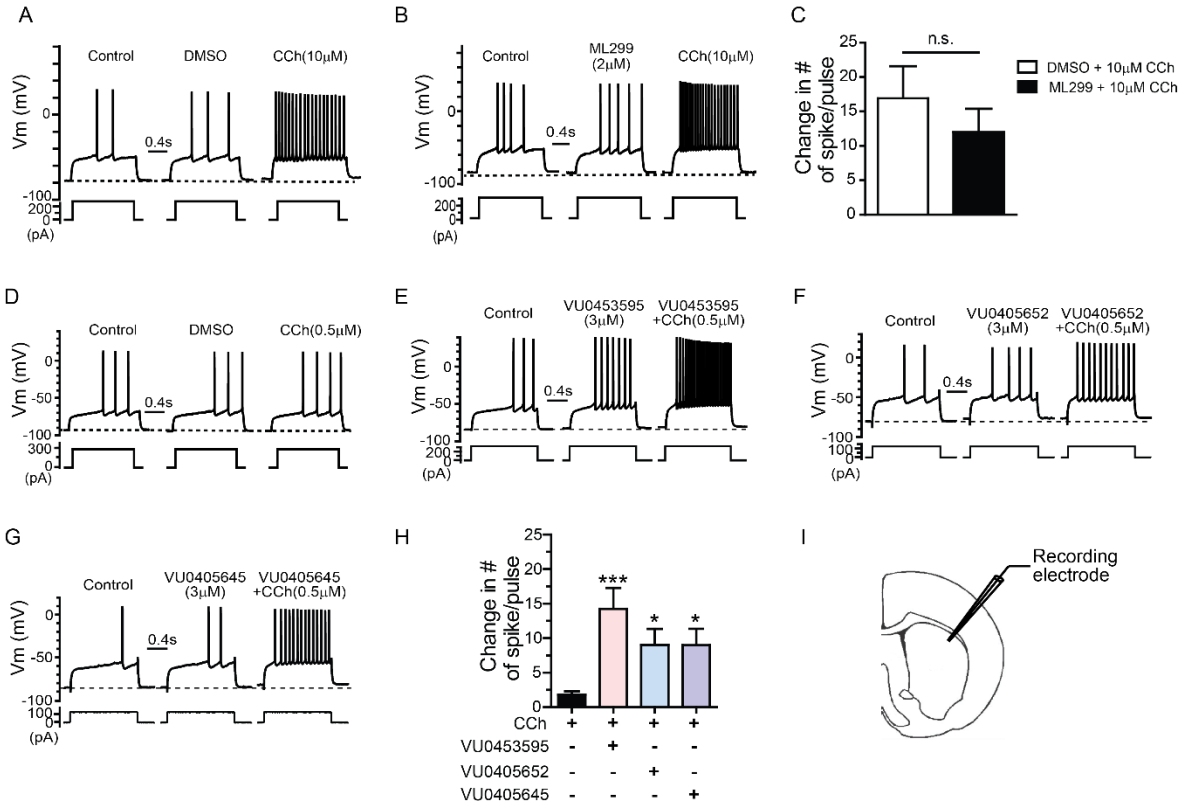

Figure 24: PLD is not necessary for M_1-dependent effects on the excitability of striatal SPNs, and both biased and nonbiased M_1 PAMs potentiate this response. (**A**) Sample traces of membrane potential responses to a depolarization current step from an SPN during baseline, in the presence of DMSO and CCh (10 μM). (**B**) Effect of pretreatment of ML299 (2 μM) then co-application of carbachol on SPN excitability (10 μM). (**C**) Bar graph summarizing the changes in the number of spikes per pulse after CCh (10 μM) application in presence of ML299 (12.0 ± 3.38, n/N = 6/5 cells/animal) or DMSO (16.9 ± 4.67, n/N = 5/5) shows no significant difference between groups (Student's t-test; P > 0.05). (**D** to **G**) Sample traces of membrane potential responses to a depolarization current step from an SPN during baseline, in the presence of M_1 PAM (3 μM) or DMSO, then M_1 PAM/DMSO + CCh (0.5 μM). (**H**) Bar graph summarizing the change in the number of spikes per pulse after CCh (0.5 μM) application in presence of DMSO (1.83 ± 0.49, n/N = 9/7), VU0453595 (14.2 ± 3.05, n/N = 6/6), VU0405652 (9.02 ± 2.31, n/N = 7/6) and VU0405645 (9.00 ± 2.37, n/N = 6/5) (one-way ANOVA $F_{3,24} = 6$; P = 0.0017, with a post-hoc Dunnett's test using CCh + DMSO as the control group, *P < 0.05, ***P < 0.001). Data are expressed as mean ± SEM. (**I**) Schematic of whole-cell recordings from SPN neurons under current clamp conditions performed in the DLS.

Discussion

A large body of clinical and preclinical research suggests that enhancing mAChR signaling can be efficacious in the treatment of the cognitive symptoms associated with Alzheimer's disease and schizophrenia (*17*, *19*, *109*, *110*). Although multiple mAChR subtypes are involved in the regulation of cognitive function, most preclinical studies point to a dominant role of the M_1 receptor and suggest that its selective modulation may provide a therapeutic potential for the treatment of these devastating cognitive symptoms (*36*, *41*, *46*, *48*, *49*, *52*, *53*, *55*, *57*, *76*, *80*, *82*, *111*). However, M_1 receptors regulate CNS function by actions on multiple signaling pathways, and M_1 receptor PAMs can display a diverse range of pharmacological properties, including signal bias. At present, little is known about the specific signaling pathways involved in the different physiological effects of M_1 receptor activation and how signal bias can affect the PAM-mediated modulation of M_1 receptor actions in identified brain circuits.

The present studies improve our understanding of at least one mechanism by which M_1 receptor activation leads to plasticity changes within a key cortical structure in the CNS. Specifically, we found that a previously described M_1-dependent LTD in the cortex was dependent on the activation of PLD. Furthermore, we identified M_1 receptor PAMs that selectively enhanced M_1 receptor coupling to PLC but not PLD, and found that these biased M_1 receptor PAMs failed to potentiate this form of M_1-dependent LTD. Finally, these biased M_1 receptor PAMs actively blocked the ability of mAChR agonists to induce this PLD-dependent LTD, consistent with the hypothesis that these PAMs stabilize a conformation of the M_1 receptor that favors activation of PLC over PLD and thereby bias M_1 receptor signaling in favor of PLC-mediated responses. Furthermore, not all M_1-

dependent responses were PLD-dependent, and biased M_1 receptor PAMs functioned similarly to nonbiased M_1 PAMs in M_1 signaling that was PLD-independent.

Although the ability of the M_1 receptor and other GPCRs to activate PLD is well established (*112*), little is known about the physiological roles of PLD in regulating CNS function. This has largely been due to the lack of selective inhibitors and other tools that enable systematic studies of PLD-mediated responses. However, the discovery of the highly selective PLD inhibitors used here (*99–101*), together with the generation of PLD KO mice and the biased M_1 receptor PAMs reported in the present studies, provided an unprecedented opportunity to determine the roles of PLD in mediating specific responses to M_1 receptor activation. With the availability of these new tools, these studies provide an example of a specific physiological role of PLD in mediating a response to GPCR activation in the CNS and reveal a previously uncharacterized role for PLD in the induction of major form of synaptic plasticity in an identified brain circuit. Furthermore, these PLD inhibitors include selective inhibitors of PLD_1 and PLD_2, the major isoforms of PLD expressed in the CNS. Experiments with these isoform-selective inhibitors, together with PLD_1 KO mice, revealed a critical role for PLD_1 as the PLD isoform involved in mediating this response to M_1 receptor activation.

M_1-dependent LTD in the mPFC has been extensively studied and has been postulated to play a critical role in regulating specific inputs to the mPFC from the hippocampus and other extrinsic afferents (*58*, *113*). Cholinergic regulation of these inputs is thought to be important for the regulation of multiple aspects of mPFC function and previous studies suggest that M_1 receptor expression and signaling in the mPFC can be impaired in some pathological states that could be relevant for schizophrenia and

Alzheimer's disease (*52*, *53*, *114–121*). However, very few studies have focused on understanding the cellular mechanisms underlying M_1-dependent LTD in the PFC. Although the current studies identify PLD_1 as being critically important in M_1-dependent cortical synaptic plasticity, the detailed molecular mechanism by which the M_1 receptor signals through PLD to induce synaptic plasticity changes in the cortex remains unknown. Rigorous molecular and biochemical studies to elucidate this signaling pathway are necessary to fully understand the signaling cascade responsible for M_1-dependent LTD.

The finding that PLD_1 is important for this form of synaptic plasticity, coupled with the finding that biased and nonbiased M_1 receptor PAMs have functionally distinct effects on this response, raises the possibility that different PAMs could have unique profiles in regulating cognitive function or other in vivo responses. It is possible that biased versus nonbiased M_1 receptor PAMs could induce markedly different effects on specific behavioral responses, as is the case for biased and nonbiased PAMs of the $mGlu_5$ subtype of metabotropic glutamate (mGlu) receptor (*122*, *123*). Unfortunately, the currently available biased M_1 receptor PAMs used in the present studies do not have appropriate properties to enable their use in behavioral studies in vivo (Table 3). However, in future studies, it may be possible to optimize biased M_1 receptor PAMs that can be used to systematically evaluate the roles of PLD in specific behavioral responses that are dependent on M_1 receptor activation. Extensive drug discovery efforts are needed to develop biased M_1 receptor PAMs that have favorable physical and pharmacokinetic properties suitable for systemic administration with high CNS penetrance to test whether systemically administered biased M_1 PAMs display functional differences in their ability to reverse the cognitive deficits in preclinical animals relevant for AD and schizophrenia.

Compound	Molecular Weight	Route [Dose]	TIME (min)	Plasma Concentration (ng/mL)	Plasma Concentration (nM)	Brain Concentration (ng/mL)	Brain Concentration (nM)
VU0405652	505.35	i.p.	15	3380	6688	68.7	135.95
		[30mg/kg]	30	1641	3247	157	310.68
VU0405645	511.51	i.p.	15	0.00	0.00	6.51	12.73
		[30mg/kg]	30	8.48	16.58	13	25.41

Table 3: Summary of the in vivo pharmacological characterization data for VU0405652 and VU0405645.
Data represent mean values (n=3).

Lastly, future studies are necessary to develop an understanding of the precise molecular mechanisms involved in conferring bias for some M_1 receptor PAMs. Whereas there are multiple examples of allosteric modulators of GPCRs that induce biased signaling, little is known about the structural basis of biased versus nonbiased signaling. Previous studies revealed multiple allosteric binding sites for some GPCRs, which could contribute to different responses to distinct classes of allosteric modulators (*124–126*). However, other studies suggest that differences in M_1 receptor PAM functionality may not be due to binding to different allosteric binding pockets, but that binding of PAMs to a single allosteric site may stabilize different receptor conformational states (*23*, *127*). Understanding how allosteric modulators of GPCRs induce their effects will help facilitate the rational design of the next generation of PAMs and negative allosteric modulators.

CHAPTER 4

SUMMARY & DISCUSSION

Summary

In conclusion, the high-profile failure of several experimental therapeutic approaches targeting the reduction of Aβ in patients with AD warrants identification and development of novel therapeutic targets for the treatment of the cognitive disruptions in AD. Furthermore, current antipsychotics do not improve and may even worsen the cognitive deficits associated with schizophrenia (*128*). The ability of M_1 PAMs to improve cognition in multiple animal models (*36*, *48*, *52*, *53*, *57*, *82*) suggest a strong potential for success in the clinic and may help mitigate the critical issue common to animal models in that they often fail to recapitulate the full range of disease symptoms and etiology. However, with the recent phase II failure of MK-7622 to significantly improve cognitive endpoints in AD patients (*74*), there is a critical need to fully characterize M_1 PAMs with respect to agonist activity, signal bias, and other pharmacological properties in order to de-risk clinical candidates and move the M_1 PAM with the highest chance of success forward into the clinic.

Discussion

Overactivation of the M_1 mAChR may be detrimental to M_1 PAM efficacy

The findings outlined in **Chapter 2** suggest that the *in vivo* cognition-enhancing efficacy of M_1 PAMs can be observed with PAMs lacking agonist activity and that intrinsic

agonist activity of M_1 PAMs may contribute to adverse effects and result in reduced efficacy in improving cognitive function. Furthermore, as receptor expression levels may vary between cell lines and between research groups, it is critical to evaluate M_1 preclinical candidates in systems with varying degrees of receptor reserve (i.e. both *in vitro* and in native tissue) to fully characterize potential ago-PAM activity.

While *in vitro* assays are ideal to screen compounds and achieve a first pass look at a ligand's pharmacological properties, cell-based assays often fail to recapitulate the exact pathways found in native tissue. Additionally, discovery and characterization of functional M_1 receptors expressed intracellularly (*129*), as well as allosteric ligands that display "signal bias" (*90*), further highlights the need to fully assess activities of allosteric modulators in native preparations. Full understanding of the pharmacological properties responsible for *in vivo* efficacy of other GPCR allosteric ligands, such as $mGlu_5$ PAMs that display stimulus bias, have provided proof-of-concept that adverse effect liability can be avoided and *in vivo* efficacy remain intact (*122*).

M_1 PAMs that display bias can have differential effects in the CNS

Characterization of a broad range of structurally diverse M_1 PAMs revealed an interesting signal bias in that some M_1 PAMs can potentiate receptor signaling through the canonical phospholipase C (PLC) pathway, but do not potentiate M_1 receptor–mediated activation of phospholipase D (PLD) (*90*). Little was known about the role of PLD in M_1 signaling in the CNS and whether PLD is necessary for any M_1-dependent signaling. First, we demonstrated that activation of the M_1 mAChR primarily couple to PLD_1 not PLD_2 in M_1 mAChR expressing CHO cells. Interestingly, these findings were

recently recapitulated in immortalized HeLa cells (*130*). These two findings suggest that while PLD_1 and PLD_2 can catalyze the same enzymatic reaction, they have non-redundant functions with respect to GPCR signaling.

Using brain slice electrophysiology, in **Chapter 3** we demonstrated that not all M_1-dependent responses in the CNS were PLD-dependent, and biased M_1 PAMs functioned similarly to nonbiased M_1 PAMs in M_1 signaling that was PLD-independent. However, M_1 PAMs that do not couple to PLD function in a dramatically different way than nonbiased M_1 PAMs in their ability to potentiate a PLD-dependent M_1-mediated plasticity in the PFC. These findings demonstrate that PLD plays a critical role in the ability of M_1 PAMs to modulate certain CNS functions and that biased M_1 PAMs function differently in synaptic plasticity in the cortex implicated in cognition.

Future Directions

Characterization of M_1 signaling pathway to phospholipase D

Although the current studies identify PLD_1 as being critically important in M_1-dependent cortical synaptic plasticity, the detailed molecular mechanism by which the M_1 receptor signals through PLD to induce synaptic plasticity changes in the cortex remains unknown. Rigorous molecular and biochemical studies to elucidate this signaling pathway are necessary to fully understand the signaling cascade responsible for M_1-dependent LTD.

In order to elucidate the molecular mechanisms that govern M_1 mAChR signaling to PLD, it would be most prudent to start in a cell culture system (e.g. M_1 mAChR expressing CHO cells) in order to quickly screen through different downstream signaling effectors. Utilizing RNAi based technologies such as small interfering RNA (siRNA) (*131–133*), in combination with the PLD assay, it would be feasible to quickly screen different downstream effectors (i.e. AKT, PLC, mTOR, various g-proteins etc.). Preliminary data in Fig. 24A suggest that neither K-Ras nor H-Ras play a role in M_1 mAChR activation of PLD. Results in Fig. 24B suggest a potential role of PI3K, AKT, Src, GSK3, PKC and possibly mTOR in M_1 activation of PLD in M_1 mAChR expressing CHO cells. While promising, these results are from just one assay and need to be replicated and the various protein knockdown confirmed by western blot analysis.

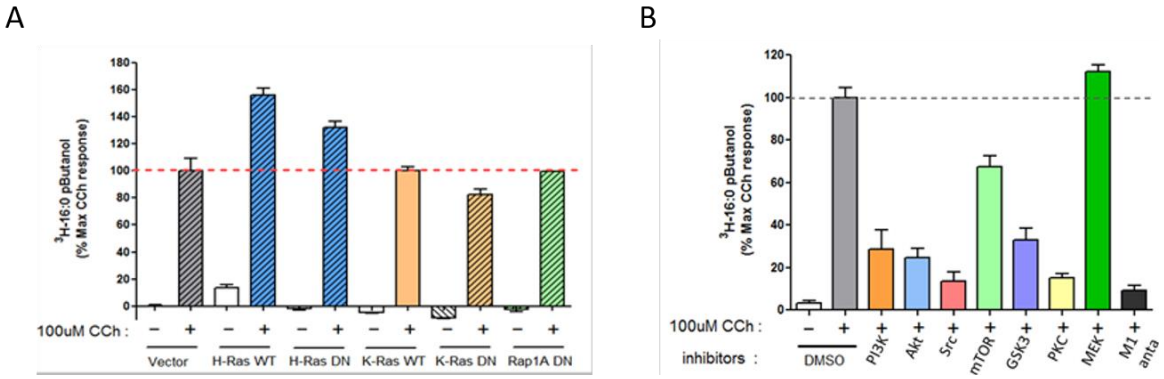

Figure 25. Preliminary data examining the signaling pathway involved in M1 mAChR activation of PLD.
(**A**) Use of CHO cells expressing normal H-Ras and K-Ras proteins or the dominant negative mutations forms of this protein. (**B**) PLD activation by CCh appears to be decreased by pharmacological inhibition of PI3K, AKT, Src, GSK3, PKC and potentially mTOR but not MEK. N=1 assay (3 lanes averaged together) per group. Data courtesy of Hyekyung Plumley.

It should be noted that siRNA technology suffers from the caveat of off target effects as well as the fact that siRNA knockdown of the transcript of interest in typically not 100% and small amounts of transcript may be sufficient to provide a full response, thereby confounding the interpretation of the results. Therefore, newer technologies using the Crispr-Cas system can be used to permanently delete or alter the gene of interest (*134*) or to selectively repress the expression of targeted genes through the use of CRISPR interference (CRISPRi) with no detectable off-target effects (*135*). Together, through these cell based experiments, we could quickly screen putative signaling molecules upstream of PLD and then determine whether the protein of interest is also critical for M_1 mAChR signaling in native tissue assays such as CCh-LTD in the mPFC.

Role of PLD downstream of other canonical $G_{\alpha q}$ GPCR signaling

The M_1 mAChR is one of many different receptors that can couple to PLD, and PLD is known to be activated by both multiple classes of GPCRs as well as receptor tyrosine kinases (*136*). Previously, it was demonstrated that the activation of mGlu receptors can lead to activation of PLD in cell lines as well as in hippocampal slice preparations (*137–139*). Furthermore, mGlu receptor activation of PLD was demonstrated to be independent of both PLC and PKC. However, the dearth of pharmacological and genetic tools available at the time prevented further investigation into the role of PLD in mGlu receptor signaling. With the recent significant advances in mGlu receptor subtype selective inhibitors, highly selective mGlu receptor PAMs, and PLD isoform selective inhibitors, we are now poised to revisit the role of PLD in mGlu receptor signaling.

Based on the previous literature, we do not know which specific mGlu receptors subtypes may or may not couple to PLD, we do know that activation of both group I and group II mGlu receptors by 1S,3R-amino-1,3-cyclopentanedicarboxylic acid (ACPD) can lead to increases in PLD. Therefore, we set out with the initial goal to determine whether group I mGlu receptors ($mGlu_1$ and $mGlu_5$) couple to PLD. Thus, we set out to test whether PLD was involved in a group I mGlu receptor-LTD at SC-CA1 in the hippocampus induced by (S)-3,5-Dihydroxyphenylglycine (DHPG), a very well characterized form of synaptic plasticity involving group I mGlu receptors. Importantly, previous studies have demonstrated that DHPG-LTD at SC-CA1 in the hippocampus is not dependent on PLC or PKC (*140*, *141*), and therefore is a good candidate for being dependent on non-canonical signaling proteins such as PLD.

Preliminary results from these studies demonstrate that, similar to the CCh-LTD in the mPFC, DHPG-LTD in the hippocampus is dependent on PLD_1 not PLD_2 (Fig. 25A-F). Confirming these results, PLD_1 KO mice have a significant deficit in DHPG-LTD compared to littermate controls. Since DHPG can activate both $mGlu_1$ and $mGlu_5$, we then probed whether an $mGlu_5$ specific LTD in the hippocampus was also dependent on PLD. We previously demonstrated that bath application of the $mGlu_5$ ago-PAM VU0424465 can produce a robust $mGlu_5$ LTD at SC-CA1 in brain slices obtained from rodents (*67*). In agreement with the previously published data, we demonstrated that VU0424465 produced a robust LTD (Fig. 25J) and that this $mGlu_5$-LTD was absent in the presence of the PLD_1 inhibitor (Fig. 25K-L). Therefore, these preliminary findings suggest that $mGlu_5$ may couple to PLD and that PLD_1 may be critical for some forms of mGlu receptor synaptic plasticity in the hippocampus.

While these preliminary findings are exciting, detailed future studies are necessary to fully probe the role of PLD in mGlu receptor signaling. In order to determine which specific mGlu receptor subtypes couple to PLD, PLD activity can be directly quantified using mGlu receptor-expressing HEK cells for the PLD assay. Furthermore, this cell-based assay can be used to probe the signaling cascade involved in mGlu receptor coupling to PLD.

While DHPG-LTD is a well characterized form of mGlu receptor synaptic plasticity in the hippocampus, it would be interesting to probe the role of PLD in other forms of mGlu-dependent synaptic plasticity including: electrically-induced LTD (low frequency stimulation (LFS) as well as paired pulse-LFS (PP-LFS), high frequency stimulation LTP and theta burst stimulation LTP. Understanding whether PLD is involved in any of these other forms of synaptic plasticity would greatly advance the field of hippocampal synaptic plasticity as well as help focus on PLD-impacted signaling pathways.

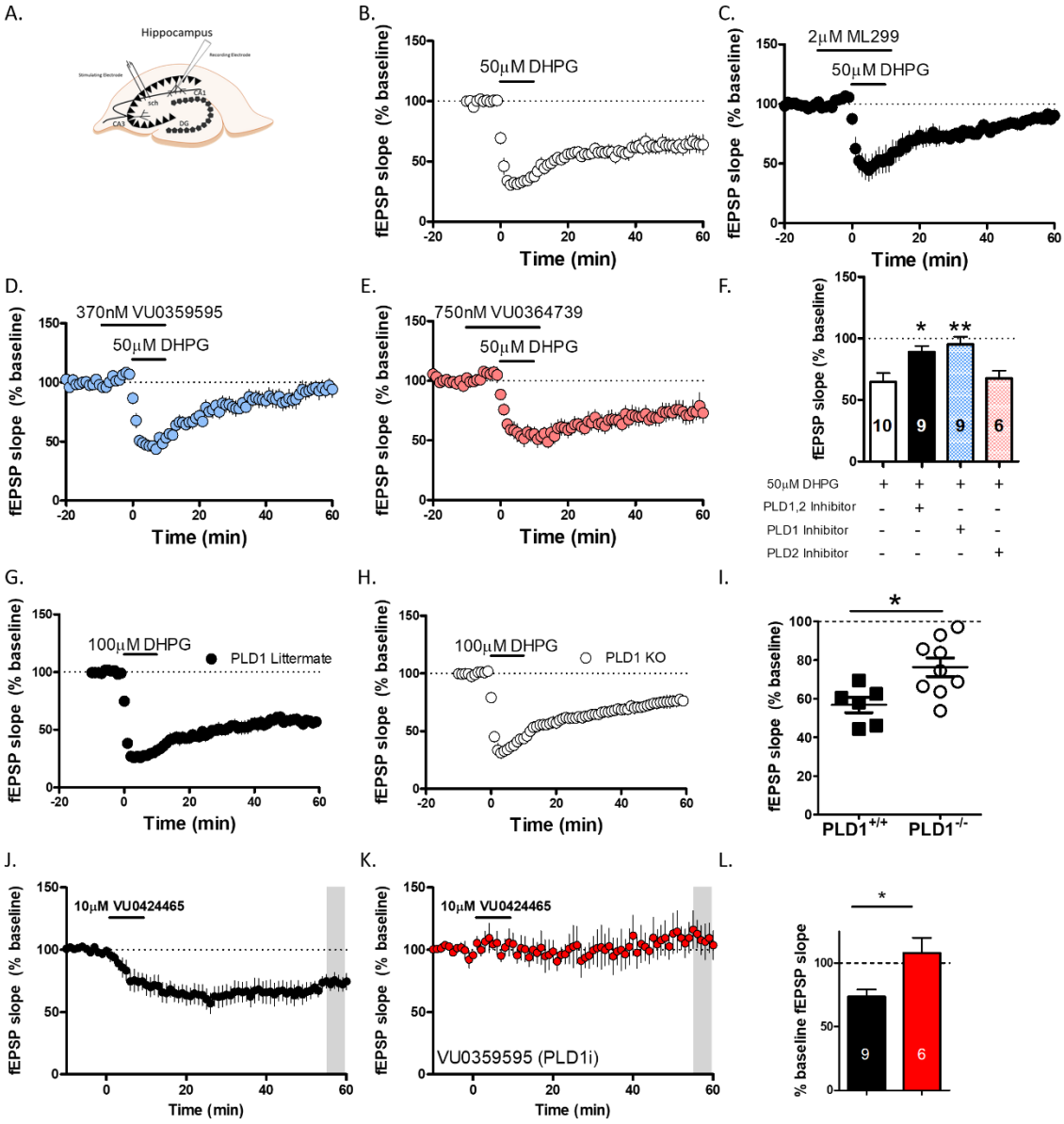

Figure 26: DHPG-LTD at SC-CA1 in the hippocampus is dependent on PLD, specifically PLD_1

(**A**) Schematic of SC-CA1 hippocampal brain slice (**B**) Bath application of 50μ M DHPG results in a long-term depression (LTD) of fEPSPs. (**C**) pretreatment with the PLD1,2 inhibitor ML299 blocks this LTD. (**D**) Inhibition of PLD_1 but not (**E**) PLD_2 blocks DHPG-LTD. (**F**) Oneway ANOVA with Dunnett's post-hoc test demonstrates a significant difference between $PLD_{1,2}$ inhibition, PLD_1 inhibition but not PLD_2 inhibition compared to DHPG alone. (**G-H**) DHPG-LTD is attenuated in PLD_1 KO mice but not littermate controls. (**I**) Student's t-test demonstrates significant difference between genotype. (**J**) $mGlu_5$ ago-PAM VU0424465 induces a $mGlu_5$-dependent LTD that is lost in the presence of the (**K**) PLD_1 inhibitor. **(L**) Student's t-test demonstrates significant difference between two groups.

Development of the next generation of biased M_1 PAMs

Extensive medicinal chemistry efforts are needed to develop biased M_1 mAChR PAMs that have favorable physical and pharmacokinetic properties suitable for systemic administration with high CNS penetrance to test whether systemically administered biased M_1 PAMs display functional differences in their ability to reverse the cognitive deficits in preclinical animals relevant for AD and schizophrenia. Results from these studies could directly impact drug discovery decisions for backup compounds and/or future clinical candidates.

Furthermore, it would be especially useful to develop M_1 PAMs that potentiate coupling to PLD but not PLC. An M_1 PAM with this pharmacological property could be very useful to test whether M_1 PAM coupling to PLC is necessary or sufficient for M_1 PAM efficacy and/or adverse effects in vivo. However, identification of a biased M_1 PAM that couples to PLD but not PLC is currently challenging due to the low-throughput manner of the PLD activity assay. A solution to this technical problem can be solved by development of a higher-throughput PLD activity assay that would likely use fluorescence as a read out instead of quantifying radioactivity using film. One possibility is to develop a fluorescent reporter that changes light emission with respect to generation of the stable PLD product phosphatidylbutanol. In theory, this could be similar to the calcium mobilization assay dye Fluo-4 AM that exhibits an increase in fluorescence upon binding of Ca^{2+}. A similar approach would be to use the recently developed PLD “click-chemistry” technology that correlates PLD activity with a change in fluorescence (*130*).

Fluorescence-activity assays are extremely amendable to high-throughput screening and therefore, a large library of compounds can be screened. One could also envision a “smart” library of small molecules that are structurally similar to established M_1 PAMs that have weak activity, no activity, or inverse agonism in the M_1 CHO cell Ca^{2+} mobilization assay. In theory, this intelligently designed “smart” library could have a higher chance of success in identifying an M_1 PAM that does not potentiate PLC but does potentiate PLD. identified leads would then need to be counter-screened in receptor subtype selectivity, in vivo pharmacokinetic assays, and native tissue assays.

Lastly, PLC and PLD are just two out of many different signaling pathways downstream of the M_1 mAChR and future studies are necessary to identify M_1 PAMs with favorable in vivo properties that may display signal bias for other signaling pathways including ERK or β-arrestin, in order to fully dissect the downstream signaling pathways important for M_1 PAM efficacy and adverse effect liability. To date, no biased M_1 PAMs with respect to ERK phosphorylation or β-arrestin recruitment have been disclosed; however, only a small number of M_1 PAMs have been tested (*41*, *44*, *45*).

Characterization of the molecular mechanisms involved in conferring bias

Future studies are necessary to develop an understanding of the precise molecular mechanisms involved in conferring bias for M_1 receptor PAMs. Whereas there are multiple examples of allosteric modulators of GPCRs that induce biased signaling, little is known about the structural basis of biased versus nonbiased signaling. Previous studies have revealed multiple allosteric binding sites for other GPCRs such as mGlu receptors, and these distinct binding sites could contribute to the different responses to distinct allosteric

modulators (*124–126*). However, investigation into the binding sites of M1 PAMs has revelaed that several structurally distinct M_1 PAMs (e.g. PF-06767832, MIPS1780, VU6004256) bind to the same binding pocket as the first described M_1 PAM, BQCA (*127*, *142*).

Therefore, differences in M_1 mAChR PAM functionality may not be due to the allosteric ligand binding to a different allosteric binding pocket, but instead be due to the binding of PAMs to the same allosteric site but stabilizing different receptor conformational states (*23*, *127*). This is further supported by the hypothesis that M_1 PAM selectivity for the M_1 mAChR, compared to the other mAChR subtypes, is not driven by binding to a unique allosteric site on the M_1 mAChR; rather, subtype-selectivity is driven by cooperativity (*142*, *143*). Thus, understanding exactly how allosteric modulators of GPCRs induce their effects may help facilitate the rational design of the next generation of PAMs and negative allosteric modulators.

M_1 PAMs with low α-values may also minimize adverse effects

According to the operational allosteric ternary complex model (*22*, *144*), allosteric modulators can exert their effects by modulating binding affinity of the orthosteric agonist (e.g. binding of ACh to the M_1 mAChR) or by modulating receptor efficacy (e.g. ACh response), termed α and β respectively (Fig. 26A). When $\alpha > 1$, the allosteric modulator increases the affinity of the orthosteric agonist whereas when $\alpha < 1$ demonstrates a decrease in receptor-agonist affinity. Conversely, when $\beta > 1$, the allosteric modulator will potentiate cellular activation whereas when $\beta < 1$, the modulator will prevent cellular activation (Fig. 26B). Importantly, α and β values are independent of each other and in

theory can occur in every combination (*144*). Several recent papers from Takeda Pharmaceutical Company Ltd suggest that M_1 PAMs that possess low α-values, such as TAK-071, have a wider **therapeutic index** in rodent models relevant for schizophrenia compared to M_1 PAMs with high α-values (*81*, *145*, *146*). However, TAK-071 was not completely devoid of adverse effects and demonstrated a concentration-dependent increase in spontaneous ileum motility (*145*). Nonetheless, TAK-071 provides a much greater margin between doses leading to cognition-enhancing effects and adverse effects (e.g. diarrhea) compared to T-662, an M_1 PAM with a high α-value (*81*, *111*, *145*). Furthermore, it is not known whether M_1 PAMs with higher α and β-values may be more beneficial in later stages of AD in which there is greater loss of endogenous ACh (*15*, *147*). Overall, while these results are promising, more extensive studies are necessary to understand the exact relationship between α-value, agonist activity, and signal bias to fully characterize the pharmacological profiles of M_1 PAMs. Lastly, it is prudent to carefully consider the appropriate α and β-values for the M_1 PAM clinical candidate depending on the stage of AD (e.g. early or late) chosen for clinical intervention.

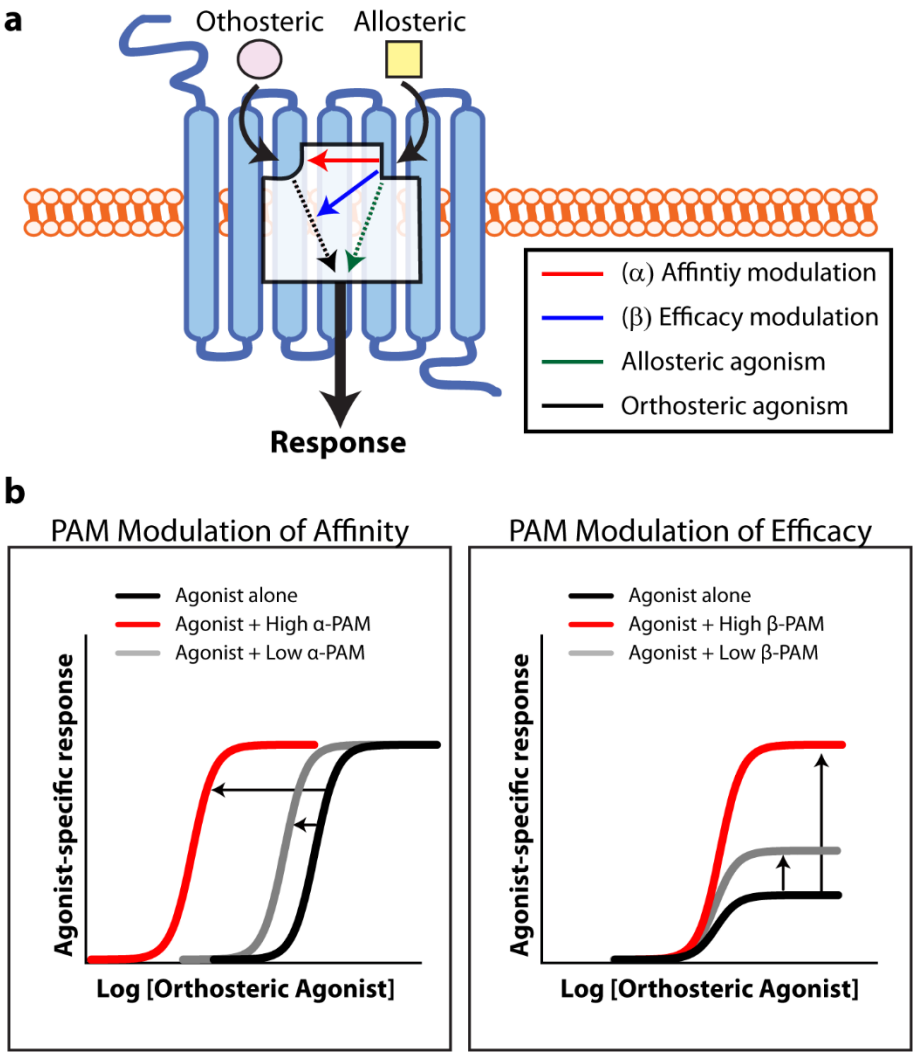

Figure 27: Allosteric modulator modes of action.
(A) Allosteric modulators (yellow square) bind to a topographically and structurally distinct site on the muscarinic receptor to modulate orthosteric agonist (acetylcholine, pink) affinity (red) and/or efficacy (blue). Binding of allosteric agonists or ago-PAMs can also directly induce receptor signaling in the absence of the orthosteric agonist (green). (B) Left: Allosteric modulators that robustly modulate agonist affinity (high α-value, red) will result in a large leftward shift in the orthosteric agonist concentration response curve. In contrast, allosteric modulators that weakly enhance agonist affinity (low α-value, grey) result in a modest leftward shift in the orthosteric agonist concentration response curve. Right: Allosteric modulators that strongly modulate agonist efficacy (high β-value, red) may result in a large increase in the orthosteric agonist maximal response. In contrast, allosteric modulators that weakly enhance agonist efficacy (low β-value, grey) result in a modest increase in the orthosteric agonist response. Sigmoidal curves were generated using Graphpad Prisim8 (www.graphpad.com).

Potential utility of M_1 allosteric modulators for the treatment of other CNS disorders

In addition to potential efficacy in reversing cognitive deficits in AD and schizophrenia patients, recent studies suggests that M_1 PAMs also improve social interactions in rodent models (*52*). Previously, xanomeline demonstrated efficacy in reducing negative symptoms in schizophrenia patients (*18*, *19*), thus, it will be important to fully evaluate the potential efficacy of M_1 PAMs in animal models that are relevant for negative symptoms. To this same end, the wide variety of M_1 and M_4 selective tool compounds developed over the past decade have identified other psychiatric and neurological disorders in which subtype-selective muscarinic modulation may be effective. Consistent with procognitive efficacy, the M_1 PAM BQCA improved learning and memory deficits in a rodent model of traumatic brain injury (*148*). An M_1 PAM was also able to enhance the consolidation and recall of fear extinction in a rodent model of posttraumatic stress disorder (PTSD) (*58*) suggesting that M_1 PAMs could improve the efficacy of exposure therapy in the clinic for the treatment of PTSD and other anxiety disorders

In addition to AD and schizophrenia, the wide variety of M_1 selective tool compounds developed over the past decade have identified other psychiatric and neurological disorders in which subtype-selective muscarinic modulation may be effective. Consistent with procognitive efficacy, the M_1 PAM BQCA improved learning and memory deficits in a rodent model of traumatic brain injury (*148*). An M_1 PAM was also able to enhance the consolidation and recall of fear extinction in a rodent model of posttraumatic stress disorder (PTSD) (*58*) suggesting that M_1 PAMs could improve the

efficacy of exposure therapy in the clinic for the treatment of PTSD and other anxiety disorders. Additionally, M_1 activation in combination with an M_4 PAM accelerated the extinction of cocaine seeking (*149*) implying that potentiating M_1 activation may broadly facilitate and/or enhance extinction learning across multiple behavioral paradigms. Therefore, future studies are needed to determine whether M_1 PAMs could be beneficial in a broader range of CNS disorders.

Conclusions

A wealth of preclinical literature over the last decade suggest that allosteric modulators of several mAChRs hold great promise for the treatment of multiple devastating CNS disorders, including AD, schizophrenia and other brain disorders, which have limited to no effective treatments. Recent advances in medicinal chemistry efforts to develop highly selective mAChR ligands have provided fundamental new insights into muscarinic receptor biology as well as provided key information for drug discovery efforts. As a consequence of these efforts, several allosteric modulators for the M_1 mAChR have already entered clinical trials with allosteric modulators for the other subtypes quickly advancing toward the clinic.

While much progress has been made in developing allosteric modulators of the various mAChR for the potential treatment of several CNS disorders, there are still many outstanding questions that the muscarinic field is primed to address. First, there is a critical need to fully characterize the pharmacological properties important for efficacy and adverse effects, in order to derisk clinical candidates and ultimately advance mAChR allosteric modulators forward into the clinic with the highest chance of success. This can

illustrated by the recent phase II failure of the M_1 ago-PAM MK-7622 to significantly improve cognitive endpoints in AD patients (*74*). Better understanding of M_1 PAM pharmacology at the preclinical research stage may have better informed drug discovery decisions and the outcome of Merck's M_1 PAM clinical trial may have been avoided. Secondly, through use of M_1 PAMs with dramatically different pharmacological properties as tool compounds, we as a field can make significant progress in understanding muscarinic receptor biology in the CNS.

Lastly, characterization of biased allosteric ligands for the M_1 mAChR has provided useful insight into the mechanism of action of these allosteric modulators. However, to date, we have only identified a limited number of biased ligands and more focused drug discovery efforts are needed to identify biased ligands for other distinct signaling pathways as well as the other mAChR subtypes. Therefore, dedicated medicinal chemistry, paired with pathway-specific but still high throughput pharmacological assays, is needed to identify a wider range of biased ligands the M_1 mAChR. Information gleaned from these studies could greatly advance our collective knowledge of mAChR biology as well as help inform drug discovery programs. Even modest investments into pharmacological characterization of the signaling pathways and pharmacological properties involved in allosteric modulator action in vivo could pay huge dividends for drug discovery efforts. Through better understanding of the pharmacological properties important for efficacy and adverse effects, we as a field can ultimately advance M1 mAChR allosteric modulators forward into the clinic with the highest chance of success.

CHAPTER 5

MATERIALS AND METHODS

Calcium mobilization assay

Briefly, M_1-CHO cells were plated in black-walled, clear-bottomed 384 well plates (Greiner Bio-One,Monroe, NC) the day before assay. The next day, cells were washed with assay buffer (Hank's balanced salt solution, 20 mM HEPES, 4.16 mM sodium bicarbonate, and 2.5 mM probenecid) and immediately incubated with 20 µL of 1.15 µM Fluo-4-acetomethoxyester (Fluo-4 AM) dye solution prepared in assay buffer for 45 min at 37 °C. M_1 PAMs were serial diluted (1:3) in DMSO for 10-point concentration−response curves (CRC), and further diluted in assay buffer at starting final concentration 30µM using Echo liquid handler (Labcyte, Sunnyvale CA). After removing dye, cells were washed with assay buffer. Immediately, calcium flux was measured using the Functional Drug Screening System (FDSS7000, Hamamatsu, Japan) The serially diluted compounds or DMSO vehicle were added to cells for 2.5 min and then an EC_{20} concentration of acetylcholine (ACh) was added and incubated for 2 min. EC_{max} concentration was also added to cells that were incubated with DMSO vehicle to ensure the EC_{20} calcium response. To determine the potency and efficacy of the agonist and PAM, data were analyzed to generate a concentration-response curve using a four-point logistical equation in GraphPad Prism 5.0 (GraphPad Software, Inc., La Jolla, CA).

PLD activity assay

Methods were adapted from a previously published procedure (*112*). Briefly, CHO cells stably transfected with the human M_1 muscarinic acetylcholine receptor were grown on growth media consisted of Ham's F-12 Nutrient Mix (ThermoFisher #11765), 10% FBS, 20 mM HEPES, 1X Antibiotic/Antimycotic, 500 µM G418. The cells were then plated on 6-well plates for a total of approximately $0.7x10^6$ cells / 2mL / well. Plating media consisted of growth media without FBS or G418. The following day, plating media was aspirated off and labeling media was prepared by adding ^{3}H-palmitic acid (5 µCi/ µL) supplemented with 2.08 µg/µL Phosphoethanolamine (PE stock, 25 mg/mL in $CHCl_3$) to serum free media supplemented with bovine serum albumin. Each well contained 1mL media with 10 to 30 µCi [^{3}H]-palmitic acid. Labeling was allowed to occur in a 37 °C incubator overnight. The next morning, the plating media was carefully aspirated off and the cells were treated for 5 min with DMSO or M_1 PAM then 30 min in the presence of 0.3% 1-butanol in serum-free assay media (1 mL media/well) or no butanol serum-free assay media as a negative control and the plates were incubated at 37 ^{o}C. ^{3}H labeling efficiency was measured by subtracting the post-labeling medium from the pre-labeling medium. All pharmacological agent stocks were used at 500 or 1000-fold higher than the final concentration. Immediately after the incubation, 600 µL ice cold acidified methanol (1:1 ratio of 0.1 N HCl to Methanol) was added and the cells were scraped off using a cell scraper and transferred to a 1.5 mL Eppendorf tube. 300 µL room-temperature $CHCl_3$ was then added and the sample which was then vortexed vigorously for approximately 20 seconds. The samples were then spun at 16,000 g for 5 min to separate phases. The bottom lipid phase was removed carefully to ensure no other phases were carried over

and transferred to a new 1.5 mL Eppendorf tube. The samples were then dried under N_2 gas until all liquid was evaporated. The lipids were then resuspended in 25 µL $CHCl_3$ and immediately spotted onto the TLC plate (Sorbtech, Norcross GA; Cat#2315126C). Non-radioactive lipid standards such as p-Butanol and phosphatidic acid were also spotted on the TLC plate. The TLC tank was prepared by placing chromatography paper 7-inch (H) x 22.5-inch (W) so that it covers approximately 75% of the tank's height. The mobile phase was then added (10 $CHCl_3$: 2 Methanol: 2 Acetic Acid: 4 Acetone: 1 H_20) and allowed to equilibrate for 1 hour before the TLC plate was added and run for 1.5 to 2 hours. The plate was then removed from the tank and allowed to completely dry before imaging using autoradiography film in conjunction with an intensifying screen (BioMax Transcreen LE, Carestream Health) and placed in a -80 ^oC freezer for 3-5 days. The film was then processed after exposure and quantified using Chemdoc (Biorad).

Animals

All animal studies were approved by the Vanderbilt University Medical Center Institutional Animal Care and Use Committee and were conducted in accordance with the National Institutes of Health Guide for the Care and Use of Laboratory Animals. Male C57BL6/J mice (Jackson laboratories) and M_1 receptor knock-out (KO) mice (with permission from J. Wess, National Institutes of Health–National Institute of Diabetes and Digestive and Kidney Diseases, Bethesda, MD) were used in electrophysiology and behavioral studies (6-10 weeks old). PLD_1 knockout (KO) mice (obtained from the trans-NIH Knock-Out Mouse Project Repository, www.komp.org) maintained on a C57BL6/J background were used in electrophysiology studies. Mice were group housed 4-5 per

cage, maintained on a 12 hr light/dark cycle, and food and water were provided *ad libitum*. Adult male Sprague-Dawley rats weighing between 280-350 grams (Envigo, Indianapolis, IN) were used in the behavioral studies. Rats were group housed 3 per cage and were maintained on a 12 hr light/dark cycle with food and water *ad libitum*.

Behavioral manifestations of seizure activity

To evaluate induction of behavioral manifestation of seizure activity, C57Bl/6J mice received administration of vehicle or 1, 3, 10, 30, or 100 mg/kg M_1 PAM. Compounds were formulated in 10% Tween 80 (pH 7.0) at a concentration of 10 mg/mL and injected intraperitoneally (i.p.) (n = 3). Animals were monitored continuously and scored for behavioral manifestations of seizure activity at 5, 10, 15, and 30 min, and 1 and 3 h. Behavioral manifestations of seizures were scored using a modified Racine scoring system (*62*, *67*). A Racine score of 0 represents no behavior alterations; score 1, immobility, mouth and facial movements, or facial clonus; score 2, head nodding, tail extension; score 3, forelimb clonus, repetitive movements; score 4, rearing and tonic-clonic seizure; and score 5, continuous rearing and falling, severe generalized tonic-clonic seizure (*62*, *67*, *73*).

Extracellular field electrophysiology

6-10 week old male C57BL6/J mice (Jackson Laboratories) were anesthetized using isoflurane then transcardially perfused with either ice cold 1)high sucrose cutting solution (in mM: 230 sucrose, 2.5 KCl, 8 $MgSO_4$, 0.5 $CaCl_2$, 1.25 NaH_2PO_4, 10 D-glucose, 26 $NaHCO_3$), or 2) NMDG-HEPES solution (in mM: 93 NMDG, 2.5 KCl, 1.2 NaH_2PO_4, 30

$NaHCO_3$, 20 HEPES, 25 D-glucose, 5 sodium ascorbate, 2 thiourea, 3 sodium pyruvate, 10 $MgSO_4$, 0.5 $CaCl_2$, 12 N-acetyl-L-cysteine, pH 7.35, <310 mOsm) and then the brains were removed and submerged in ice-cold solution that was the same as the perfusion solution (e.g. high sucrose or NMDG solution). Coronal slices containing the prelimbic prefrontal cortex were cut at 400 µm and were transferred to a holding chamber containing NMDG-HEPES recovery solution (in mM: 93 NMDG, 2.5 KCl, 1.2 NaH_2PO_4, 30 $NaHCO_3$, 20 HEPES, 25 D-glucose, 5 sodium ascorbate, 2 thiourea, 3 sodium pyruvate, 10 $MgSO_4$, 0.5 $CaCl_2$, 12 N-acetyl-L-cysteine, pH 7.3, <310 mOsm) for 8-10 minutes at 32 ºC. Slices were then transferred to a room temperature holding chamber for 1.0 hour containing ACSF (in mM: 126 NaCl, 1.25 NaH_2PO_4, 2.5 KCl, 10 D-glucose, 26 $NaHCO_3$, 2 $CaCl_2$, 1 $MgSO_4$) supplemented with 600-µM sodium ascorbate for slice viability. All buffers were continuously bubbled with 95% O_2/5% CO_2. Subsequently, slices were transferred to a 30-32 ºC submersion recording chamber (Warner Instruments) where they were perfused with ACSF at a rate of 2 mL/min. Recording pipettes were constructed from thin-walled borosilicate capillary glass tubing (I.D.=1.17 mm, O.D. 1.50 mm; Warner Instruments, Hamden, CT), pulled with a horizontal pipette puller (P-97 Sutter Instrument Co., Novata, CA) to a resistance of 1-3MΩ when filled with ACSF. Field excitatory postsynaptic potentials (fEPSPs) were recorded from layer V of the prelimbic cortex and evoked electrically by a concentric bipolar stimulating electrode (200 µs duration, 0.05 Hz; inter-pulse interval of 50 ms) in the superficial layers II-III. Layer II/III was visualized using a Olympus BX50WI upright microscope (Olympus, Lake Success, NY) microscope according to landmarks illustrated in the Allen mouse brain atlas(*150*) and the recording electrode was laterally placed approximately 200µM

away from layer 2/3 into layer V so that the recording and stimulating electrodes were parallel to each other. Input-output curves were generated to determine the stimulus intensity that produced approximately 70% of the maximum fEPSP slope before each experiment, which was then used as the baseline stimulation. Data were digitized using a Multiclamp 700B, using a sampling rate of 20,000kHz and were filtered at 0.5kHz, with a Digidata 1322A, pClamp 9.2 and Clampex 10.6.2 software (Molecular Devices) running on a Dell PC (Round Rock, TX). All test compounds, with the exception of CCh (Tocris Bioscience, Bristol, UK) which was diluted in H_2O, were diluted to the appropriate concentrations in DMSO (<0.1% final) in ACSF and applied to the bath for 20 minutes using a peristaltic pump perfusion system. Offline data analysis to calculate fEPSP slope was performed using Clampfit 10.2 (Molecular Devices).

Whole cell electrophysiology

Mice were anesthetized with isoflurane then transcardially perfused and the brains were removed then as described above. Coronal slices containing either dorsal striatum or prelimbic prefrontal cortex (PFC) were cut at 250 µm or 300 µm, respectively, and were transferred to a holding chamber containing NMDG-HEPES recovery solution (in mM: 93 NMDG, 2.5 KCl, 1.2 NaH_2PO_4, 30 $NaHCO_3$, 20 HEPES, 25 D-glucose, 5 sodium ascorbate, 2 thiourea, 3 sodium pyruvate, 10 $MgSO_4$, 0.5 $CaCl_2$, 12 N-acetyl-L-cysteine, pH 7.35, <310 mOsm) for 8-10 minutes at 32 ºC. Slices were then transferred to a room temperature holding chamber for 1.0 hour containing ACSF (in mM: 126 NaCl, 1.25 NaH_2PO_4, 2.5 KCl, 10 D-glucose, 26 $NaHCO_3$, 2 $CaCl_2$, 1 $MgSO_4$) supplemented with 600-µM sodium ascorbate for slice viability. All buffers were continuously bubbled with

95% O_2/5% CO_2. Subsequently, slices were transferred to a 30-31 ºC submersion recording chamber (Warner Instruments) where they were perfused with ACSF at a rate of 2 mL/min. Recording pipettes were constructed from thin-walled borosilicate capillary glass tubing (I.D.=1.17 mm, O.D. 1.50 mm; Warner Instruments, Hamden, CT), pulled with a horizontal pipette puller (P-97 Sutter Instrument Co., Novato, CA) to a resistance of 4-6 MΩ when filled with potassium-based internal solution: (mM) 125 K-gluconate, 4 NaCl, 10 HEPES, 4 MgATP, 0.3 NaGTP, 10 Tris-phosphocreatine.

For the PFC recordings, pyramidal neurons were visualized based on morphology with a 40X water-immersion lens with oblique illumination coupled with an Olympus BX50WI upright microscope (Olympus). After a stable gigaohm seal was formed, light suction was applied to break through the cell membrane and achieve whole-cell access. The access resistance was checked at the beginning and the end of each experiment and neurons with an access resistance of neurons greater than 30 mOhm were not used for analysis. Pyramidal neurons were further identified by their regular spiking pattern following depolarizing current injections induced by a series of 500 ms current steps (−150pA to +100 pA) incremented in +25 pA performed in current clamp mode. Spontaneous EPSCs were recorded at a holding potential of -70 mV (the reversal potential for $GABA_A$ channels) and the junction potential was not compensated. The voltage clamp signal was low pass filtered at 5 kHz and digitized at 10 kHz using a Digidata 1322A and acquired using Axon MultiClamp 700B (Molecular Devices, Sunnyvale, CA) and controlled by pClamp 9.2 and Clampex 10.6.2 running on a Dell PC. After a stable baseline was recorded for 5-10 min, test compounds were diluted to the appropriate concentrations in DMSO (<0.1% final) in ACSF and applied to the bath using

a peristaltic pump perfusion system. Cumulative probability plots of inter-event-intervals (IEI) were constructed using 2 min episodes of baseline and peak effect during drug application. In order to determine whether M_1 receptor PAM potentiation of sEPSC frequency was dependent on PLC, we included 1μM U73122 (Tocris Bioscience, Bristol, UK) or DMSO in the internal solution and constantly perfused in 10μM U73122 or DMSO (0.2%) ACSF throughout the entire experiment. All sEPSC analyses were performed using MiniAnalysis (Synaptosoft Inc., Decatur, GA) or Clampfit 10.2 (Molecular Devices).

For striatal spiny projection neurons (SPN) recordings the change in excitability of MSN was assessed in current clamp mode by monitoring the change in the number of spike discharges in response to a near rheobase depolarization current step (1.5 s). The access resistance was checked at the beginning and the end of each experiment, which were compensated using “bridge balance”. The change in spike number was calculated by averaging the number of spikes during the baseline subtracted from the peak drug-effect (60 seconds). Offline data analysis to calculate change in SPN excitability was performed using Clampfit 10.2 (Molecular Devices).

Novel object recognition task

Rats were habituated for 10 min for 2 consecutive days in an empty novel object recognition arena consisting of dark-colored plexiglass box (40 × 64 × 33 cm3). On day 3, rats were administered vehicle 0.5% methylcellulose (for MK-7622 and 20% b-cyclodextrin for VU0453595) or M_1 PAM (0.3−10 mg/kg, per os (p.o.), 3 mL/kg, n = 11-12) and returned to their home cage for 90 min. Rats were then placed in the novel object recognition arena containing two identical objects for 10 min. Following the exposure

period, rats were placed back into their home cages for 24 h. The rats were then returned to the arena in which one of the previously exposed (familiar) objects was replaced by a novel object and were video recorded for 5 min while they explored the two objects. Time spent exploring each object was scored by an observer blinded to the experimental conditions and the recognition index was calculated as [(time spent exploring novel object) − (time spent exploring familiar object)]/total time exploring objects.

In vivo pharmacokinetic analysis

VU0405652 and VU0405645 compound were formulated as 10% Tween 80 in sterile water at the concentration of 3 mg/mL and administered intraperitoneally to male C57/bl6J mice and dosed at 10 mg/kg. Mice blood (cardiac puncture) and brain were collected at 15 and 30min. Animals were euthanized and decapitated, and the brains were removed, thoroughly washed in ice-cold (4 °C) phosphate-buffered saline, and immediately frozen on dry ice. Brain samples were processed and concentrations of compound were determined via electrospray ionization on an AB Sciex API-4000 (Foster City, CA) triple-quadrupole instrument that was coupled with Shimadzu LC-10AD pumps (Columbia, MD) and a Leap Technologies CTC PAL auto-sampler (Carrboro, NC). All data were analyzed using AB Sciex Analyst 1.5.1 software. Compound exposures, in the form of area-under-the-curve were calculated by trapezoidal method employing PRISM software (GraphPad, La Jolla, CA).

Western blot analysis of PLD_1 protein

Total protein was extracted from the cortex of PLD_1 KO mice and littermate controls by homogenization in RIPA buffer (Sigma) with protease inhibitors. After homogenization, samples were spun for 20 min at 15,000*g* at 4 °C. The supernatant was kept and protein concentration was determined using a bicinchoninic acid (BCA) protein assay (Pierce). 50 µg protein per sample was electrophoretically separated using a 4–20% SDS polyacrylamide gel and transferred onto a nitrocellulose membrane using the iBlot2 (Thermo Fisher). The membrane was blocked with Odyssey blocking buffer (LI-COR) for 1 h at room temperature. Membranes were probed with the following primary antibodies: rabbit anti-PLD1 (1:500, Cell Signaling Technology #3832) and mouse anti-tubulin (1:5000, Abcam ab44928) overnight at 4 °C. Membranes were washed with TBST (25 mM Tris, 150 mM NaCl, 0.05% Tween 20) and incubated with fluorescently labeled secondary antibodies (Goat anti-rabbit 800 and goat anti-mouse 680, 1:5000, LI-COR) for one hour at room temperature. Blots were washed again and imaged using a LI-COR Odyssey

Statistical analyses

For the novel object recognition task groups were compared using a one-way analysis of variance (ANOVA), followed by Dunnett's multiple comparison tests with the vehicle treated rats as the control group. Changes in sEPSC frequency before and during drug add (peak effect) was compared using a paired t-test after data passed the Kohmogrov-Sminov normality test. For LTD experiments where only 2 experimental conditions were compared, a paired t-test was performed to calculate statistical significance after data

passed the Kohmogrov-Sminov normality test. For electrophysiological comparisons with more than one group, a one-way ANOVA was performed followed by Dunnett's Multiple Comparison test. For all statistical comparison, the critical p value was considered to be 0.05. The numbers of animals to be used for each experiment outlined within the manuscript were determined using a power calculation statistical analysis using the Power and Sample Size Calculation software program available at Vanderbilt University (Dupont and Plummer, PS Controlled Clinical Trials. 18:274 1997). Animal numbers are based on a power calculation using standard errors from published studies and previous experience to detect >20% difference for each outlined experiment with an 80% power (alpha=0.05, power=80%, delta=0.2, sigma=0.18).

REFERENCES

1. M. R. Picciotto, M. J. Higley, Y. S. Mineur, Acetylcholine as a neuromodulator: cholinergic signaling shapes nervous system function and behavior. *Neuron*. **76**, 116–129 (2012).

2. H. Soreq, Checks and balances on cholinergic signaling in brain and body function. *Trends Neurosci.* **38**, 448–458 (2015).

3. M. Sarter, C. Lustig, W. M. Howe, H. Gritton, A. S. Berry, Deterministic functions of cortical acetylcholine. *Eur. J. Neurosci.* **39**, 1912–1920 (2014).

4. M. E. Hasselmo, M. Sarter, Modes and models of forebrain cholinergic neuromodulation of cognition. *Neuropsychopharmacology*. **36**, 52–73 (2011).

5. J. Wess, R. M. Eglen, D. Gautam, Muscarinic acetylcholine receptors: mutant mice provide new insights for drug development. *Nat. Rev. Drug Discov.* **6**, 721–733 (2007).

6. J. van Os, S. Kapur, Schizophrenia. *Lancet*. **374**, 635–645 (2009).

7. C. A. Ross, R. L. Margolis, S. A. J. Reading, M. Pletnikov, J. T. Coyle, Neurobiology of schizophrenia. *Neuron*. **52**, 139–153 (2006).

8. J. T. Coyle, Schizophrenia: basic and clinical. *Adv. Neurobiol.* **15**, 255–280 (2017).

9. J. P. McEvoy, The costs of schizophrenia. *J. Clin. Psychiatry*. **68 Suppl 14**, 4–7 (2007).

10. J. A. Lieberman, T. S. Stroup, J. P. McEvoy, M. S. Swartz, R. A. Rosenheck, D. O. Perkins, R. S. E. Keefe, S. M. Davis, C. E. Davis, B. D. Lebowitz, J. Severe, J. K. Hsiao, Clinical Antipsychotic Trials of Intervention Effectiveness (CATIE) Investigators, Effectiveness of antipsychotic drugs in patients with chronic schizophrenia. *N. Engl. J. Med.* **353**, 1209–1223 (2005).

11. J. Lally, J. H. MacCabe, Antipsychotic medication in schizophrenia: a review. *Br Med Bull*. **114**, 169–179 (2015).

12. C. L. Masters, R. Bateman, K. Blennow, C. C. Rowe, R. A. Sperling, J. L. Cummings, Alzheimer's disease. *Nat. Rev. Dis. Primers*. **1**, 15056 (2015).

13. Alzheimer's Association, 2016 Alzheimer's disease facts and figures. *Alzheimers Dement.* **12**, 459–509 (2016).

14. C. A. Lane, J. Hardy, J. M. Schott, Alzheimer's disease. *Eur. J. Neurol.* **25**, 59–70 (2018).

15. P. J. Whitehouse, D. L. Price, A. W. Clark, J. T. Coyle, M. R. DeLong, Alzheimer disease: evidence for selective loss of cholinergic neurons in the nucleus basalis. *Ann. Neurol.* **10**, 122–126 (1981).

16. J. Birks, Cholinesterase inhibitors for Alzheimer's disease. *Cochrane Database Syst. Rev.*, CD005593 (2006).

17. N. C. Bodick, W. W. Offen, A. I. Levey, N. R. Cutler, S. G. Gauthier, A. Satlin, H. E. Shannon, G. D. Tollefson, K. Rasmussen, F. P. Bymaster, D. J. Hurley, W. Z.

Potter, S. M. Paul, Effects of xanomeline, a selective muscarinic receptor agonist, on cognitive function and behavioral symptoms in Alzheimer disease. *Arch. Neurol.* **54**, 465–473 (1997).

18. A. M. Bender, C. K. Jones, C. W. Lindsley, Classics in chemical neuroscience: xanomeline. *ACS Chem. Neurosci.* **8**, 435–443 (2017).

19. A. Shekhar, W. Z. Potter, J. Lightfoot, J. Lienemann, S. Dubé, C. Mallinckrodt, F. P. Bymaster, D. L. McKinzie, C. C. Felder, Selective muscarinic receptor agonist xanomeline as a novel treatment approach for schizophrenia. *Am. J. Psychiatry*. **165**, 1033–1039 (2008).

20. E. Callegari, B. Malhotra, P. J. Bungay, R. Webster, K. S. Fenner, S. Kempshall, J. L. LaPerle, M. C. Michel, G. G. Kay, A comprehensive non-clinical evaluation of the CNS penetration potential of antimuscarinic agents for the treatment of overactive bladder. *Br. J. Clin. Pharmacol.* **72**, 235–246 (2011).

21. P. J. Conn, C. K. Jones, C. W. Lindsley, Subtype-selective allosteric modulators of muscarinic receptors for the treatment of CNS disorders. *Trends Pharmacol. Sci.* **30**, 148–155 (2009).

22. P. J. Conn, A. Christopoulos, C. W. Lindsley, Allosteric modulators of GPCRs: a novel approach for the treatment of CNS disorders. *Nat. Rev. Drug Discov.* **8**, 41–54 (2009).

23. D. M. Thal, B. Sun, D. Feng, V. Nawaratne, K. Leach, C. C. Felder, M. G. Bures, D. A. Evans, W. I. Weis, P. Bachhawat, T. S. Kobilka, P. M. Sexton, B. K. Kobilka,

A. Christopoulos, Crystal structures of the M1 and M4 muscarinic acetylcholine receptors. *Nature*. **531**, 335–340 (2016).

24. K. Haga, A. C. Kruse, H. Asada, T. Yurugi-Kobayashi, M. Shiroishi, C. Zhang, W. I. Weis, T. Okada, B. K. Kobilka, T. Haga, T. Kobayashi, Structure of the human M2 muscarinic acetylcholine receptor bound to an antagonist. *Nature*. **482**, 547–551 (2012).

25. A. C. Kruse, J. Hu, A. C. Pan, D. H. Arlow, D. M. Rosenbaum, E. Rosemond, H. F. Green, T. Liu, P. S. Chae, R. O. Dror, D. E. Shaw, W. I. Weis, J. Wess, B. K. Kobilka, Structure and dynamics of the M3 muscarinic acetylcholine receptor. *Nature*. **482**, 552–556 (2012).

26. H. Liu, J. Hofmann, I. Fish, B. Schaake, K. Eitel, A. Bartuschat, J. Kaindl, H. Rampp, A. Banerjee, H. Hübner, M. J. Clark, S. G. Vincent, J. T. Fisher, M. R. Heinrich, K. Hirata, X. Liu, R. K. Sunahara, B. K. Shoichet, B. K. Kobilka, P. Gmeiner, Structure-guided development of selective M3 muscarinic acetylcholine receptor antagonists. *Proc. Natl. Acad. Sci. USA*. **115**, 12046–12050 (2018).

27. Z. Vuckovic, P. R. Gentry, A. E. Berizzi, K. Hirata, S. Varghese, G. Thompson, E. T. van der Westhuizen, W. A. C. Burger, R. Rahmani, C. Valant, C. J. Langmead, C. W. Lindsley, J. Baell, A. B. Tobin, P. M. Sexton, A. Christopoulos, D. M. Thal, Crystal structure of the M5 muscarinic acetylcholine receptor. *BioRxiv* (2019), doi:10.1101/730622.

28. Y. Miao, S. E. Nichols, P. M. Gasper, V. T. Metzger, J. A. McCammon, Activation and dynamic network of the M2 muscarinic receptor. *Proc. Natl. Acad. Sci. USA*. **110**, 10982–10987 (2013).

29. W. A. C. Burger, P. M. Sexton, A. Christopoulos, D. M. Thal, Toward an understanding of the structural basis of allostery in muscarinic acetylcholine receptors. *J. Gen. Physiol.* **150**, 1360–1372 (2018).

30. S. J. Y. Macalino, V. Gosu, S. Hong, S. Choi, Role of computer-aided drug design in modern drug discovery. *Arch. Pharm. Res.* **38**, 1686–1701 (2015).

31. D. Dencker, G. Wörtwein, P. Weikop, J. Jeon, M. Thomsen, T. N. Sager, A. Mørk, D. P. D. Woldbye, J. Wess, A. Fink-Jensen, Involvement of a subpopulation of neuronal M4 muscarinic acetylcholine receptors in the antipsychotic-like effects of the M1/M4 preferring muscarinic receptor agonist xanomeline. *J. Neurosci.* **31**, 5905–5908 (2011).

32. M. L. Woolley, H. J. Carter, J. E. Gartlon, J. M. Watson, L. A. Dawson, Attenuation of amphetamine-induced activity by the non-selective muscarinic receptor agonist, xanomeline, is absent in muscarinic M4 receptor knockout mice and attenuated in muscarinic M1 receptor knockout mice. *Eur. J. Pharmacol.* **603**, 147–149 (2009).

33. J. Wei, E. A. Walton, A. Milici, J. J. Buccafusco, m1-m5 muscarinic receptor distribution in rat CNS by RT-PCR and HPLC. *J. Neurochem.* **63**, 815–821 (1994).

34. J. E. Davoren, M. Garnsey, B. Pettersen, M. A. Brodney, J. R. Edgerton, J.-P. Fortin, S. Grimwood, A. R. Harris, S. Jenkinson, T. Kenakin, J. T. Lazzaro, C.-W.

Lee, S. M. Lotarski, L. Nottebaum, S. V. O'Neil, M. Popiolek, S. Ramsey, S. J. Steyn, C. A. Thorn, L. Zhang, D. Webb, Design and Synthesis of γ- and δ-Lactam M1 Positive Allosteric Modulators (PAMs): Convulsion and Cholinergic Toxicity of an M1-Selective PAM with Weak Agonist Activity. *J. Med. Chem.* **60**, 6649–6663 (2017).

35. M. Miyauchi, N. M. Neugebauer, T. Sato, H. Ardehali, H. Y. Meltzer, Muscarinic receptor signaling contributes to atypical antipsychotic drug reversal of the phencyclidine-induced deficit in novel object recognition in rats. *J. Psychopharmacol. (Oxford)*. **31**, 1588–1604 (2017).

36. R. W. Gould, D. Dencker, M. Grannan, M. Bubser, X. Zhan, J. Wess, Z. Xiang, C. Locuson, C. W. Lindsley, P. J. Conn, C. K. Jones, Role for the M1 Muscarinic Acetylcholine Receptor in Top-Down Cognitive Processing Using a Touchscreen Visual Discrimination Task in Mice. *ACS Chem. Neurosci.* **6**, 1683–1695 (2015).

37. S. G. Anagnostaras, G. G. Murphy, S. E. Hamilton, S. L. Mitchell, N. P. Rahnama, N. M. Nathanson, A. J. Silva, Selective cognitive dysfunction in acetylcholine M1 muscarinic receptor mutant mice. *Nat. Neurosci.* **6**, 51–58 (2003).

38. E. P. Lebois, C. Thorn, J. R. Edgerton, M. Popiolek, S. Xi, Muscarinic receptor subtype distribution in the central nervous system and relevance to aging and Alzheimer's disease. *Neuropharmacology*. **136**, 362–373 (2018).

39. D. J. Foster, J. P. Conn, Allosteric Modulation of GPCRs: New Insights and Potential Utility for Treatment of Schizophrenia and Other CNS Disorders. *Neuron* (2017).

40. M. Bubser, N. Byun, M. R. Wood, C. K. Jones, Muscarinic receptor pharmacology and circuitry for the modulation of cognition. *Handb Exp Pharmacol*, 121–166 (2012).

41. L. Ma, M. A. Seager, M. Wittmann, M. Jacobson, D. Bickel, M. Burno, K. Jones, V. K. Graufelds, G. Xu, M. Pearson, A. McCampbell, R. Gaspar, P. Shughrue, A. Danziger, C. Regan, R. Flick, D. Pascarella, S. Garson, S. Doran, C. Kreatsoulas, L. Veng, C. W. Lindsley, W. Shipe, S. Kuduk, C. Sur, G. Kinney, G. R. Seabrook, W. J. Ray, Selective activation of the M1 muscarinic acetylcholine receptor achieved by allosteric potentiation. *Proc. Natl. Acad. Sci. USA*. **106**, 15950–15955 (2009).

42. D. J. Gerber, T. D. Sotnikova, R. R. Gainetdinov, S. Y. Huang, M. G. Caron, S. Tonegawa, Hyperactivity, elevated dopaminergic transmission, and response to amphetamine in M1 muscarinic acetylcholine receptor-deficient mice. *Proc. Natl. Acad. Sci. USA*. **98**, 15312–15317 (2001).

43. C. Chambon, C. Jatzke, N. Wegener, A. Gravius, W. Danysz, Using cholinergic M1 receptor positive allosteric modulators to improve memory via enhancement of brain cholinergic communication. *Eur. J. Pharmacol.* **697**, 73–80 (2012).

44. H. R. Yeatman, J. R. Lane, K. H. C. Choy, N. A. Lambert, P. M. Sexton, A. Christopoulos, M. Canals, Allosteric modulation of M1 muscarinic acetylcholine receptor internalization and subcellular trafficking. *J. Biol. Chem.* **289**, 15856–15866 (2014).

45. A. Abdul-Ridha, J. R. Lane, P. M. Sexton, M. Canals, A. Christopoulos, Allosteric modulation of a chemogenetically modified G protein-coupled receptor. *Mol. Pharmacol.* **83**, 521–530 (2013).

46. J. K. Shirey, A. E. Brady, P. J. Jones, A. A. Davis, T. M. Bridges, J. P. Kennedy, S. B. Jadhav, U. N. Menon, Z. Xiang, M. L. Watson, E. P. Christian, J. J. Doherty, M. C. Quirk, D. H. Snyder, J. J. Lah, A. I. Levey, M. M. Nicolle, C. W. Lindsley, P. J. Conn, A selective allosteric potentiator of the M1 muscarinic acetylcholine receptor increases activity of medial prefrontal cortical neurons and restores impairments in reversal learning. *J. Neurosci.* **29**, 14271–14286 (2009).

47. J. Maksymetz, S. P. Moran, J. P. Conn, J. Maksymetz, S. Moran, J. Conn, Targeting metabotropic glutamate receptors for novel treatments of schizophrenia. *Mol. Brain* (2017).

48. J. M. Uslaner, D. Eddins, V. Puri, C. E. Cannon, J. Sutcliffe, C. S. Chew, M. Pearson, J. A. Vivian, R. K. Chang, W. J. Ray, S. D. Kuduk, M. Wittmann, The muscarinic M1 receptor positive allosteric modulator PQCA improves cognitive measures in rat, cynomolgus macaque, and rhesus macaque. *Psychopharmacology*. **225**, 21–30 (2013).

49. J. D. Vardigan, C. E. Cannon, V. Puri, M. Dancho, A. Koser, M. Wittmann, S. D. Kuduk, J. J. Renger, J. M. Uslaner, Improved cognition without adverse effects: novel M1 muscarinic potentiator compares favorably to donepezil and xanomeline in rhesus monkey. *Psychopharmacology*. **232**, 1859–1866 (2015).

50. V. Puri, X. Wang, J. D. Vardigan, S. D. Kuduk, J. M. Uslaner, The selective positive allosteric M1 muscarinic receptor modulator PQCA attenuates learning and memory deficits in the Tg2576 Alzheimer's disease mouse model. *Behav. Brain Res.* **287**, 96–99 (2015).

51. S. J. Bradley, J.-M. Bourgognon, H. E. Sanger, N. Verity, A. J. Mogg, D. J. White, A. J. Butcher, J. A. Moreno, C. Molloy, T. Macedo-Hatch, J. M. Edwards, J. Wess, R. Pawlak, D. J. Read, P. M. Sexton, L. M. Broad, J. R. Steinert, G. R. Mallucci, A. Christopoulos, C. C. Felder, A. B. Tobin, M1 muscarinic allosteric modulators slow prion neurodegeneration and restore memory loss. *J. Clin. Invest.* **127**, 487–499 (2017).

52. A. Ghoshal, J. M. Rook, J. W. Dickerson, G. N. Roop, R. D. Morrison, N. Jalan-Sakrikar, A. Lamsal, M. J. Noetzel, M. S. Poslusney, M. R. Wood, B. J. Melancon, S. R. Stauffer, Z. Xiang, J. S. Daniels, C. M. Niswender, C. K. Jones, C. W. Lindsley, P. J. Conn, Potentiation of M1 muscarinic receptor reverses plasticity deficits and negative and cognitive symptoms in a schizophrenia mouse model. *Neuropsychopharmacology*. **41**, 598–610 (2016).

53. M. D. Grannan, C. A. Mielnik, S. P. Moran, R. W. Gould, J. Ball, Z. Lu, M. Bubser, A. J. Ramsey, M. Abe, H. P. Cho, K. D. Nance, A. L. Blobaum, C. M. Niswender,

P. J. Conn, C. W. Lindsley, C. K. Jones, Prefrontal Cortex-Mediated Impairments in a Genetic Model of NMDA Receptor Hypofunction Are Reversed by the Novel M1 PAM VU6004256. *ACS Chem. Neurosci.* **7**, 1706–1716 (2016).

54. K. H. C. Choy, D. M. Shackleford, D. T. Malone, S. N. Mistry, R. T. Patil, P. J. Scammells, C. J. Langmead, C. Pantelis, P. M. Sexton, J. R. Lane, A. Christopoulos, Positive allosteric modulation of the muscarinic M1 receptor improves efficacy of antipsychotics in mouse glutamatergic deficit models of behavior. *J. Pharmacol. Exp. Ther.* **359**, 354–365 (2016).

55. J. E. Davoren, S. V. O'Neil, D. P. Anderson, M. A. Brodney, L. Chenard, K. Dlugolenski, J. R. Edgerton, M. Green, M. Garnsey, S. Grimwood, A. R. Harris, G. W. Kauffman, E. LaChapelle, J. T. Lazzaro, C.-W. Lee, S. M. Lotarski, D. M. Nason, R. S. Obach, V. Reinhart, R. Salomon-Ferrer, S. J. Steyn, D. Webb, J. Yan, L. Zhang, Design and optimization of selective azaindole amide M1 positive allosteric modulators. *Bioorg. Med. Chem. Lett.* **26**, 650–655 (2016).

56. J. E. Davoren, C.-W. Lee, M. Garnsey, M. A. Brodney, J. Cordes, K. Dlugolenski, J. R. Edgerton, A. R. Harris, C. J. Helal, S. Jenkinson, G. W. Kauffman, T. P. Kenakin, J. T. Lazzaro, S. M. Lotarski, Y. Mao, D. M. Nason, C. Northcott, L. Nottebaum, S. V. O'Neil, B. Pettersen, M. Popiolek, V. Reinhart, R. Salomon-Ferrer, S. J. Steyn, D. Webb, L. Zhang, S. Grimwood, Discovery of the Potent and Selective M1 PAM-Agonist N-[(3R,4S)-3-Hydroxytetrahydro-2H-pyran-4-yl]-5-methyl-4-[4-(1,3-thiazol-4-yl)benzyl]pyridine-2-carboxamide (PF-06767832):

Evaluation of Efficacy and Cholinergic Side Effects. *J. Med. Chem.* **59**, 6313–6328 (2016).

57. S. P. Moran, J. W. Dickerson, H. P. Cho, Z. Xiang, J. Maksymetz, D. H. Remke, X. Lv, C. A. Doyle, D. H. Rajan, C. M. Niswender, D. W. Engers, C. W. Lindsley, J. M. Rook, P. J. Conn, M1-positive allosteric modulators lacking agonist activity provide the optimal profile for enhancing cognition. *Neuropsychopharmacology*. **43**, 1763–1771 (2018).

58. J. Maksymetz, M. E. Joffe, S. P. Moran, B. J. Stansley, B. Li, K. Temple, D. W. Engers, J. J. Lawrence, C. W. Lindsley, P. J. Conn, M1 Muscarinic Receptors Modulate Fear-Related Inputs to the Prefrontal Cortex: Implications for Novel Treatments of Posttraumatic Stress Disorder. *Biol. Psychiatry*. **85**, 989–1000 (2019).

59. S. H. Dennis, F. Pasqui, E. M. Colvin, H. Sanger, A. J. Mogg, C. C. Felder, L. M. Broad, S. M. Fitzjohn, J. T. R. Isaac, J. R. Mellor, Activation of Muscarinic M1 Acetylcholine Receptors Induces Long-Term Potentiation in the Hippocampus. *Cereb. Cortex*. **26**, 414–426 (2016).

60. Y. Cui, D. Wang, W. Si, W. Lv, Y. Niu, X. Lei, Y. Hu, X. Cao, Enhancement of memory function in aged mice by a novel derivative of xanomeline. *Cell Res.* **18**, 1151–1153 (2008).

61. C.-H. Xiong, M.-G. Liu, L.-X. Zhao, M.-W. Chen, L. Tang, Y.-H. Yan, H.-Z. Chen, Y. Qiu, M1 muscarinic receptors facilitate hippocampus-dependent cognitive

flexibility via modulating GluA2 subunit of AMPA receptors. *Neuropharmacology*. **146**, 242–251 (2019).

62. J. M. Rook, M. Abe, H. P. Cho, K. D. Nance, V. B. Luscombe, J. J. Adams, J. W. Dickerson, D. H. Remke, P. M. Garcia-Barrantes, D. W. Engers, J. L. Engers, S. Chang, J. J. Foster, A. L. Blobaum, C. M. Niswender, C. K. Jones, P. J. Conn, C. W. Lindsley, Diverse Effects on M1 Signaling and Adverse Effect Liability within a Series of M1 Ago-PAMs. *ACS Chem. Neurosci.* **8**, 866–883 (2017).

63. S. E. Hamilton, M. D. Loose, M. Qi, A. I. Levey, B. Hille, G. S. McKnight, R. L. Idzerda, N. M. Nathanson, Disruption of the m1 receptor gene ablates muscarinic receptor-dependent M current regulation and seizure activity in mice. *Proc. Natl. Acad. Sci. USA*. **94**, 13311–13316 (1997).

64. F. P. Bymaster, P. A. Carter, M. Yamada, J. Gomeza, J. Wess, S. E. Hamilton, N. M. Nathanson, D. L. McKinzie, C. C. Felder, Role of specific muscarinic receptor subtypes in cholinergic parasympathomimetic responses, in vivo phosphoinositide hydrolysis, and pilocarpine-induced seizure activity. *Eur. J. Neurosci.* **17**, 1403–1410 (2003).

65. J. M. Rook, J. L. Bertron, H. P. Cho, P. M. Garcia-Barrantes, S. P. Moran, J. T. Maksymetz, K. D. Nance, J. W. Dickerson, D. H. Remke, S. Chang, J. M. Harp, A. L. Blobaum, C. M. Niswender, C. K. Jones, S. R. Stauffer, P. J. Conn, C. W. Lindsley, A Novel M1 PAM VU0486846 Exerts Efficacy in Cognition Models without Displaying Agonist Activity or Cholinergic Toxicity. *ACS Chem. Neurosci.* **9**, 2274–2285 (2018).

66. S. P. Moran, H. P. Cho, J. Maksymetz, D. H. Remke, R. M. Hanson, C. M. Niswender, C. W. Lindsley, J. M. Rook, P. J. Conn, PF-06827443 Displays Robust Allosteric Agonist and Positive Allosteric Modulator Activity in High Receptor Reserve and Native Systems. *ACS Chem. Neurosci.* **9**, 2218–2224 (2018).

67. J. M. Rook, M. J. Noetzel, W. A. Pouliot, T. M. Bridges, P. N. Vinson, H. P. Cho, Y. Zhou, R. D. Gogliotti, J. T. Manka, K. J. Gregory, S. R. Stauffer, F. E. Dudek, Z. Xiang, C. M. Niswender, J. S. Daniels, C. K. Jones, C. W. Lindsley, P. J. Conn, Unique signaling profiles of positive allosteric modulators of metabotropic glutamate receptor subtype 5 determine differences in in vivo activity. *Biol. Psychiatry*. **73**, 501–509 (2013).

68. D. Beshore, in *MEDI: Division of Medicinal Chemistry* (2017).

69. A. Alt, A. Pendri, R. L. Bertekap, G. Li, Y. Benitex, M. Nophsker, K. L. Rockwell, N. T. Burford, C. S. Sum, J. Chen, J. J. Herbst, M. Ferrante, A. Hendricson, M. E. Cvijic, R. S. Westphal, J. O'Connell, M. Banks, L. Zhang, R. G. Gentles, S. Jenkins, J. Loy, J. E. Macor, Evidence for Classical Cholinergic Toxicity Associated with Selective Activation of M1 Muscarinic Receptors. *J. Pharmacol. Exp. Ther.* **356**, 293–304 (2016).

70. X. Lv, J. W. Dickerson, J. M. Rook, C. W. Lindsley, P. J. Conn, Z. Xiang, M1 muscarinic activation induces long-lasting increase in intrinsic excitability of striatal projection neurons. *Neuropharmacology*. **118**, 209–222 (2017).

71. H. G. S. Martin, A. Bernabeu, O. Lassalle, C. Bouille, C. Beurrier, A.-L. Pelissier-Alicot, O. J. Manzoni, Endocannabinoids Mediate Muscarinic Acetylcholine Receptor-Dependent Long-Term Depression in the Adult Medial Prefrontal Cortex. *Front. Cell Neurosci.* **9**, 457 (2015).

72. D. J. Sheffler, R. Williams, T. M. Bridges, Z. Xiang, A. S. Kane, N. E. Byun, S. Jadhav, M. M. Mock, F. Zheng, L. M. Lewis, C. K. Jones, C. M. Niswender, C. D. Weaver, C. W. Lindsley, P. J. Conn, A novel selective muscarinic acetylcholine receptor subtype 1 antagonist reduces seizures without impairing hippocampus-dependent learning. *Mol. Pharmacol.* **76**, 356–368 (2009).

73. T. M. Bridges, J. M. Rook, M. J. Noetzel, R. D. Morrison, Y. Zhou, R. D. Gogliotti, P. N. Vinson, Z. Xiang, C. K. Jones, C. M. Niswender, C. W. Lindsley, S. R. Stauffer, P. J. Conn, J. S. Daniels, Biotransformation of a novel positive allosteric modulator of metabotropic glutamate receptor subtype 5 contributes to seizure-like adverse events in rats involving a receptor agonism-dependent mechanism. *Drug Metab. Dispos.* **41**, 1703–1714 (2013).

74. T. Voss, J. Li, J. Cummings, M. Farlow, C. Assaid, S. Froman, H. Leibensperger, L. Snow-Adami, K. B. McMahon, M. Egan, D. Michelson, Randomized, controlled, proof-of-concept trial of MK-7622 in Alzheimer's disease. *Alzheimers Dement (N Y)*. **4**, 173–181 (2018).

75. T. P. Kenakin, Receptor reserve as a tissue misnomer. *Trends Pharmacol. Sci.* **7**, 93–95 (1986).

76. G. J. Digby, M. J. Noetzel, M. Bubser, T. J. Utley, A. G. Walker, N. E. Byun, E. P. Lebois, Z. Xiang, D. J. Sheffler, H. P. Cho, A. A. Davis, N. E. Nemirovsky, S. E. Mennenga, B. W. Camp, H. A. Bimonte-Nelson, J. Bode, K. Italiano, R. Morrison, J. S. Daniels, C. M. Niswender, M. F. Olive, C. W. Lindsley, C. K. Jones, P. J. Conn, Novel allosteric agonists of M1 muscarinic acetylcholine receptors induce brain region-specific responses that correspond with behavioral effects in animal models. *J. Neurosci.* **32**, 8532–8544 (2012).

77. G. J. Digby, T. J. Utley, A. Lamsal, C. Sevel, D. J. Sheffler, E. P. Lebois, T. M. Bridges, M. R. Wood, C. M. Niswender, C. W. Lindsley, P. J. Conn, Chemical modification of the M(1) agonist VU0364572 reveals molecular switches in pharmacology and a bitopic binding mode. *ACS Chem. Neurosci.* **3**, 1025–1036 (2012).

78. A. C. Porter, F. P. Bymaster, N. W. DeLapp, M. Yamada, J. Wess, S. E. Hamilton, N. M. Nathanson, C. C. Felder, M1 muscarinic receptor signaling in mouse hippocampus and cortex. *Brain Res.* **944**, 82–89 (2002).

79. M. J. Noetzel, J. M. Rook, P. N. Vinson, H. P. Cho, E. Days, Y. Zhou, A. L. Rodriguez, H. Lavreysen, S. R. Stauffer, C. M. Niswender, Z. Xiang, J. S. Daniels, C. K. Jones, C. W. Lindsley, C. D. Weaver, P. J. Conn, Functional impact of allosteric agonist activity of selective positive allosteric modulators of metabotropic glutamate receptor subtype 5 in regulating central nervous system function. *Mol. Pharmacol.* **81**, 120–133 (2012).

80. E. P. Lebois, J. P. Schroeder, T. J. Esparza, T. M. Bridges, C. W. Lindsley, P. J. Conn, D. L. Brody, J. S. Daniels, A. I. Levey, Disease-Modifying Effects of M1 Muscarinic Acetylcholine Receptor Activation in an Alzheimer's Disease Mouse Model. *ACS Chem. Neurosci.* **8**, 1177–1187 (2017).

81. E. Kurimoto, M. Nakashima, H. Kimura, M. Suzuki, TAK-071, a muscarinic M1 receptor positive allosteric modulator, attenuates scopolamine-induced quantitative electroencephalogram power spectral changes in cynomolgus monkeys. *PLoS One*. **14**, e0207969 (2019).

82. H. S. Lange, C. E. Cannon, J. T. Drott, S. D. Kuduk, J. M. Uslaner, The M1 muscarinic positive allosteric modulator PQCA improves performance on translatable tests of memory and attention in rhesus monkeys. *J. Pharmacol. Exp. Ther.* **355**, 442–450 (2015).

83. W. Y. Chan, D. L. McKinzie, S. Bose, S. N. Mitchell, J. M. Witkin, R. C. Thompson, A. Christopoulos, S. Lazareno, N. J. M. Birdsall, F. P. Bymaster, C. C. Felder, Allosteric modulation of the muscarinic M4 receptor as an approach to treating schizophrenia. *Proc. Natl. Acad. Sci. USA*. **105**, 10978–10983 (2008).

84. M. R. Wood, M. J. Noetzel, M. S. Poslusney, B. J. Melancon, J. C. Tarr, A. Lamsal, S. Chang, V. B. Luscombe, R. L. Weiner, H. P. Cho, M. Bubser, C. K. Jones, C. M. Niswender, M. W. Wood, D. W. Engers, N. J. Brandon, M. E. Duggan, P. J. Conn, T. M. Bridges, C. W. Lindsley, Challenges in the development of an M4 PAM in vivo tool compound: The discovery of VU0467154 and unexpected DMPK profiles of close analogs. *Bioorg. Med. Chem. Lett.* **27**, 171–175 (2017).

85. D. Wootten, A. Christopoulos, M. Marti-Solano, M. M. Babu, P. M. Sexton, Mechanisms of signalling and biased agonism in G protein-coupled receptors. *Nat. Rev. Mol. Cell Biol.* **19**, 638–653 (2018).

86. L. M. Bohn, R. J. Lefkowitz, R. R. Gainetdinov, K. Peppel, M. G. Caron, F. T. Lin, Enhanced morphine analgesia in mice lacking beta-arrestin 2. *Science*. **286**, 2495–2498 (1999).

87. K. M. Raehal, C. L. Schmid, C. E. Groer, L. M. Bohn, Functional selectivity at the μ-opioid receptor: implications for understanding opioid analgesia and tolerance. *Pharmacol. Rev.* **63**, 1001–1019 (2011).

88. C. L. Schmid, N. M. Kennedy, N. C. Ross, K. M. Lovell, Z. Yue, J. Morgenweck, M. D. Cameron, T. D. Bannister, L. M. Bohn, Bias factor and therapeutic window correlate to predict safer opioid analgesics. *Cell*. **171**, 1165–1175.e13 (2017).

89. A. E. Conibear, E. Kelly, A Biased View of μ-Opioid Receptors? *Mol. Pharmacol.* **96**, 542–549 (2019).

90. J. E. Marlo, C. M. Niswender, E. L. Days, T. M. Bridges, Y. Xiang, A. L. Rodriguez, J. K. Shirey, A. E. Brady, T. Nalywajko, Q. Luo, C. A. Austin, M. B. Williams, K. Kim, R. Williams, D. Orton, H. A. Brown, C. W. Lindsley, C. D. Weaver, P. J. Conn, Discovery and characterization of novel allosteric potentiators of M1 muscarinic receptors reveals multiple modes of activity. *Mol. Pharmacol.* **75**, 577–588 (2009).

91. H. A. Brown, L. G. Henage, A. M. Preininger, Y. Xiang, J. H. Exton, *Biochemical analysis of phospholipase D.* (2007), vol. 434.

92. S. Pepitoni, R. G. Mallon, J. K. Pai, J. A. Borkowski, M. A. Buck, R. D. McQuade, Phospholipase D activity and phosphatidylethanol formation in stimulated HeLa cells expressing the human m1 muscarinic acetylcholine receptor gene. *Biochem. Biophys. Res. Commun.* **176**, 453–458 (1991).

93. F. R. McKenzie, K. Seuwen, J. Pouysségur, Stimulation of phosphatidylcholine breakdown by thrombin and carbachol but not by tyrosine kinase receptor ligands in cells transfected with M1 muscarinic receptors. Rapid desensitization of phosphocholine-specific (PC) phospholipase D but sustained activity of PC-phospholipase C. *J. Biol. Chem.* **267**, 22759–22769 (1992).

94. R. K. Nelson, M. A. Frohman, Physiological and pathophysiological roles for phospholipase D. *J. Lipid Res.* **56**, 2229–2237 (2015).

95. T. Kenakin, Is the quest for signaling bias worth the effort? *Mol. Pharmacol.* **93**, 266–269 (2018).

96. A. Ghoshal, S. P. Moran, J. W. Dickerson, M. E. Joffe, B. A. Grueter, Z. Xiang, C. W. Lindsley, J. M. Rook, P. J. Conn, Role of mGlu5 receptors and inhibitory neurotransmission in M1 dependent muscarinic LTD in the prefrontal cortex: implications in schizophrenia. *ACS Chem. Neurosci.* **8**, 2254–2265 (2017).

97. J. H. Exton, Regulation of phospholipase D. *FEBS Lett.* **531**, 58–61 (2002).

98. S. B. Bocckino, P. B. Wilson, J. H. Exton, Ca^{2+}-mobilizing hormones elicit phosphatidylethanol accumulation via phospholipase D activation. *FEBS Lett.* **225**, 201–204 (1987).

99. S. A. Scott, M. C. O'Reilly, J. S. Daniels, R. Morrison, R. Ptak, E. S. Dawson, N. Tower, J. L. Engers, D. W. Engers, T. Oguin, P. Thomas, L. White, H. A. Brown, C. W. Lindsley, in *Probe Reports from the NIH Molecular Libraries Program* (National Center for Biotechnology Information (US), Bethesda (MD), 2010).

100. J. A. Lewis, S. A. Scott, R. Lavieri, J. R. Buck, P. E. Selvy, S. L. Stoops, M. D. Armstrong, H. A. Brown, C. W. Lindsley, Design and synthesis of isoform-selective phospholipase D (PLD) inhibitors. Part I: Impact of alternative halogenated privileged structures for PLD1 specificity. *Bioorg. Med. Chem. Lett.* **19**, 1916–1920 (2009).

101. R. Lavieri, S. A. Scott, J. A. Lewis, P. E. Selvy, M. D. Armstrong, H. Alex Brown, C. W. Lindsley, Design and synthesis of isoform-selective phospholipase D (PLD) inhibitors. Part II. Identification of the 1,3,8-triazaspiro[4,5]decan-4-one privileged structure that engenders PLD2 selectivity. *Bioorg. Med. Chem. Lett.* **19**, 2240–2243 (2009).

102. P. R. Reid, T. M. Bridges, D. J. Sheffler, H. P. Cho, L. M. Lewis, E. Days, J. S. Daniels, C. K. Jones, C. M. Niswender, C. D. Weaver, P. J. Conn, C. W. Lindsley, M. R. Wood, Discovery and optimization of a novel, selective and brain penetrant M1 positive allosteric modulator (PAM): the development of ML169, an MLPCN probe. *Bioorg. Med. Chem. Lett.* **21**, 2697–2701 (2011).

103. A. G. Walker, C. J. Wenthur, Z. Xiang, J. M. Rook, K. A. Emmitte, C. M. Niswender, C. W. Lindsley, P. J. Conn, Metabotropic glutamate receptor 3 activation is required

for long-term depression in medial prefrontal cortex and fear extinction. *Proc. Natl. Acad. Sci. USA*. **112**, 1196–1201 (2015).

104. M. E. Joffe, C. I. Santiago, J. L. Engers, C. W. Lindsley, P. J. Conn, Metabotropic glutamate receptor subtype 3 gates acute stress-induced dysregulation of amygdalo-cortical function. *Mol. Psychiatry*. **24**, 916–927 (2017).

105. M. E. Joffe, C. I. Santiago, B. J. Stansley, J. Maksymetz, R. G. Gogliotti, J. L. Engers, F. Nicoletti, C. W. Lindsley, P. J. Conn, Mechanisms underlying prelimbic prefrontal cortex mGlu3/mGlu5-dependent plasticity and reversal learning deficits following acute stress. *Neuropharmacology*. **144**, 19–28 (2018).

106. J. R. Lane, L. T. May, R. G. Parton, P. M. Sexton, A. Christopoulos, A kinetic view of GPCR allostery and biased agonism. *Nat. Chem. Biol.* **13**, 929–937 (2017).

107. T. P. Kenakin, Biased signalling and allosteric machines: new vistas and challenges for drug discovery. *Br. J. Pharmacol.* **165**, 1659–1669 (2012).

108. Z. Xiang, A. D. Thompson, C. K. Jones, C. W. Lindsley, P. J. Conn, Roles of the M1 muscarinic acetylcholine receptor subtype in the regulation of basal ganglia function and implications for the treatment of Parkinson's disease. *J. Pharmacol. Exp. Ther.* **340**, 595–603 (2012).

109. F. P. Bymaster, C. A. Whitesitt, H. E. Shannon, N. DeLapp, J. S. Ward, D. O. Calligaro, L. A. Shipley, J. L. Buelke-Sam, N. C. Bodick, L. Farde, M. J. Sheardown, P. H. Olesen, K. T. Hansen, P. D. Suzdak, M. D. B. Swedberg, P. Sauerberg, C.

H. Mitch, Xanomeline: A selective muscarinic agonist for the treatment of Alzheimer's disease. *Drug Dev Res*. **40**, 158–170 (1997).

110. H. Hall, M. F. Iulita, P. Gubert, L. Flores Aguilar, A. Ducatenzeiler, A. Fisher, A. C. Cuello, AF710B, an M1/sigma-1 receptor agonist with long-lasting disease-modifying properties in a transgenic rat model of Alzheimer's disease. *Alzheimers Dement.* **14**, 811–823 (2018).

111. E. Kurimoto, S. Matsuda, Y. Shimizu, Y. Sako, T. Mandai, T. Sugimoto, H. Sakamoto, H. Kimura, An Approach to Discovering Novel Muscarinic M1 Receptor Positive Allosteric Modulators with Potent Cognitive Improvement and Minimized Gastrointestinal Dysfunction. *J. Pharmacol. Exp. Ther.* **364**, 28–37 (2018).

112. S. J. Walker, H. A. Brown, Molecular and Cellular Biology, Cornell University, Ithaca, NY, USA, Measurement of G protein-coupled receptor-stimulated phospholipase D activity in intact cells. *Methods Mol. Biol.* **237**, 89–97 (2004).

113. A. Ghoshal, P. J. Conn, The hippocampo-prefrontal pathway: a possible therapeutic target for negative and cognitive symptoms of schizophrenia. *Future Neurol.* **10**, 115–128 (2015).

114. E. Scarr, S. Hopper, V. Vos, M. S. Seo, I. P. Everall, T. D. Aumann, G. Chana, B. Dean, Low levels of muscarinic M1 receptor-positive neurons in cortical layers III and V in Brodmann areas 9 and 17 from individuals with schizophrenia. *J. Psychiatry Neurosci.* **43**, 338–346 (2018).

115. E. Scarr, S. Sundram, D. Keriakous, B. Dean, Altered hippocampal muscarinic M4, but not M1, receptor expression from subjects with schizophrenia. *Biol. Psychiatry*. **61**, 1161–1170 (2007).

116. B. Dean, S. Hopper, P. J. Conn, E. Scarr, Changes in BQCA Allosteric Modulation of [(3)H]NMS Binding to Human Cortex within Schizophrenia and by Divalent Cations. *Neuropsychopharmacology*. **41**, 1620–1628 (2016).

117. B. Dean, M. McLeod, D. Keriakous, J. McKenzie, E. Scarr, Decreased muscarinic1 receptors in the dorsolateral prefrontal cortex of subjects with schizophrenia. *Mol. Psychiatry*. **7**, 1083–1091 (2002).

118. E. Scarr, M. Udawela, E. A. Thomas, B. Dean, Changed gene expression in subjects with schizophrenia and low cortical muscarinic M1 receptors predicts disrupted upstream pathways interacting with that receptor. *Mol. Psychiatry*. **23**, 295–303 (2016).

119. E. Scarr, T. F. Cowie, S. Kanellakis, S. Sundram, C. Pantelis, B. Dean, Decreased cortical muscarinic receptors define a subgroup of subjects with schizophrenia. *Mol. Psychiatry*. **14**, 1017–1023 (2009).

120. A. Caccamo, S. Oddo, L. M. Billings, K. N. Green, H. Martinez-Coria, A. Fisher, F. M. LaFerla, M1 receptors play a central role in modulating AD-like pathology in transgenic mice. *Neuron*. **49**, 671–682 (2006).

121. R. Medeiros, M. Kitazawa, A. Caccamo, D. Baglietto-Vargas, T. Estrada-Hernandez, D. H. Cribbs, A. Fisher, F. M. LaFerla, Loss of muscarinic M1 receptor

exacerbates Alzheimer's disease-like pathology and cognitive decline. *Am. J. Pathol.* **179**, 980–991 (2011).

122. J. M. Rook, Z. Xiang, X. Lv, A. Ghoshal, J. W. Dickerson, T. M. Bridges, K. A. Johnson, D. J. Foster, K. J. Gregory, P. N. Vinson, A. D. Thompson, N. Byun, R. L. Collier, M. Bubser, M. T. Nedelcovych, R. W. Gould, S. R. Stauffer, J. S. Daniels, C. M. Niswender, H. Lavreysen, C. Mackie, S. Conde-Ceide, J. Alcazar, J. M. Bartolomé-Nebreda, G. J. Macdonald, J. C. Talpos, T. Steckler, C. K. Jones, C. W. Lindsley, P. J. Conn, Biased mGlu5-Positive Allosteric Modulators Provide In Vivo Efficacy without Potentiating mGlu5 Modulation of NMDAR Currents. *Neuron*. **86**, 1029–1040 (2015).

123. S. Parmentier-Batteur, P. H. Hutson, K. Menzel, J. M. Uslaner, B. A. Mattson, J. A. O'Brien, B. C. Magliaro, T. Forest, C. A. Stump, R. M. Tynebor, N. J. Anthony, T. J. Tucker, X.-F. Zhang, R. Gomez, S. L. Huszar, N. Lambeng, H. Fauré, E. Le Poul, S. Poli, T. W. Rosahl, J.-P. Rocher, R. Hargreaves, T. M. Williams, Mechanism based neurotoxicity of mGlu5 positive allosteric modulators--development challenges for a promising novel antipsychotic target. *Neuropharmacology*. **82**, 161–173 (2014).

124. D. E. O'Brien, D. M. Shaw, H. P. Cho, A. J. Cross, S. S. Wesolowski, A. S. Felts, J. Bergare, C. S. Elmore, C. W. Lindsley, C. M. Niswender, P. J. Conn, Differential Pharmacology and Binding of mGlu2 Receptor Allosteric Modulators. *Mol. Pharmacol.* **93**, 526–540 (2018).

125. A. S. Hammond, A. L. Rodriguez, S. D. Townsend, C. M. Niswender, K. J. Gregory, C. W. Lindsley, P. J. Conn, Discovery of a Novel Chemical Class of mGlu(5) Allosteric Ligands with Distinct Modes of Pharmacology. *ACS Chem. Neurosci.* **1**, 702–716 (2010).

126. A. L. Rodriguez, J. C. Tarr, Y. Zhou, R. Williams, K. J. Gregory, T. M. Bridges, J. S. Daniels, C. M. Niswender, P. J. Conn, C. W. Lindsley, S. R. Stauffer, in *Probe Reports from the NIH Molecular Libraries Program* (National Center for Biotechnology Information (US), Bethesda (MD), 2010).

127. E. Khajehali, C. Valant, M. Jörg, A. B. Tobin, P. J. Conn, C. W. Lindsley, P. M. Sexton, P. J. Scammells, A. Christopoulos, Probing the binding site of novel selective positive allosteric modulators at the M1 muscarinic acetylcholine receptor. *Biochem. Pharmacol.* **154**, 243–254 (2018).

128. D. Elie, M. Poirier, J. Chianetta, M. Durand, C. Grégoire, S. Grignon, Cognitive effects of antipsychotic dosage and polypharmacy: a study with the BACS in patients with schizophrenia and schizoaffective disorder. *J. Psychopharmacol. (Oxford)*. **24**, 1037–1044 (2010).

129. A. S. M. Anisuzzaman, J. Uwada, T. Masuoka, H. Yoshiki, M. Nishio, Y. Ikegaya, N. Takahashi, N. Matsuki, Y. Fujibayashi, Y. Yonekura, T. Momiyama, I. Muramatsu, Novel contribution of cell surface and intracellular M1-muscarinic acetylcholine receptors to synaptic plasticity in hippocampus. *J. Neurochem.* **126**, 360–371 (2013).

130. D. Liang, K. Wu, R. Tei, T. W. Bumpus, J. Ye, J. M. Baskin, A real-time, click chemistry imaging approach reveals stimulus-specific subcellular locations of phospholipase D activity. *Proc. Natl. Acad. Sci. USA*. **116**, 15453–15462 (2019).

131. T. Ahmadzada, G. Reid, D. R. McKenzie, Fundamentals of siRNA and miRNA therapeutics and a review of targeted nanoparticle delivery systems in breast cancer. *Biophys. Rev.* **10**, 69–86 (2018).

132. D. W. Kang, M. H. Park, Y. J. Lee, H. S. Kim, C. W. Lindsley, H. Alex Brown, D. S. Min, Autoregulation of phospholipase D activity is coupled to selective induction of phospholipase D1 expression to promote invasion of breast cancer cells. *Int. J. Cancer*. **128**, 805–816 (2011).

133. R. C. Bruntz, H. E. Taylor, C. W. Lindsley, H. A. Brown, Phospholipase D2 mediates survival signaling through direct regulation of Akt in glioblastoma cells. *J. Biol. Chem.* **289**, 600–616 (2014).

134. M. Adli, The CRISPR tool kit for genome editing and beyond. *Nat. Commun.* **9**, 1911 (2018).

135. L. S. Qi, M. H. Larson, L. A. Gilbert, J. A. Doudna, J. S. Weissman, A. P. Arkin, W. A. Lim, Repurposing CRISPR as an RNA-guided platform for sequence-specific control of gene expression. *Cell*. **152**, 1173–1183 (2013).

136. P. E. Selvy, R. R. Lavieri, C. W. Lindsley, H. A. Brown, Phospholipase D: enzymology, functionality, and chemical modulation. *Chem. Rev.* **111**, 6064–6119 (2011).

137. V. Boss, P. J. Conn, Metabotropic excitatory amino acid receptor activation stimulates phospholipase D in hippocampal slices. *J. Neurochem.* **59**, 2340–2343 (1992).

138. V. Boss, K. M. Nutt, P. J. Conn, L-cysteine sulfinic acid as an endogenous agonist of a novel metabotropic receptor coupled to stimulation of phospholipase D activity. *Mol. Pharmacol.* **45**, 1177–1182 (1994).

139. D. E. Pellegrini-Giampietro, S. A. Torregrossa, F. Moroni, Pharmacological characterization of metabotropic glutamate receptors coupled to phospholipase D in the rat hippocampus. *Br. J. Pharmacol.* **118**, 1035–1043 (1996).

140. C. M. Gladding, S. M. Fitzjohn, E. Molnár, Metabotropic glutamate receptor-mediated long-term depression: molecular mechanisms. *Pharmacol. Rev.* **61**, 395–412 (2009).

141. C. Lüscher, K. M. Huber, Group 1 mGluR-dependent synaptic long-term depression: mechanisms and implications for circuitry and disease. *Neuron*. **65**, 445–459 (2010).

142. A. Abdul-Ridha, J. R. Lane, S. N. Mistry, L. López, P. M. Sexton, P. J. Scammells, A. Christopoulos, M. Canals, Mechanistic insights into allosteric structure-function relationships at the M1 muscarinic acetylcholine receptor. *J. Biol. Chem.* **289**, 33701–33711 (2014).

143. A. E. Berizzi, A. M. Bender, C. W. Lindsley, P. J. Conn, P. M. Sexton, C. J. Langmead, A. Christopoulos, Structure-Activity Relationships of Pan-Gαq/11

Coupled Muscarinic Acetylcholine Receptor Positive Allosteric Modulators. *ACS Chem. Neurosci.* **9**, 1818–1828 (2018).

144. T. Kenakin, Theoretical Aspects of GPCR-Ligand Complex Pharmacology. *Chem. Rev.* **117**, 4–20 (2017).

145. Y. Sako, E. Kurimoto, T. Mandai, A. Suzuki, M. Tanaka, M. Suzuki, Y. Shimizu, M. Yamada, H. Kimura, TAK-071, a novel M1 positive allosteric modulator with low cooperativity, improves cognitive function in rodents with few cholinergic side effects. *Neuropsychopharmacology*. **44**, 950–960 (2019).

146. T. Mandai, M. Kasahara, E. Kurimoto, M. Tanaka, M. Suzuki, A. Nakatani, H. Kimura, In Vivo Pharmacological Comparison of TAK-071, a Positive Allosteric Modulator of Muscarinic M1 Receptor, and Xanomeline, an Agonist of Muscarinic M1/M4 Receptor, in Rodents. *Neuroscience* (2019), doi:10.1016/j.neuroscience.2019.07.003.

147. J. T. Coyle, D. L. Price, M. R. DeLong, Alzheimer's disease: a disorder of cortical cholinergic innervation. *Science*. **219**, 1184–1190 (1983).

148. D. P. Holschneider, Y. Guo, Z. Wang, M. Vidal, O. U. Scremin, Positive Allosteric Modulation of Cholinergic Receptors Improves Spatial Learning after Cortical Contusion Injury in Mice. *J. Neurotrauma* (2019), doi:10.1089/neu.2018.6036.

149. K. Stoll, R. Hart, C. W. Lindsley, M. Thomsen, Effects of muscarinic M1 and M4 acetylcholine receptor stimulation on extinction and reinstatement of cocaine

seeking in male mice, independent of extinction learning. *Psychopharmacology*. **235**, 815–827 (2018).

150. E. S. Lein, M. J. Hawrylycz, N. Ao, M. Ayres, A. Bensinger, A. Bernard, A. F. Boe, M. S. Boguski, K. S. Brockway, E. J. Byrnes, L. Chen, L. Chen, T.-M. Chen, M. C. Chin, J. Chong, B. E. Crook, A. Czaplinska, C. N. Dang, S. Datta, N. R. Dee, A. L. Desaki, T. Desta, E. Diep, T. A. Dolbeare, M. J. Donelan, H.-W. Dong, J. G. Dougherty, B. J. Duncan, A. J. Ebbert, G. Eichele, L. K. Estin, C. Faber, B. A. Facer, R. Fields, S. R. Fischer, T. P. Fliss, C. Frensley, S. N. Gates, K. J. Glattfelder, K. R. Halverson, M. R. Hart, J. G. Hohmann, M. P. Howell, D. P. Jeung, R. A. Johnson, P. T. Karr, R. Kawal, J. M. Kidney, R. H. Knapik, C. L. Kuan, J. H. Lake, A. R. Laramee, K. D. Larsen, C. Lau, T. A. Lemon, A. J. Liang, Y. Liu, L. T. Luong, J. Michaels, J. J. Morgan, R. J. Morgan, M. T. Mortrud, N. F. Mosqueda, L. L. Ng, R. Ng, G. J. Orta, C. C. Overly, T. H. Pak, S. E. Parry, S. D. Pathak, O. C. Pearson, R. B. Puchalski, Z. L. Riley, H. R. Rockett, S. A. Rowland, J. J. Royall, M. J. Ruiz, N. R. Sarno, K. Schaffnit, N. V. Shapovalova, T. Sivisay, C. R. Slaughterbeck, S. C. Smith, K. A. Smith, B. I. Smith, A. J. Sodt, N. N. Stewart, K.-R. Stumpf, S. M. Sunkin, M. Sutram, A. Tam, C. D. Teemer, C. Thaller, C. L. Thompson, L. R. Varnam, A. Visel, R. M. Whitlock, P. E. Wohnoutka, C. K. Wolkey, V. Y. Wong, M. Wood, M. B. Yaylaoglu, R. C. Young, B. L. Youngstrom, X. F. Yuan, B. Zhang, T. A. Zwingman, A. R. Jones, Genome-wide atlas of gene expression in the adult mouse brain. *Nature*. **445**, 168–176 (2007).